CZECH TECHNICAL UNIVERSITY IN PRAGUE

FACULTY OF MECHANICAL ENGINEERING

Department of production machines and equipment

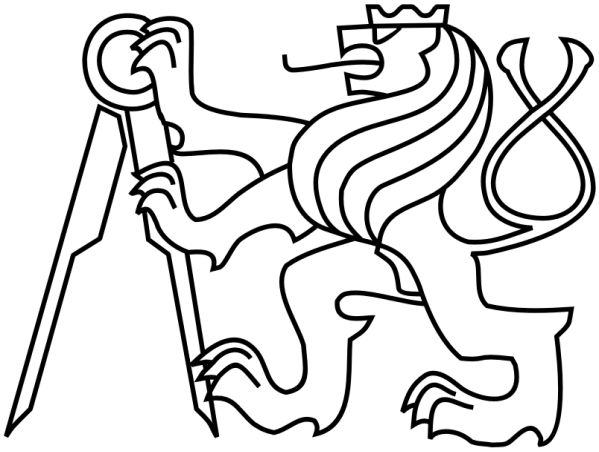

Master thesis

Active control of hydrostatic pocket throttling gap height

2016 **Bc. Tomáš Lazák**

Vysoká škola:	**ČVUT v Praze**
Fakulta:	**strojní**
Ústav:	**Výrobní stroje a zařízení**
Akademický rok:	**2015/2016**

ZADÁNÍ DIPLOMOVÉ PRÁCE

pro	**Bc. Tomáš Lazák**
Program:	Strojní inženýrství
Obor:	Výrobní stroje a zařízení

Téma práce: **Aktivní řízení výšky škrticí mezery hydrostatické buňky**
Active control of hydrostatic pocket throttling gap height

Stručná osnova zadání:

Úkolem práce je provedení návrhu aktivního řízení výšky škrtící mezery hydrostatických kapes. Aktivní řízení umožňuje na základě vnějšího signálu měnit výšku škrticí mezery a umožňuje společné řízení více hydrostatických kapes najednou (např. celá pohybová osa) s cílem kompenzovat geometrické chyby nebo známé výrobní nepřesnosti stroje. Navržený princip aktivního řízení bude experimentálně ověřen na testovací stolici STD30 v laboratoři ústavu.

Práce bude obsahovat tyto hlavní body:

1. Rešerše problematiky hydrostatických (HS) vedení obráběcích strojů zaměřená na stávající stav regulace a aktivního řízení průtoku kapsou.
2. Návrh vhodného způsobu aktivního řízení jedné HS buňky.
3. Návrh řízení výšky a naklopení posuvného stolu uloženého na hydrostatickém vedení.
4. Realizace a experimentální ověření na testovací stolici STD30.

Declaration

I declare that I developed and wrote enclosed master thesis independently, using only cited sources accordingly to Guidelines adhering to ethical principles addressing undergraduate thesis, issued by Czech Technical University in Prague on June 1, 2009.

I do not have a relevant reason against the use of this academic work in accordance with § 60 of the Act No.121 / 2000 Coll., on copyright, rights related to copyright and amending some laws (Copyright Act).

Prague, July 15, 2016

……
Signature

Acknowledgement

I would like to express my gratitude and appreciation to my supervisor Ing. Eduard Stach. This work would have never been finished without his patience and guidance. My thanks also belong to Ing. Lukáš Novotný, Ph.D. for his counsel regarding mechatronics and machine control. I would like to thank to my family for their support.

Anotace

Autor:	Tomáš Lazák
Název BP:	Aktivní řízení výšky škrtící mezery hydrostatické buňky
Rozsah práce:	80 str., 68 obr., 5 tab.
Školní rok vyhotovení	2016
Škola	ČVUT – Fakulta strojní
Ústav:	Ú12135 - Ústav výrobních strojů a zařízení
Vedoucí bakalářské práce:	Ing. Stach Eduard
Konzultant:	Ing. Lukáš Novotný, Ph.D.
Zadavatel:	ČVUT – FS
Využití:	Kompenzace geometrických chyb výrobních strojů
Klíčová slova:	Hydrostatická kapsa, Hydrostatická buňka, Hydrostatické vedení, Zpětnovazební řízení, Řízení polohy, Kompenzace
Anotace:	Tato práce se zabývá návrhem a experimentálním ověřením systému pro aktivní řízení výšky škrtící mezery hydrostatických kapes, které jsou součástí hydrostatického vedení. Společné řízení více hydrostatických kapes umožňuje kompenzování geometrických chyb nebo známých výrobních nepřesností obráběcích strojů. Na základě provedených experimentů lze uvést, že navržený systém je vhodný pro použití ve výrobních strojích, nicméně další výzkum by se měl zaměřit na dynamické chování systému.

Annotation:

Author:	Tomas Lazak
Title of bachelor dissertation:	Active control of hydrostatic pocket throttling gap height.
Extent:	80 p., 68 fig., 5 tab.
University:	CTU – Faculty of Mechanical Engineering
Department:	Ú12135 – Department of Production Machines and equipment
Supervisor:	Ing. Stach Eduard.
Consultant:	Ing. Lukáš Novotný, Ph.D.
Submitter of the Theme:	CTU – Faculty of Mechanical Engineering
Application	Compensation of geometrical errors of Machine tool.
Key words:	Hydrostatics cell, Hydrostatics guideway, Hydrostatic pocket, Hydrostatic pad, Feedback control system, Displacement control. Compensations
Annotation:	This thesis aims to develop and experimentally verify a system for active control of a hydrostatic cell throttling gap height. Hydrostatic cells are part of Hydrostatic guideway. Simultaneous control of several hydrostatic cells enable us to compensate geometrical errors and known manufacturing errors of machine tools. On the basis of conducted experiments can be concluded that proposed compensation principle is feasible for use in machine tool industry, nevertheless further research should address its dynamical behaviour.

Contents

List of used variables and units

a	HS pocket width	[m]
A	Effective area of hydrostatic (HS) pocket	[m^2]
b	HS pocket depth	[m]
d	HS pocket land length	[m]
h	Throttling gap height	[m]
h_0	Designed throttling gap height	[m]
h_r	Actual (measured) throttling gap height	[m]
Δh	Throttling gap height difference	[m]
I	Electric current	[A]
K_R	PM controller design constant	[-]
l	HS pocket land width	[m]
l_C	Capillary length	[m]
p	Pressure	[Pa]
p_p	Pump pressure	[Pa]
p_T	Pressure in pocket cavity	[Pa]
Δp	Pressure difference	[Pa]
Q	Fluid flow rate	[m^3s^{-1}]
Q_K	Fluid flow rate thru capillary	[m^3s^{-1}]
Q_0	Fluid flow rate thru PM controller for zero HS pocket pressure	[m^3s^{-1}]
Q_R	Fluid flow rate thru PM controller	[m^3s^{-1}]
Q_T	Fluid flow rate thru HS pocket	[m^3s^{-1}]
$Q_{K,T}$	Fluid flow rate thru capillary and HS pocket	[m^3s^{-1}]
r	Radius	[m]
r_c	Inner radius of capillary	[m]
r_p	Radius of inner pocket corner	[m]

R_K	Hydraulic resistance of capillary	[$kgs^{-1}m^{-4}$]
R_T	Hydraulic resistance of HS pocket	[$kgs^{-1}m^{-4}$]
t	Time	[s]
T_z	Transformation matrix for translation in z	[m]
T_{φ_x}	Transformation matrix for rotation around x axis	[-]
T_{φ_y}	Transformation matrix for rotation around y axis	[-]
u	Flow velocity	[ms^{-1}]
U	Voltage	[V]
V	Velocity	[ms^{-1}]
x, X	Coordinate in the direction of the flow	[m]
x_G	Point coordinate in direction of x axis in global coordinate system	[m]
X_G	Vector of point in global coordinate system	[m]
x_L	Point coordinate in direction of x axis in local coordinate system	[m]
X_L	Vector of point in local coordinates	[m]
y	Coordinate in the direction of gap height	[m]
y_G	Point coordinate in direction of y axis in global coordinate system	[m]
y_L	Point coordinate in direction of y axis in local coordinate system	[m]
z	Coordinate perpendicular to x and y	[m]
z_G	Point coordinate in direction of z axis in global coordinate system	[m]
z_L	Point coordinate in direction of z axis in local coordinate system	[m]
Δ	Throttling gap height error	[m]
μ	Dynamic viscosity	[$kgm^{-1}s^{-1}$]
υ	Kinematic viscosity	[m^2s^{-1}]
ρ	Fluid density	[kgm^{-3}]
φ_x	Angle of rotation around x axis	[rad]
φ_y	Angle of rotation around y axis	[rad]
ϕ	Angle	[rad]

1 Introduction

Hydrostatics (HS) guideways are machine tool components enabling a linear movement of machine parts. HS guideways closely relates with hydrostatics bearings that enables rotational movement. Difference is in the nature of movement, however, working principle is similar. In comparison with other guiding systems, hydrostatic (HS) guideways possess advantages such as, high precision, load capacity, stiffness, damping and low friction. Therefore they have been used in machine tools (MT) since seventies of 20th century. HS guideways have been used also in heavy and precise MT such as, lathes and horizontal machine tools.

Accuracy of machine tools is adversely affected by external and internal influences, e.g., thermal deformations, gravity, inertial force, cutting force. To diminish these influences, MT are being compensated by means of various compensation methods.

This thesis proposes a new method feasible for machine tool compensation that actively controls HS guideway. Actively controlled HS guideways consist of HS cells. These cells contain one part with HS pocket with a cavity and the second part a prism with guiding surface. Between the HS pocket and prism is a throttling gap. Each gap height of actively controlled HS guideways is independently controlled and thus a supported structure can be displaced in the direction perpendicular to HS guideway and also tilled. Consequently, it is possible to compensate geometrical errors of MT and manufacturing errors of MT. The proposed system conveniently makes use of HS guideways that are already implemented to the machine structure. This thesis demonstrates use of actively controlled HS guideways on example of a cutting tool position compensation. Analogically, actively controlled HS cells can be applied to different machines.

2 Thesis objectives

This thesis aims to design an actively controlled HS cell and a system for control of multiple HS cells and experimentally verify functionality of the designed system. Firstly, a research is carried out in order to investigate current technologies addressing HS guideways and their throttling gap height control systems that are not used only in machine tools. Based on the research, the most feasible system for HS cell control is selected and designed. The design includes mathematical description of problem, hydraulic circuit design and control system design. Subsequent development is focused on the control of multitude HS pockets in order to control the gap height and small rotation of supported structure (e.g. table or carriage). The system is set up and several experiments are conducted in order to proof its functionality. Measured data of throttling gap height and rotation around axes are evaluated and interpreted. The conclusion is recorded on final pages of this thesis.

3 State of the art

Hydrostatics (HS) guideways are machine tool components enabling a linear movement of machine parts. Typical HS guideway is shown in fig. 1. HS guideways closely relates with hydrostatics bearings that enables rotational movement. Difference is in the nature of movement, however, working principle is similar. Therefore, in the text of this thesis both terms occurs.

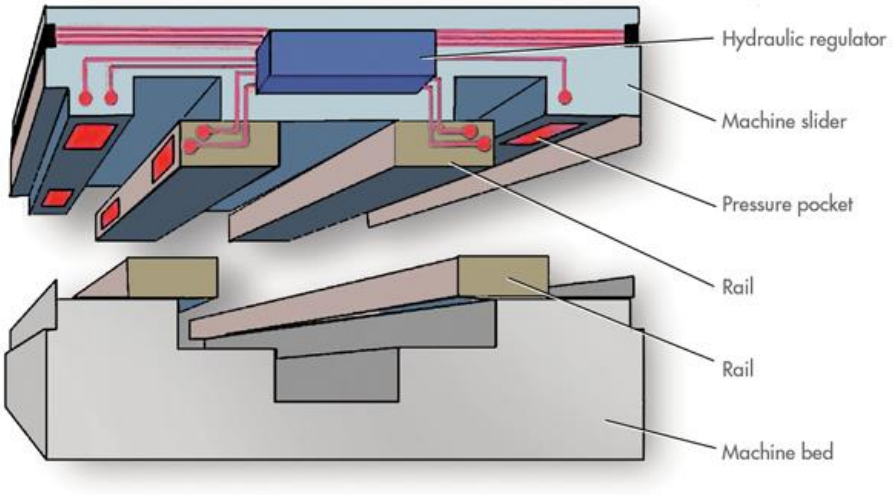

fig. 1: Example of HS guideway [1]

At the beginning of the thesis work a research addressing current technologies concerning HS guideways used not only in machine tools was made. Results of a research are listed below. Firstly, standard designs for (HS) guideways are described. Secondly, approaches with different kind of feedback are presented. Then systems with active control of throttling gap height are explained. Finally, described designs are compared and the best approach for further development is chosen.

For proper function of HS guideways, it is necessary that each HS pocket is supplied with hydraulic pressure oil independently. This ensures that in case of not equally distributed forces applied to structure, no HS pocket collide with rails. Different regulation systems addressing this problem are described in this section. [2]

HS guideways are being used in machine tools (MT) since 1970 because of their advantages over other guidance types. HS guideways meet requirements for high precision MT, hard turning MT, heavy MT such as lathes and horizontal boring machines, and machines for minute steps in positioning. HS guideways excels in high precision, damping, stiffness and low friction – no stick slip effect. They are practically wear free. Another benefit is error averaging ability. The

drawback is high operating cost, challenging manufacturing and possibly complicated design. [3], [4], [5] Another disadvantages are: [6]

- High accuracy of rails is required for lowering oil loses and preventing mechanical collisions.
- Current throttling gap height affect stiffness of HS guideways. Higher throttling gap prevents mechanical collision of pocket and guideway, however, simultaneously increases consumption if oil and decreases stiffness.
- Guideways and a machine structure warm as a consequence of throttling of high pressure oil. Thus thermal deformation adversely influences accuracy.

HS cell consists of HS pocket and guiding prism (rail). The hydrostatic pocket comprises a cavity and a land (fig. 2). Depending on the arrangement, HS guideway is open or closed. Open HS guideway is preloaded by gravitational force of a supported structure whereas closed HS guideway is preloaded by two opposed pads as shown in fig. 3. [2], [7], [4]

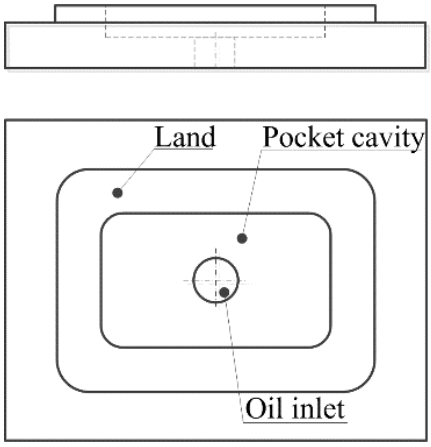

fig. 2: HS pocket

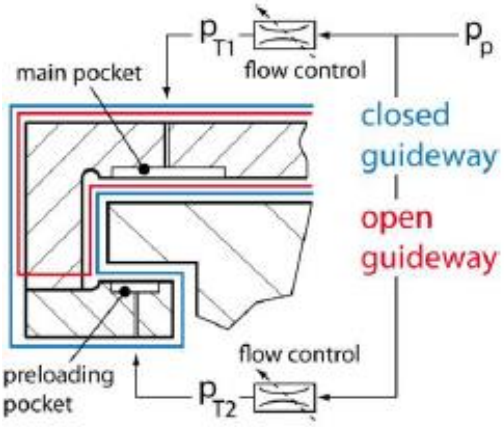

fig. 3: Open and closed HS guideway [4]

3.1 Standard flow regulators for hydrostatic guideways

This section address practices commonly used in industry to regulate oil flow rate to HS pockets. None of these methods enables active regulation of hydrostatic throttling gap height. [6]

3.1.1 Constant flow rate regulation

A constant oil flow rate thru each HS pocket is achieved by one pressure pump for each HS pocket or by a gear flow – divider. Such system has a high payload capacity because pressure in the pocket is limited just by maximal pump pressure. An advantage over other regulation methods is

lower energetic consumption since pressure in the system depends only on applied load. No extra hydraulic resistor is added into a hydraulic circuit. Required energy $E = p \cdot Q$ is lower in comparison with other regulation methods especially when the HS guideway is not fully loaded. The constant flow rate regulation is suitable for applications that require high stiffness or require small pocket size. The drawback is relatively high cost of flow dividers or pumps. It is used for both, open and closed guideways. Schematic is depicted in fig. 4. [8] [9] [10]

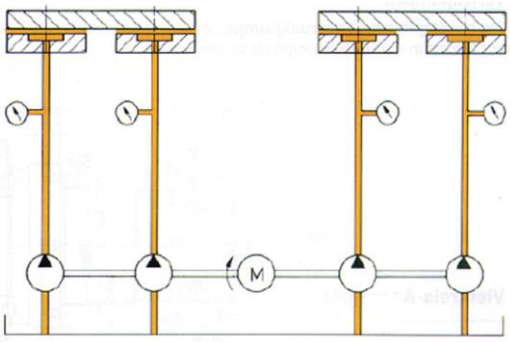

fig. 4: Constant flow rate regulation [10]

3.1.2 Constant flow resistance regulation

The most widely used approach for gap height control is using of constant hydraulic resistance such as a capillary tube or other narrow groove. The fundamental characteristics of capillaries is expressed by Hagen-Poiseuille's equation and is also shown in the fig. 5. [8]

$$\Delta p = \frac{8 \mu l_C Q}{\pi r_C^4} \qquad (1)$$

Where Δp means pressure drop along the capillary length, Q means oil flow rate, μ means dynamic viscosity, l_C means length of capillary and r_C means inner radius of capillary. Constant hydraulic resistance $(R = p/Q)$ denotes constant geometrical resistance, since viscosity is temperature dependent. [8]

Capilaries exhibit the ower load carring capacity and stiffness than constant flow rate regulation. Siffness can be improved by increasing capillary resistance, nevertheless the load carring capacity is consequently decreased. It is a cost-effective solution. [2]

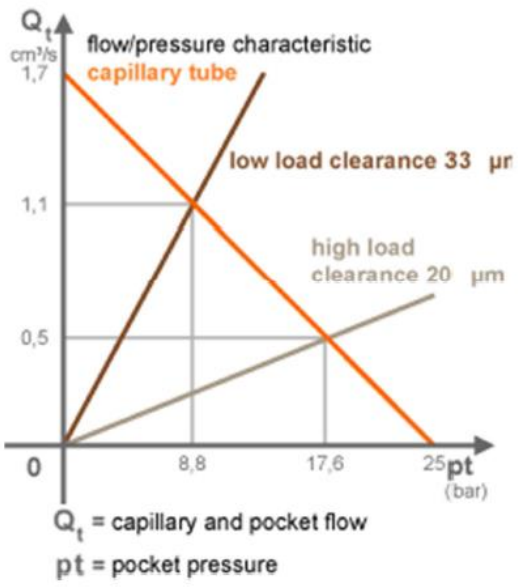

fig. 5: Capillary characteristic curve [10]

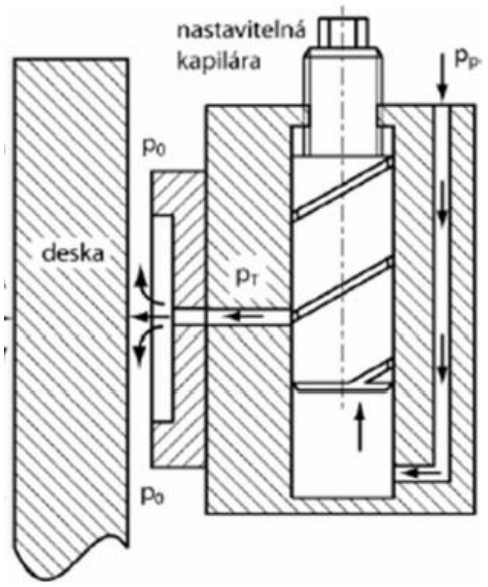

fig. 6: Device for adjustable capillary length [10]

A device for easier setting of capillary resistance is shown in fig. 6. The device has adjustable capillary length. [10]

3.2 Systems increasing stiffness of HS guideways

These systems improve stiffness by using different feedback principles. The systems are therefore more complex. Throttling gap height is set when systems are designed. Next sections states these systems.

3.2.1 Progressive regulation of oil flow

Currently prevailing progressive regulators of oil flow are PM controllers from Hyprostatic Schönfeld GmbH. [11] Therefore, its operating principle is demonstrated by PM controller example. The designation of PM controller stands for the "Progressiv Mengen (Progressive Quantities)" controller behaviour. The controller progressive characteristic curve is shown in fig. 7. When the pressure p_T in HS pocket rises the supplied oil flow is increased. Contrary, in case the pressure p_T in HS pocket declines the oil flow also decreases. As a result, a throttling gap height is changed less compared to capillary. Therefore, hydrostatic pocket has higher stiffness. [11]

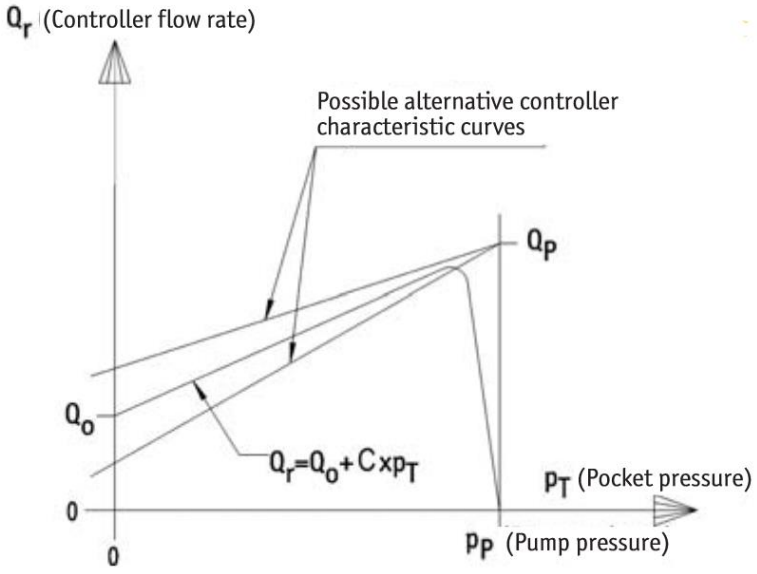

fig. 7: PM controller characteristic [11]

Advantages of PM regulator are listed below: [11]

- Practically wear free
- Excellent dynamic behaviour
- Self-ventilating designs are available
- Small space requirements, low weight
- Corrosion resistant
- Pump pressure can be utilized up to 90 %
- PM controller operates mechanically and don't require external power supply

fig. 8: PM controller in "series construction" [11]

The oil flow rate of the PM controller is described by:

$$Q_r(p_T) = Q_0 \times (1 + (K_r - 1) \times \frac{p_T}{p_P}) \quad (2)$$

where p_T means pocket pressure, p_P means pump pressure, Q_0 flow rate for $p_T = 0$, Q_r flow rate for pocket pressure p_T, Q_p means maximum flow rate and $K_r = Q_p/Q_0$. An impact of these parameters and parameters of HS pocket on a step response is discussed in [12]. PM controller consist of a fixed hydraulic resistance, a regulating hydraulic resistance and a membrane. Pressure difference at the membrane is induced by this two different hydraulic resistances. The pressure difference bends the membrane and consequently changes the regulating hydraulic resistance. For this reason, the oil flow rate is changed accordingly to pocket pressure. fig. 8 shows PM controller used in industry. Progressive controllers use pressure feedback to control constant throttling gap height. Once a PM controller is matched with HS cell it tends to keep constant throttling gap. Therefore, gap height cannot be set in real time.

3.2.2 Self-regulating systems

An approach to a bearing clearance compensation is presented by prof. Slocum and ZOLLERN GmbH. The clearance compensation relies on a preliminary throttling system and connection of two opposing hydrostatics pockets. Such system is referred to as a "Zollern bearing clearance compensator" [13], but similar systems may by presented under different names.

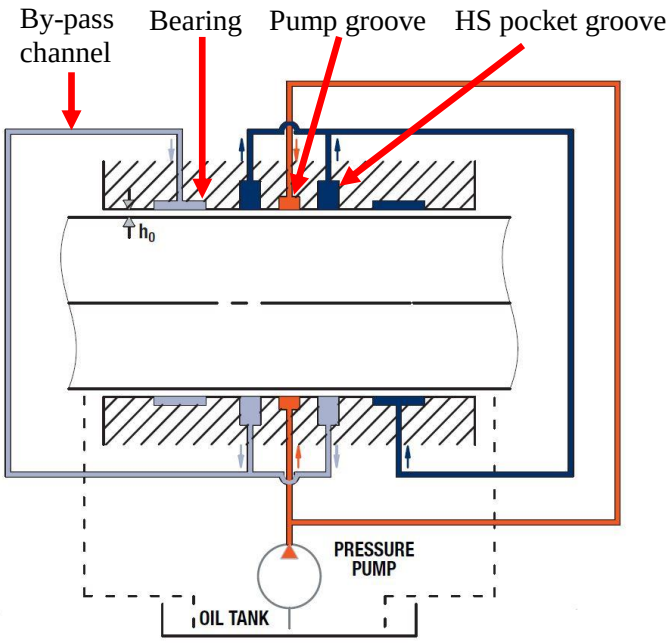

fig. 9: Hydrostatics pockets and principle of auto regulating system [13]

The self-regulating system operating principle is depicted in fig. 9, and its description follows. Several grooves are milled in the plateau of the hydrostatics pocket. First, a pump groove is located in the middle of the pocket. Second, pocket grooves are placed on both sides of the pump groove. An area between them performs as preliminary hydraulic resistance. A bearing groove is arranged around previously mentioned grooves. The bearing groove is connected with pocket grooves of the opposite side pocket by bypass channels. The second throttling gap is situated on the outer edge of bearing groove. Both throttling gaps have the same height and all HP are manufactured in one plateau. The pump groove links pressure pump with a pocket groves. The compressed oil flows from the pump groove to the pocket grooves and then through the bypass channel to the bearing grove of the opposite mounted bearing pocket. In the next step the oil flows through the second throttling gap out of HP. This provides a load capacity of a bearing. [13] [14]

In case a downward force is applied to a bearing shaft the shaft is displaced. This cause that a throttling gap height at bottom side of bearing decreases and a gap at the top side increases. Consequently, the oil flow from top pump grove to pocket groves rises. As a result, the flow through bypass channels to bottom bearing pocket increases. The pressure in the bottom pocket rises. Analogically, the oil flow to top bearing groove is reduced and pressure decreased. As a result, the displacement of the shaft is eliminated. Thus, the stiffness of bearing is higher than in case of using capillaries. [13]

Application of self-regulating systems on HS guideways is described in [15] and [16]. The self-regulating system is also discussed in [17] and [18]. The self-regulating system applied for a hydrostatic rotary bearing with angled surface is described in [19] and [20]. These examples demonstrate similar principle applied to different arrangement of HS bearing/guideway.

3.3 Systems with active control of throttling gap height

Systems with active control of throttling gap height primarily increases stiffness and accuracy of HS guideways. Such improvement is attained by using of different feedback principles. Set gap height (desired gap height) is provided by an external signal. The systems are therefore more complex.

3.3.1 Servostatic guideways

Servostatic guideways are HS guideways equipped with extra components realizing a mechanical position feedback that primarily increases stiffness of guideways. These extra components consist of a mechanical reference structure (ruler) and hydrostatics control blocks. Design of hydrostatics

control blocks enables low friction and minimal pressure oil losses. The position feedback reduces machine inaccuracy caused by for example thermal dilatations, cutting force deformations and inertial forces of moving parts. [6] [21]

Description of servostatic guideways

fig. 10 shows a scheme of the hydrostatic block and the reference structure. The hydrostatic block consist of two floating hydrostatic pockets, which are in balance, and a miniature hydraulic control valve. This block is mounted to the supported structure and moves with it. A spool of control valve copies the shape of the reference structure and opens or closes passage of oil to HS pockets and thus controls oil flow rate.

HS pocket has a special design that is referred to as a floating hydrostatic pockets. HS pocket is manufactured in HS pocket slide that is located in cavity of the hydraulic control block. The HS pocket slide moves as the cavity is filled with oil and thus height is controlled. The narrow throttling gap is between HS pocket and the guiding prism. Moreover, another groove is manufactured around the outer side of HS pocket. This groove collets the oil leakage and transport it back to tank. A groove outer edge is equipped with a sealing. Since the oil flow rate is low a small pump is needed. Another advantage of low oil flow rate is lower heat generated by throttling. [6] [21]

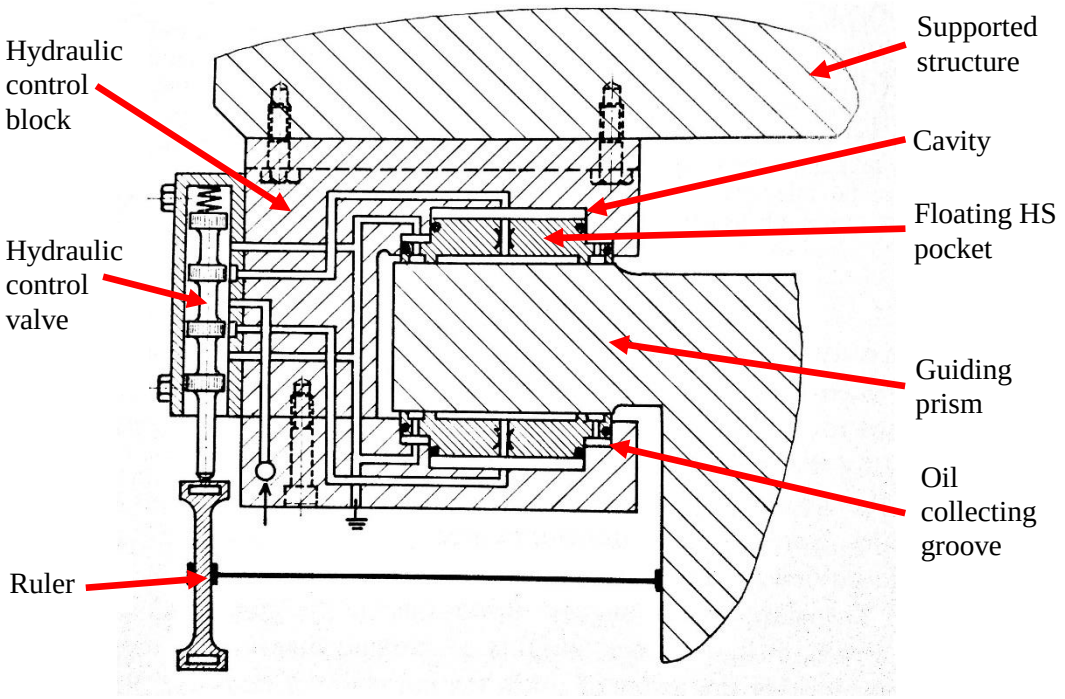

fig. 10: Servostatics guideway [6]

The system is equipped with two mechanical structures. The first supporting structure carries all loads. The second structure serves as the reference for measuring throttling gap height. Therefore, even if the support structure is inaccurate or deformed the position of working table is exact. Servostatic guideways usually requires using of six servostatic blocks per each axis of machine tool. Such axis is depicted in fig. 11. [6] [21]

Operating principle

Let's assume that a working table is loaded by vertical force pointing downwards. Then, the table is displaced in the direction of the force. Consequently, the spool of control valve is shifted, the oil pressure in the top pocket rises. Analogically, the oil pressure in bottom pocket decreases. As a result, pressure difference induces a counterforce and moves the table to its original position. [6] [21]

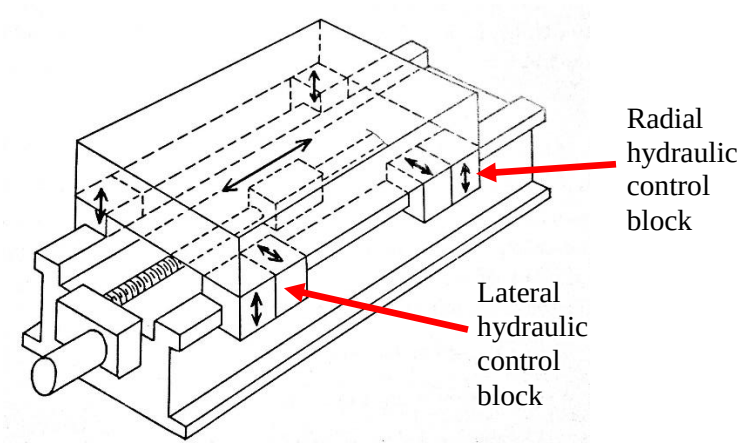

fig. 11: Six hydrostatic blocks mounted to working table [6]

Servostatic guideways have some disadvantages, such as a need for measuring structure and difficulties concerning cleanness of measuring surfaces. Servostatic guideways enable the linear axis to hold constant throttling gap height and thus increase stiffness significantly and also to follow programed path (gap height). However, modification of programed path is challenging.

3.3.2 Actively controlled capillaries (ACC)

Actively controlled capillaries are suitable for high-precision motion error compensation of a hydrostatic feed table. It is possible to compensate motion errors in five degrees of freedom (DOF). Accuracy is equal to the currently reachable measuring accuracy. Accuracy is in the order of hundredths of a micrometers. Compensation of five DOF is realized by using five ACC. Micro step response test is carried out to adjust gains of the ACC. For improving measurement accuracy, a combination of different measuring techniques is used. [22] [23]

Operating principle

ACC consists of three main parts, top and bottom body and a membrane (leaf spring). The bottom body is housing for a piezoelectric actuator. The top body serves as oil inlet and outlet. An annular capillary is formed by the top body inlet and the membrane. Deformation of membrane induced by a piezoelectric actuator changes clearance and thus resistance of the capillary. Therefore, the oil flow is changed. fig. 12 shows schematics of ACC. [22]

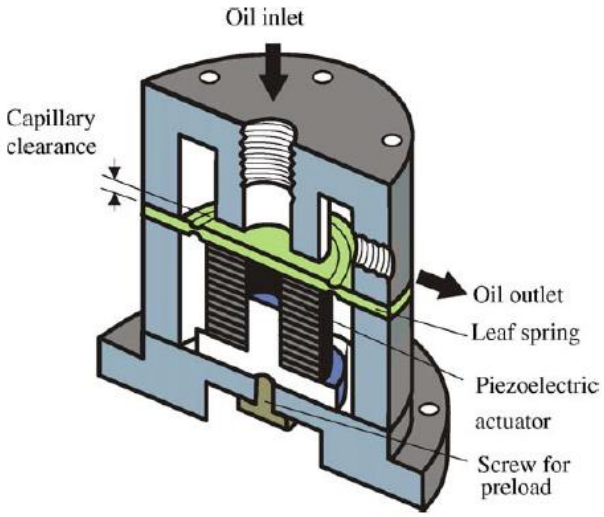

fig. 12: Schematics of actively controlled capillary [22]

fig. 13 depicts an operating principle of hydrostatics system equipped with two ACC. ACC control oil flow thru top pockets and capillaries regulates oil flow thru bottom pockets. HS guideway is the closed type. The right ACC is depicted with the bended membrane. Therefore, throttling gap of ACC is reduced and oil flow is lower than in case of the second ACC. [22] [23]

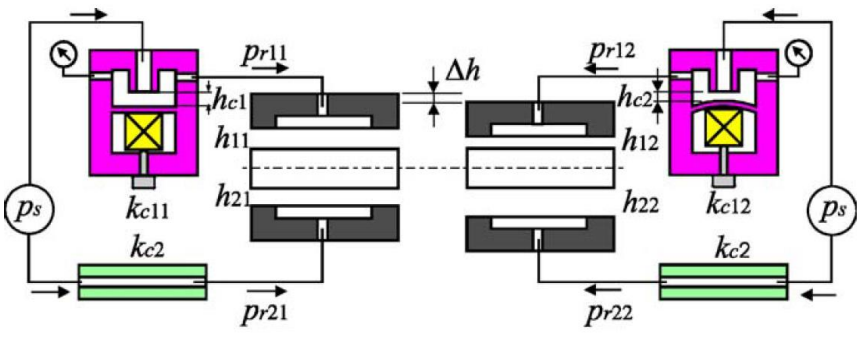

fig. 13: Operating principle of throttling gap height regulation [22]

3.3.3 Active hydrostatic bearing with magnetorheological fluid

Compared to standard HS bearings, a bearing using a magnetorheological (MR) fluid is equipped with coil that induces magnetic field. This field affects viscosity of MR fluid. The higher the intensity of the magnetic field the higher the viscosity is. This behaviour occurs until magnetic saturation. Then increasing of magnetic field have no effect. [24], [25] The consequence of magnetic field applied to MR fluid is shown in fig. 14. Magnetic particles that are carried in the oil create chains and increase the viscosity.

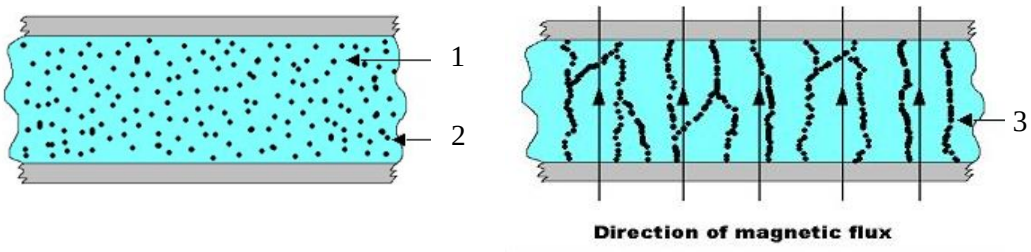

fig. 14: MR fluid behaviour (carrier oil (1), magnetic particles (2), chains of particles (3)) [26]

The load capacity of the bearing is induced by hydrostatic pressure supplied by a pump. In case that load applied to bearing varies, the height of throttling gap changes. Common practise is to compensate this changes by regulation of oil flow rate by external devices as mentioned above. In this case, the viscosity of oil is controlled and thus the throttling gap is stabilized. Major advantage is that viscosity is controlled directly in the pocket and therefore reaction time for load change is faster. [27], [28] MR fluid also enhances damping capacity of HS guideway to some extent. [29]

Characteristic of hydrostatics pocket gap height in relation to applied force for different intensities of magnetic field is in fig. 15. When a load of 100 N is applied, the throttling gap height equals 310 μm (point A). As the applied load increases to 160 N the gap height decreases. In case that magnetic increases the gap height remains constant (point B) [24].

MR fluid can also be used in hydrodynamics plain bearings. Permanent magnets keep lubricant inside the glide and thus significantly reduce lubricant loses. [30]

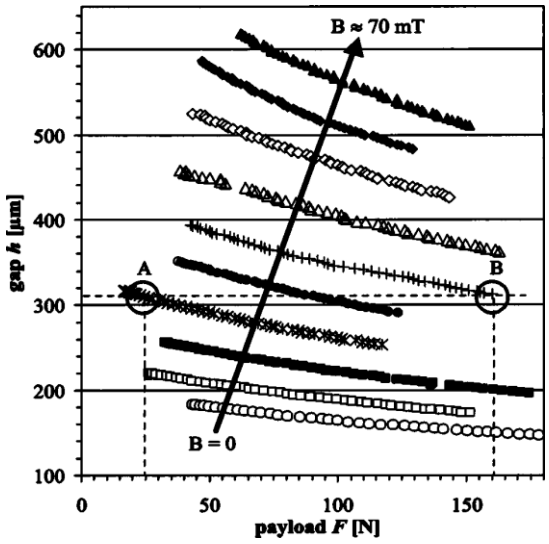

fig. 15: Change of bearing gap with the payload for different magnetic fields [24]

Advantage of MR HS guideways is short response time for load change. As a disadvantage appears viscosity thermal stability of MR fluid and its high price. MR fluid should not be contaminated with impurities such as cutting fluid and chips. Therefore proper covers are needed. Studied papers address problem of keeping constant throttling gap height. However, application of MR fluid HS guideway to rotate with working table was not found. However, described principle theoretically enables rotating with working table.

3.3.4 System with electronics closed loop system

Infinite stiffness water hydrostatic thrust bearing is presented in [31]. Article describes an electronic closed loop system for displacement control of water hydrostatic thrust bearing. Conventional constant flow restrictors and one proportional flow control valve are used to control thrust bearing displacement. This technology is suitable for high-precision machine tools. The article address problem of HS bearings with constant pressure regulation where the displacement of the bearing is proportional to its load. This technology increases stiffness of the thrust bearing. Water is used because higher thermal stability since water has higher conductivity and lower viscosity than oil. Vertical position of rotary table is controlled by using constant restrictors and one proportional valve as shown in fig. 16. Comparison of conventional design of flow restrictor for multiple HS cells and design with additional flow control valve is in fig. 17. [31]

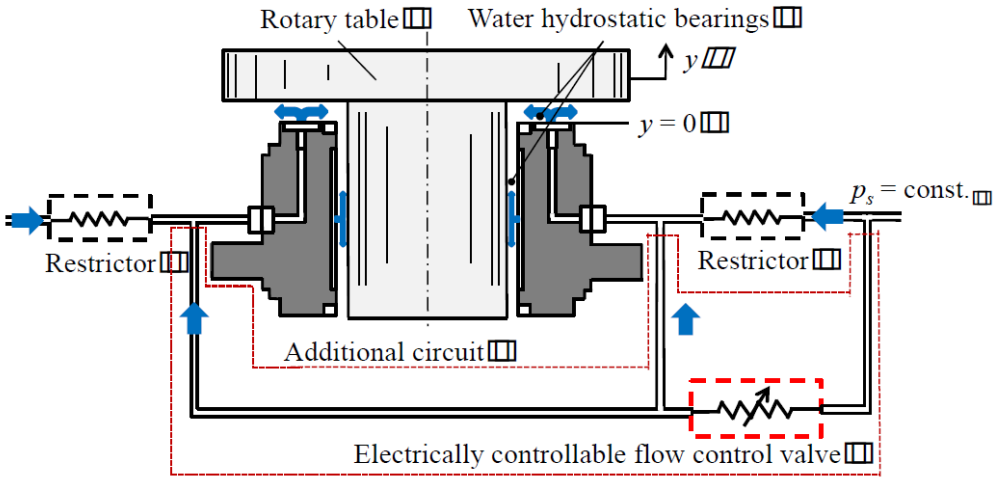

fig. 16: Water HS bearing with constant flow restrictors and flow rate control valve [31]

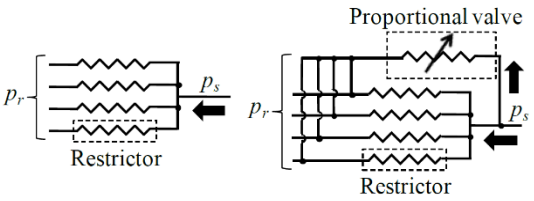

fig. 17: Conventional flow restrictor for multiple HS pockets (left), advanced design with flow control valve (right) [31]

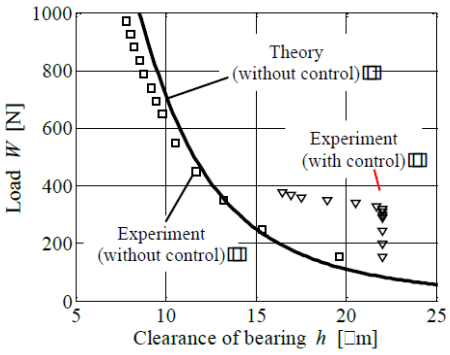

fig. 18: Infinite steady state stiffness when a controller is turned on [31]

When a load of working table rises proportional valve opens and increases pressure in HS pocket and thus eliminates displacement. fig. 18 displays results of experiment where load of HS bearing was increased by steps. As can be seen, steady state stiffness is infinite for certain range of applied load. Another experiment shown in fig. 19 describes behaviour of the system when step response is measured. Step size is 0,2 μm. Settling time equals approximately 6 s. A response to a force pulse is illustrated in fig. 20. When a load is applied an instant displacement equals 1 μm. [31]

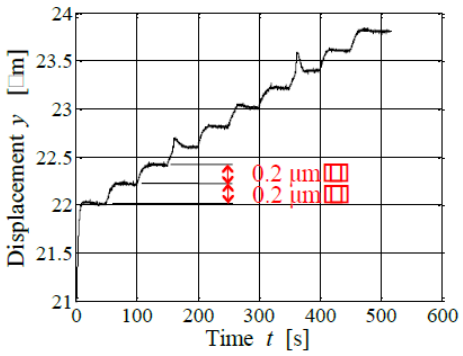

fig. 19: Step response test [31]

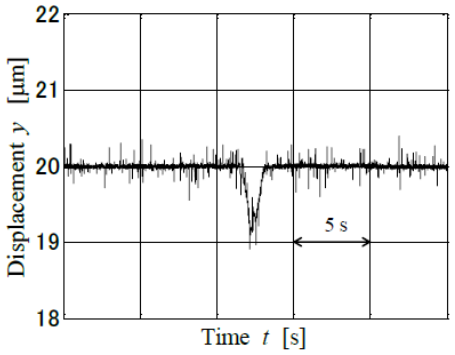

fig. 20: A response of system to force pulse [31]

From an experiment can be concluded that the system with constant restrictors and one proportional flow control valve in position feedback can increase stiffness. In steady state the stiffness is infinite. It is also possible to index the displacement by $0{,}2\ \mu m$ steps. An impact stiffness is sufficient. [31] As a result, similar system can be used to control position and rotation of working table equipped with HS guideways. Another system with electronical feedback is described in [32].

3.4 HS control systems research conclusion

Results of research are concluded in a tab. 1. Three major criteria were considered. First criterion is possibility of controller to increase the stiffness of HS guideways. Second criterion is possibility to compensate errors of HS guideways. The third criterion is possibility to actively, simultaneously and independently control several HS pocket gap heights in order to rotate with supported structure as shown for example in fig. 64 and fig. 65.

As can be seen, all methods enable us to increase the stiffness of HS guideway. Self-regulating systems and progressive regulators cannot compensate HS guideway rail inaccuracy since this systems keep constant gap height. Thus, working table follows inaccuracy of guiding prism when moving. Other systems can be equipped with additional measuring system to keep a movement of working table straight. The gap height is varying along the length of rail accordingly to inaccuracy of rail but the working table sustain a same height level. Self-regulating systems and progressive regulators cannot rotate with working table because it is not possible to actively control them by external signal. Servostatic guideway can rotate with the working table but programming of movement is very challenging since servostatic guideways use mechanical feedback. Therefore, any change in the program presents a complicated procedure. Other systems can theoretically rotate with the table, however, research on this topic were not found.

tab. 1: Comparison of different regulating systems for HS guideways

	Increased HS guideway stiffness	HG guideway error compensation	Active, simultaneous, independent control of several HS pockets
Self-regulating systems	yes	no	no
Progressive regulators	yes	no	no
Servostatic guideways	yes	yes	challenging
HS guideway with MR fluid	yes	yes	possible
Actively controlled capillaries	yes	yes	possible
Electronic closed loop systems	yes	yes	yes

HS guideway with MR fluid is characterized by very short response time. Nevertheless, MR fluid is rather expensive and also sensitive for contamination. This represents a limit for application in MT. Actively controlled capillaries control oil flow rate very precisely and have sufficient response time. They are suitable for precise applications. Disadvantage is a need for a special low controller. Electronic closed loop systems contain measuring device to measure gap height, proportional valve to control oil flow and control system. Response time is sufficient and an advantage is using of standardised parts. Therefore electronic closed loop systems are further elaborated.

3.5 Additional information addressing hydrostatics

More information relating to the topics is available in following patents. Patents concerning PM regulator describe various designs of PM controller:

- DE 35 33 037 C1 (invalid, published in 1986), Robert Schoenfeld (DE)
- DE19645535 (C2) (valid from 1986), Robert Schoenfeld (DE)
- EP1007861 (B1) (2002), Robert Schoenfeld (DE)

Following patents addresses hydrostatic screws.

- EP 0429155 A1(valid from 1991), NIPPON TELEGRAPH & TELEPHONE CORP. (JP)
- EP 0736700 A2 (valid from 1996), TOYODA MACHINE WORKS LTD (JP)
- WO 2011135247 A1 (valid from 2011), A.R.G. CONSEILS (FR)

3.6 Example of possible application for actively controlled HS cells

The following chapter describes possible application of actively controlled HS cell on an example of a horizontal milling machine. Horizontal milling machines are adversely affected by external and internal influences, which induce machine tool structural deformations and thus decrease accuracy of the manufacturing process. Therefore, a compensation of cutting tool position is required in order to maintain manufacturing accuracy. Known compensation methods are described and a method using the actively controlled HS guideway is proposed.

3.6.1 Systems for ram deflection compensation for horizontal milling machines

A patent research addressing ram displacement compensation systems for horizontal milling machines was carried out. [33] Compensation systems were divided in to the five groups accordingly to compensation principle. A list of patents is a part of an annex.

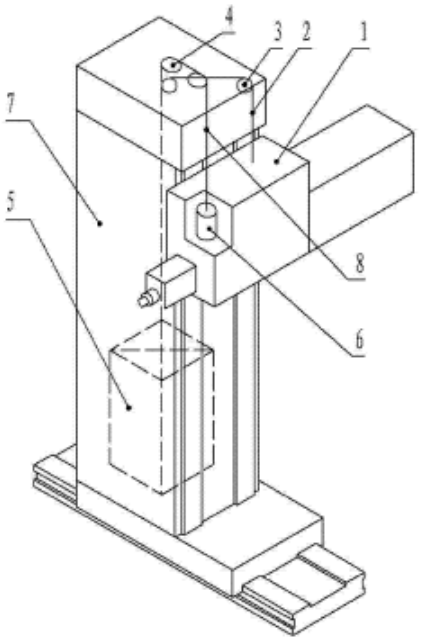

fig. 21: Counter-balance compensation system [33]

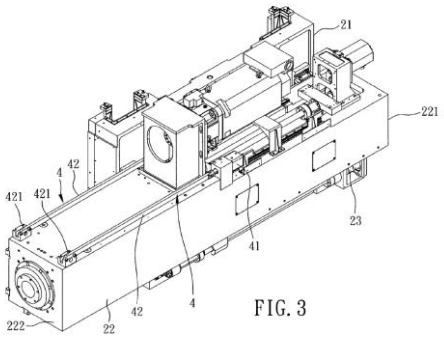

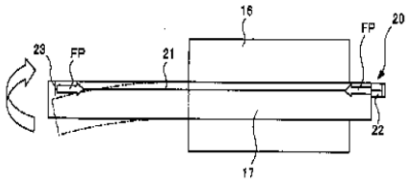

fig. 22: System for compensation that strengthen the ram [33]

First group is represented by counter-balance systems that are shown in fig. 21. They serve to counter balance mass of the ram in various positions. Ram and/or slider is hanging on ropes/chains and is connected to counter balance mass or counter balance hydraulic piston. The slider and hydraulic piston are connected by the system of pulleys. Counter balance mass is located in a column. Counter-balance systems enable a ram to be freely extended and compensate a shift of its centre of gravity. It is achieved by controlling length of ropes and thus adjusting forces in ropes. As a result, a ram is balanced in all positions and tilting of ram or slider is compensated. A number of systems hangs a ram in its centre of gravity. Consequently, a ram is bent to the same extent in all extension positions. In such case, height displacement is compensated. However, rotation at the end of ram is not compensated. More complex systems can rotate with a ram in way that the rotation of the ram end is also compensated. [33]

Second group compensation systems strengthen a ram and thus compensate cutting tool position. Schematics of the system is depicted in fig. 22. When a ram is extended it bends and its upper side extends due to a tensile stress. Compensation systems contain pull rods in upper part of a ram. A force applied to pull rod shorten the upper side of a ram and thus compensate its bending. Nevertheless, the disadvantage is shortening of the whole ram and also its deformation in case of unsymmetrical ram construction. Advanced methods compensate this effect by adding push rods in bottom part of the ram. This method compensate only bending of a ram. It does not compensate rotation of ram and slider. [33]

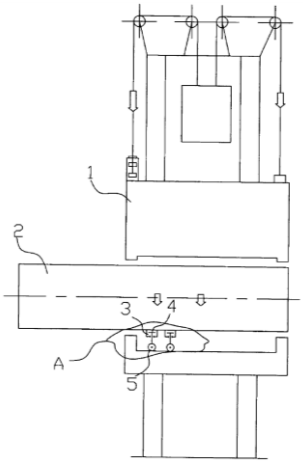

fig. 23: Compensation by ram rotation performed by linear hydro motor [33]

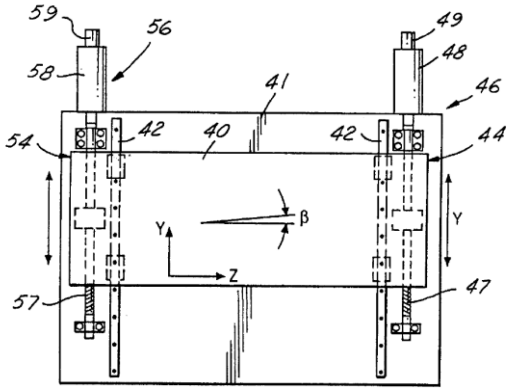

fig. 24: Compensation by slider rotation performed by two ball screws [33]

Third group does not compensate bending of the ram but its consequence. It is cutting tool displacement caused by rotation of the ram. When the ram is rotated, it does not change the extent of its bending but cutting tool position is shifted. Rotating can be achieved by linear hydro motor

or by elastic deformation of elements caring carriages of linear guideway. Deformation is performed by actuator. Ram rotation performed by linear hydro motor is illustrated in fig. 23. [33]

Next group systems rotate with the slide that is carrying the ram. The ram bending is not compensated but cutting tool position is compensated. The slider is equipped with two ball screws as can be seen in fig. 24. When both screws rotate the same angle a height of slider is changed. In case that the angle of rotation is different the system is pre-stressed and slide is rotating to some extent. Proper slide rotation compensate cutting tool position. [33]

Last group addresses compensation by means of hydrostatic guideway. It is equipped with special HS pockets with controllable oil pressure. As a result, throttling gap height can be controlled. These pockets are located in front bottom and rear top part of the slide. Pressure is controlled by pressure relief valve and its change rotates with the ram. [33]

The horizontal milling machine cutting tool displacement is obtained by two basis approaches. Firs approach measure the cutting tool displacement when MT is equipped with different equipment by means of a number of methods. Measured data are analysed and saved to MT control system. A disadvantage is that measured values can differ in time when MT is wearing off and when different equipment is used. Second approach includes methods for real time measuring of cutting tool deflection. Mostly, optical measuring methods are utilized. Measured values are then read by control system. [33]

3.6.2 Example of application of actively controlled HS cells

In the fig. 25 is shown a horizontal milling machine. It consists of a ram, slide, column, bed and a table. Y axis is equipped with HS guideway. It contain four HS pockets and two prisms. Only HS pockets needed for this application example are shown.

When a ram is extended, it bends because of gravity and a position of cutting tool is shifted. In order to compensate the shift, a ram is rotated as depicted by two arrows. The rotation is performed by the HS guideway.

Detail A shows a detail of one HS cell. Throttling gap is located between vertical prism and HS pocket. During normal operation, the gap height remains almost constant as described in chapters 3.1 and 3.2. However, through a control of all four HS pocket gap heights it is possible to rotate with slide and consequently with a ram. Specifically, top right and left bottom pocket gap height is increased and the gap height of two remaining pocket is decreased. As a result, ram is rotating.

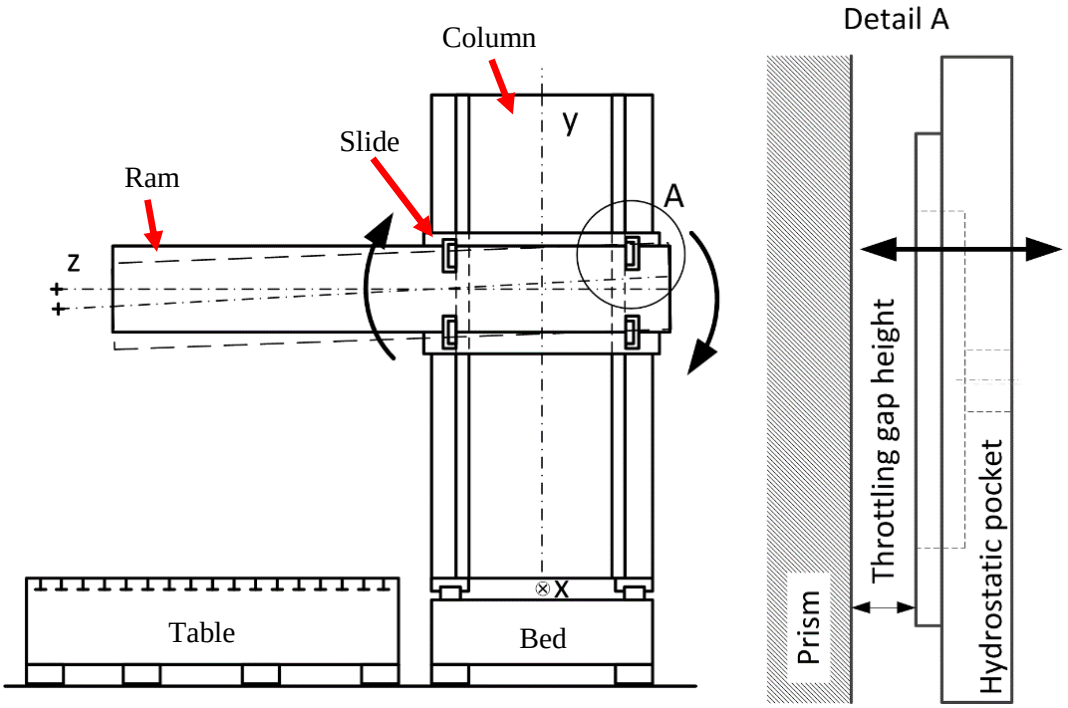

fig. 25: Horizontal milling machine – cutting tool position compensation

Advantage in comparison with other compensation method is that no extra, expensive parts are required in machine tool structure since HS guideway is already part of the machine. Moreover, HS guideways are compact.

4 Hydrostatic cell gap height control

As mentioned above, HS cell consists of a HS pocket and a rail (prism). HS pocket comprise of a cavity and a land. Between the HS pocket and the rail is located a throttling gap height. The gap height is varying accordingly to working conditions. In order to investigate an impact of different influences on throttling gap height a study was carried out. The hydraulic circuit and a control system is designed based on a results of the study.

4.1 Mathematical description of hydrostatic cell

HS pockets usually have a shape of rectangle with rounded corners as can be seen in fig. 26. For purpose of calculation the land is divided into a rectangular and a circular areas. The rectangular areas are analysed by a Cartesian form of Navier-Stokes equation. Four circular areas form full annulus and are analysed by a polar form of Navier-Stokes equation. Rectangular parts are solved first. [16] Tilting of HS pocket is neglected.

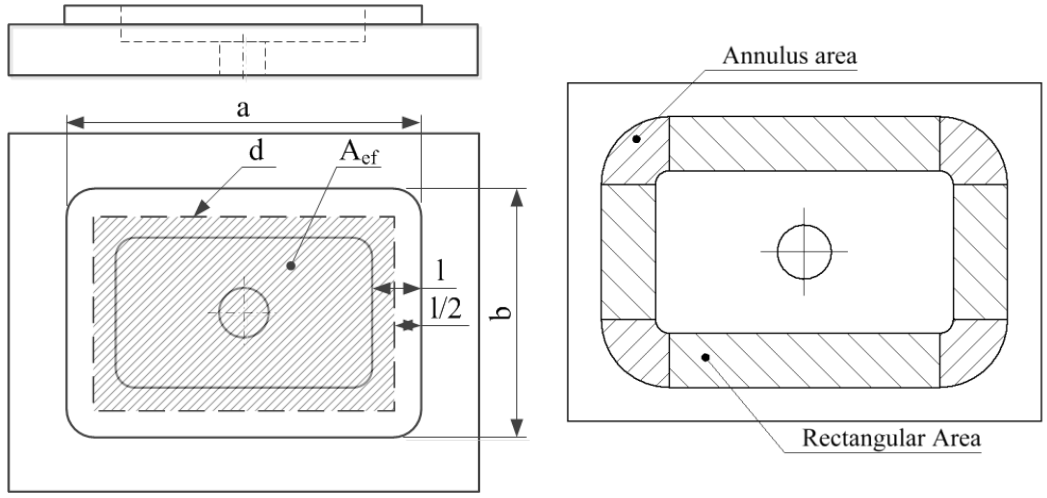

fig. 26: HS pocket dimensions (left) and HS pocket land areas (right)

It is assumed that flow thru throttling gap is non-turbulent and steady. Fluid is incompressible. Velocity profile is considered laminar since the ratio of throttling gap height to land circumference is minute. Then we can assume fully developed velocity profile and Navier-Stokes equation has a form [16]:

$$\frac{1}{\rho}\frac{\partial p}{\partial X} = \upsilon \frac{\partial^2 u}{\partial y^2} \qquad (3)$$

Where ∂p⁄∂X means pressure gradient in the direction of flow and (∂^2 u)⁄(∂y^2) denotes fluid velocity second derivative u with respect to vertical position in the throttling gap. [16]

It is assumed that HS pocket does not move. Therefore fluid velocity at pocket-fluid interface and rail-fluid inerface equals 0. That provides boundary conditions $u(0) = 0$ and $u(h) = 0$. After double integration a velocity profile is obtained [16]:

$$u = \frac{1}{2\rho v}\frac{\partial p}{\partial X}(y^2 - yh) \qquad (4)$$

An inspection of the equation (4) clarifies that the velocity profile is parabolic. In case that the HS pocket moves another term $V\,{}^{y}/_{h}$ is superinposed to parabolic profile. V denotes relative velocity of the pocket and the rail. [16]

Knowing the velocity profile, a flow rate can be determinated. A dynamic viscosity μ $[kgm^{-1}s^{-1}]$ is computed as $\mu = \rho v$ where ρ denotes fluid density and v $[m^2s^{-1}]$ a kinematic viscosity. Flow rate is obtaind by integration of the velocity ovear an area A. Depth d is a length of all rectangular areas of the land. Depth d is approximatelly depicted in fig. 26 and is computed by $d = 2\left(a + b - 4\left(l + r_p\right)\right)$. Annulus areas are excluded. Flow rate is [16]:

$$Q = \int u dA = \frac{1}{2\mu}\frac{\partial p}{\partial X}\int_0^d\int_0^h (y^2 - yh)dydz = -\frac{dh^3}{12\mu}\frac{\partial p}{\partial X} \qquad (5)$$

A pressure is decreasing linearly over the land widht x from pocket pressure p_p to zero atmospheric pressure. [16]

$$\int_{p_p}^{0} dp = \frac{-12\mu Q}{dh^3}\int_0^l dx \qquad (6)$$

After the integration across the land [16]:

$$p_p = \frac{12\mu l Q}{dh^3} \qquad (7)$$

This yields in [16]:

$$h = \sqrt[3]{\frac{12l\mu}{dp_p}Q} \qquad (8)$$

The throttling gap height of rectangular areas is a function of pocket shape (its dimensions), fluid flow rate, fluid viscosity and pocket pressure. [16]

The impact of rounded corners to pocket characteristic is studied in the next section. Four corners form a full annulus. Therefore calculating with polar form of Navier-Stokes equation is beneficial. It is assumed that flow thru throttling gap is non-turbulent and steady. Fluid is incompressible. Velocity profile is considered laminar since the ratio of throttling gap height to land circumference is minute. Then we can assume fully developed velocity profile and Navier-Stokes equation has a form [16]:

$$\frac{1}{\mu}\frac{\partial p}{\partial r} = \frac{1}{r}\frac{\partial}{\partial r}\left(r\frac{\partial u}{\partial r}\right) + \frac{\partial^2 u}{\partial z^2} - \frac{u}{r^2} \qquad (9)$$

Radius is much greater than the gap height. This yields in [16]:

$$\frac{1}{\mu}\frac{\partial p}{\partial r} = \frac{\partial^2 u}{\partial z^2} \qquad (10)$$

Again, we assume that HS pocket and the guiding prism (rail) does not move. That provides boundary conditions $u(0) = 0$ and $u(h) = 0$. A velocity profile is then derived as [16]:

$$u = \frac{1}{2\mu}\frac{\partial p}{\partial r}(z^2 - zh) \qquad (11)$$

Flow rate is then [16]:

$$Q = \int u dA = \frac{1}{2\mu}\frac{\partial p}{\partial r}\int_0^{2\pi}\int_0^h (z^2 - zh) dz d\phi = \frac{-\pi h^3 r}{6\mu}\frac{\partial p}{\partial r} \qquad (12)$$

Pressure is decreasing along the width of land [16]:

$$\int_{p_p}^{0} dp = \frac{6\mu Q}{\pi h^3}\int_{r_p}^{r_p+l}\frac{1}{r}dr \qquad (13)$$

Then pressure equals [16]:

$$p_p = \frac{6\mu Q \ln\left(\frac{r_p + l}{r_p}\right)}{\pi h^3} \qquad (14)$$

From this yields throttling gap height [16]:

$$h = \sqrt[3]{\frac{6\mu Q \log_e\left(\frac{r_p + l}{r_p}\right)}{\pi p_p}} \qquad (15)$$

Inspection of equations (8) and (15) follows and recommendations for gap height control are made. The throttling gap height depends on pocket dimensions, fluid viscosity, flow rate and pocket pressure. Pocket dimensions can be affected only during design phase. Therefore, controlling of a pocket size is not suitable for active HS cell control. An oil viscosity is temperature dependent. This dependency is highly nonlinear. Quick and precise oil temperature control is challenging since oil has thermal capacity and thus temperature change requires time. When the oil is passing through the throttling gap a heat is generated and oil temperature is changed undesirably. As a result, oil temperature control by its heating and cooling is challenging and probably ineffective. Different approach to control oil viscosity is to use magnetorheological (MR) fluid. Disadvantages of MR fluid were discussed in previous chapter. Therefore, oil viscosity control is not further elaborated in this thesis. The pocket pressure is next parameter in equation. It is a function of pocket load and behaves as a disturbance variable. The last parameter suitable to control the throttling gap height is flow rate. Flow rate is relatively easily controlled by valves. Regulation of pockets flow rate seems feasible and therefore is further studied.

4.2 Hydraulic circuit

For purpose of control and hydraulic system, a hydraulic circuit was designed. The hydraulic circuit serves for throttling gap height controling. As shown in previous text, the gap height is controlled thru flow rate control. In the first stage a proportional valve PV_2 was used as shown in fig. 27. Unfortunately, as experiments indicate this arrangement tends to be unstable. It is challenging to set values for PI controller and even with slow response regulation setting a regulation gets unstable. Possible reason is nonlinear behaviour of HS cell (8), (15).

A problem with stability is solved by using a capillary and the proportional valve that are connected in parallel (fig. 28). The flow rate thru the capillary C_1 establishes a default minimum gap height. As a result, a control range is decreased. Such arrangement improves stability of gap height control. The proportional valve PV_2 bypasses the capillary. This valve increases flow rate thru HS pocket and thus gap height rises above minimum gap height. The designation of valve is SR1P2-A2. This valve is not initially designed to control flow rate but pressure. Nevertheless, flow rate and pressure are mutually dependant and when used in closed loop, flow rate can be

controlled. The flow rate of the proportional valve depends on a poppet position and a pressure difference. The pressure difference is given by a load of HS pocket and pump pressure. Then the poppet position is indirectly controlled by a signal from the PI controller.

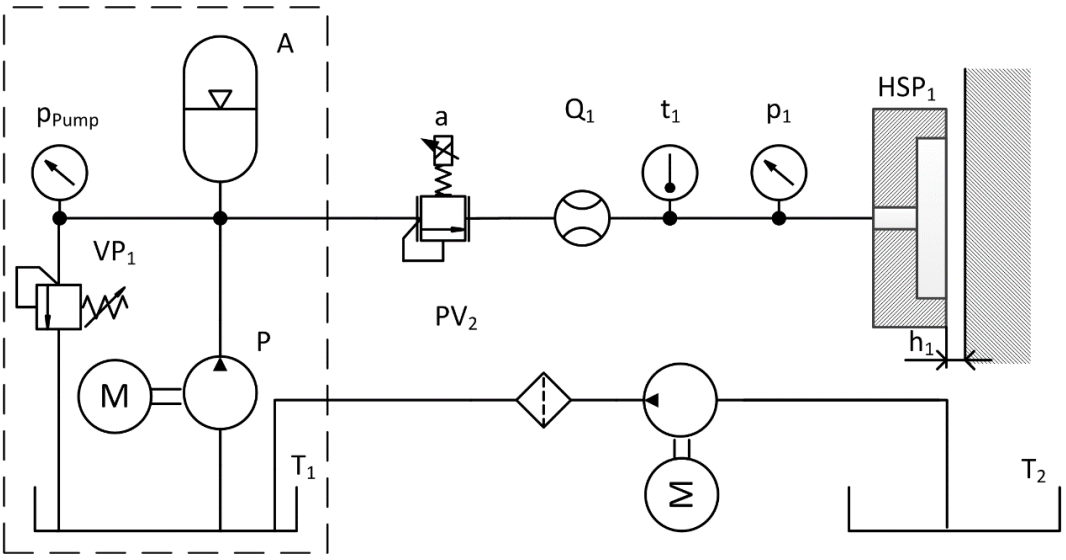

fig. 27: Hydraulic circuit for gap height control

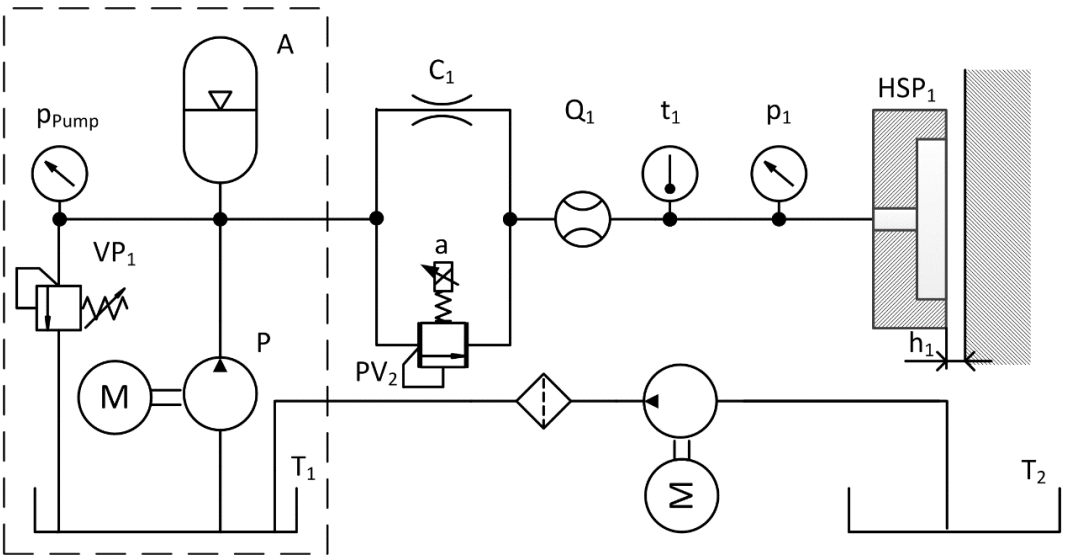

fig. 28: Hydraulic circuit for gap height control with capillary bypassing proportional valve

A valve VP1 sets pump pressure. Moreover, the circuit is equipped with pocket pressure gauge, thermometer PT100 and oval wheel flow meter. A hydraulic accumulator A provides extra flow when needed. An oil leaking from HS cell is collected into a drainpipe and then to the second tank T_2. Afterwards, the oil is pumped through a filter to main tank T_1.

4.2.1 Estimating of capillary length

In order to verify described hydraulic circuit and conduct experiments a capillary dimensions need to be estimated. The capillary is a flow restrictor and as such it is designed for specific HS cell. Testing apparatus for the experiment is a feed drive axis with HS guideway. Therefore, dimensions of HS cells are given. A capillary radius is chosen from available dimensions. HS pocket is loaded by 1800 N. Mentioned constants are written in tab. 2. Meaning of constants is clear from fig. 26.

tab. 2: HS cell and capillary dimensions

a	b	l	d	h_0	pp	F	A_{ef}	r_c
mm	mm	mm	mm	mm	bar	N	mm^2	mm
40	40	8	128	0,05	50	1800	1024	0,35

A length of the capillary must be computed to set initial throttling gap height to 50 μm. Calculations include impact of capillary resistance and a HS cell resistance. Based on (7) HS pocket resistance is expressed as (16).

$$R_T = \frac{p_T - 0}{Q_T} = \frac{12\mu l}{dh^3} \qquad (16)$$

The capillary resistance R_k is derived from Hagen–Poiseuille's equation with assumptions that the fluid is incompressible and Newtonian. The equation describes laminar flow thru a pipe of constant circular cross-section. The capillary radius is significantly lower than its length and fluid do not accelerate. Then the equation has a shape (17).

$$R_k = \frac{\Delta p}{Q_K} = \frac{p_p - p_T}{Q_K} = \frac{8\mu l_C}{\pi r_C^4} \qquad (17)$$

The capillary and HS cell are connected in series and thus flow rate is the same for both. It is expressed by a continuity equation (18).

$$Q_k = Q_T = Q_{k,T} \qquad (18)$$

Equations (16), (17) and (18) yields in:

$$\frac{p_t}{R_t} = \frac{p_p}{R_T + R_k} \qquad (19)$$

This yields in:

$$\frac{p_t}{R_t} = \frac{p_p}{R_T + R_k} \qquad (20)$$

Finally, a capillary length is computed:

$$l_C = \frac{3\pi r_c^4 l}{2dh^3}\left(\frac{p_p}{p_T} - 1\right) = 66\ mm \qquad (21)$$

The computed capillary length is 66 mm.

Conclusion

In this chapter, the hydraulic circuit for gap height control was described. Since its stability was low the improved circuit was designed with the proportional valve bypassed by the capillary. The capillary inner radius $0{,}35\ mm$ was chosen and the capillary length computed as 66 mm. Initial throttling gap height was set to $50\ \mu m$. Experimentally was proved that the capillary has stabilising effect on regulation.

4.2.2 Valve selection

For application in actively controlled HS cell, requirement for the proportional valve is a working range from 0,05 to $1{,}5\ l \cdot \mathrm{min}^{-1}$. Standardly produced proportional flow control valves has maximal flow rate above $1{,}5\ l \cdot \mathrm{min}^{-1}$ and in range close to $0\ l \cdot \mathrm{min}^{-1}$ are insensitive to control. Therefore, they are not suitable. Possible solution is to use a special valve for small flow rate control.

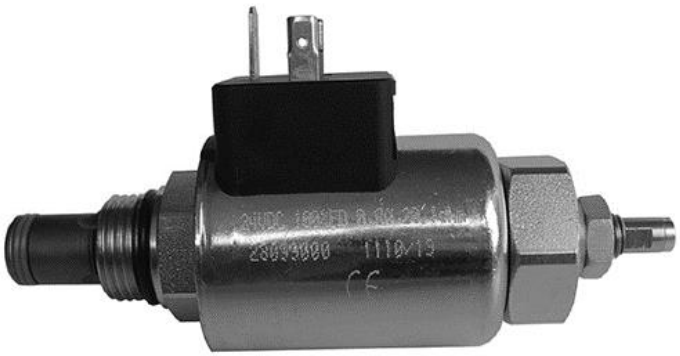

fig. 29: Proportional valve SR1P2-A2/H12-24 [35]

Example of such valve is 2-way proportional flow control valve with designation DUR 1,6 L 06 P K NBR from Parker. [34] Nevertheless, its cost is approximately 16 800 CZK. Another approach is to use a proportional pressure relief valve that is initially designed as a pilot valve for pilot operated pressure relief valves. The valve is economical. A disadvantage is unknown relation between operating signal and flow rate. Nonetheless, this obstacle can be solved by using PI controller that do not need mathematical model of controlled system. For this reason, proportional directly operated pressure relief valve SR1P2-A2/H12-24 was chosen. It cost is approximately 3 000 ZCK. [35]

4.3 Control system

As a definition states, a control system is device that controls other systems. In this case, the control system controls throttling gap height. Two major control systems are known, an open loop control system and a closed loop control system. Benefits and drawbacks of these systems are listed and evaluated and a suitable system for this application is chosen.

The open loop control system is depicted in fig. 30. It is characterised by absence of feedback. Output value is determined only by set value and system controller. The system controller has no information about actual value of a process (controlled system). It mean that it is sensitive to disturbances. An impact of disturbance is not compensated. The controller includes model of the controlled system.

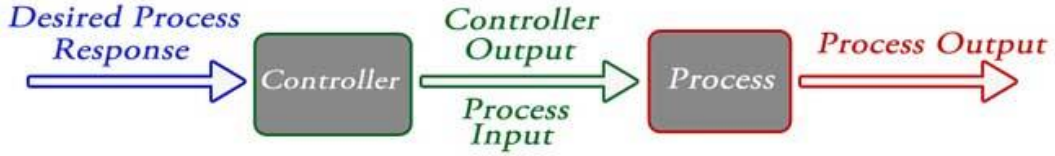

fig. 30: Open loop control system [36]

The open loop control is suitable for systems where it is possible to determine relationship between input and output and impact of the disturbance variable is rather small. The relationship can be a mathematical model or a formula. Advantages are simple construction and design and thus lower cost. The system can be faster because of absence of feedback. Disadvantages are lower accuracy, unreliability and absence of output autocorrect. [36] [37]

An impact of disturbance can be decreased when a relationship between disturbance variable and controlled system output is known and modelled. Then the control system can measure the disturbance variable and correct its impact (fig. 31). However, extent of correction depends on accuracy of the model. On the other hand, reaction on disturbance variable change is faster than

for systems with feedback. [36] [37] An application of open loop controller to throttling gap height control has several difficulties. First and the most serious difficulty is lack of proportional valve model. Relation between input current and output flow rate for various pressure differences is not known. Possibly, it could be obtained by CFD modelling of the valve. However, it is not objective of this thesis. Another challenge is a model of a disturbance variables impact. Disturbance variables are HS pocket load and oil temperature. For this reasons, open loop control is not suitable for HS cell control.

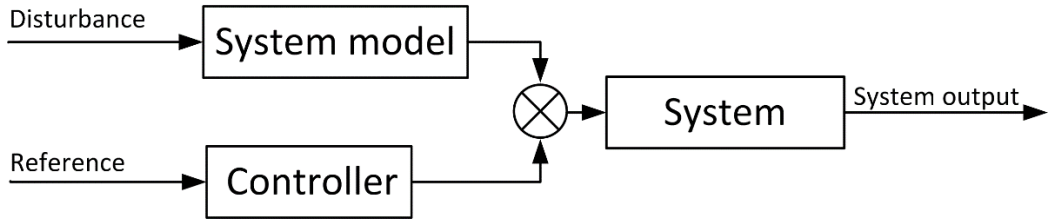

fig. 31: Open loop control system with disturbance compensation

Ffig. 32 shows a closed loop control block diagram that is characterized by feedback. Output value is compared with reference (set value) and an error is computed. A controller sets controlled system input in order to minimize difference between reference and measured output (actual value). That means to minimize the error. A magnitude of the error and time required to reach set value depends mainly on a type of controller and its parameters setting. The error caused by disturbance variables can be corrected automatically. [37]

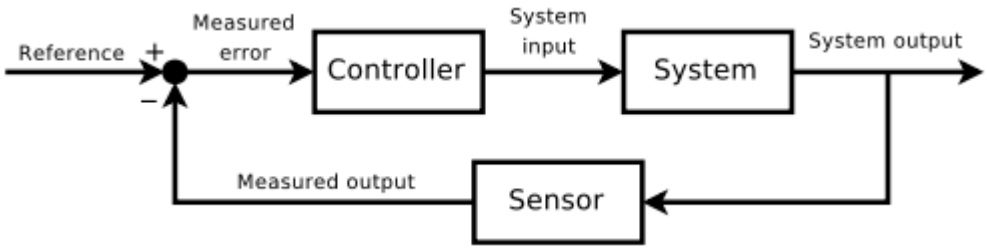

fig. 32: Closed loop control system [36]

In comparison with the open loop control system, advantages of the closed loop control system are higher accuracy even for nonlinear controlled systems, possibility to correct an impact of disturbance variable, no need for the controlled system model. For purpose of HS cell control is beneficial that model for disturbance correction is not needed. Disadvantages are higher cost, more complex design, risk of oscillation and stability issues, and slower response than the open loop system. [36] Stability of closed loop system depends on controller parameters. The most commonly used controller is a Proportional–Integral–Derivative controller (**PID** controller).

Proportional and integral controllers can be used independently or in combination with derivative controller. PID controller is illustrated in fig. 33.

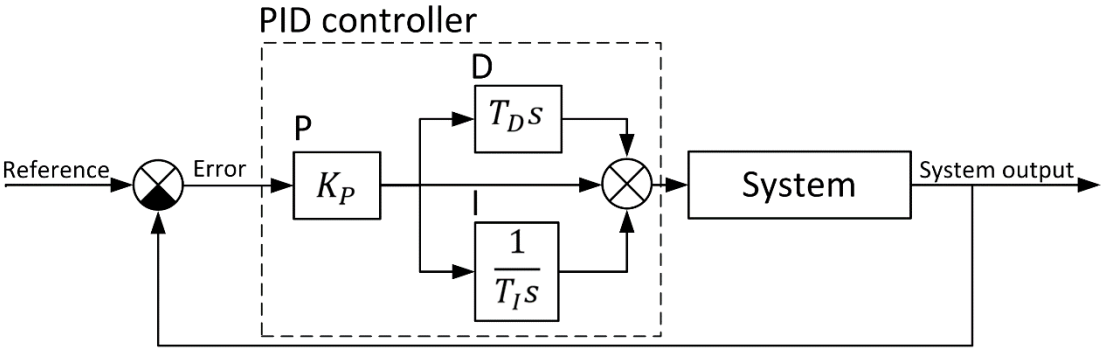

fig. 33: PID controller block schematics

P denotes proportional gain of an error. Proportional gain $\mathbf{K_p}$ causes large change in the control variable (manipulated variable) without delay. If proportional gain is too high, it can make the system unstable. The proportional controller always has a steady state error. Therefore it is not suitable for HS cell control, since position error is not acceptable.

I denotes an integral controller. It sums errors over time and computes accumulated offset that should be corrected. In steady state, I controller eliminates steady state error because it has an infinite gain for frequencies approaching zero Hz. Its characteristic constant is time constant $\mathbf{T_I}$. The smaller the constant is, the faster the error is eliminated. Nevertheless, when $\mathbf{T_I}$ is too small the system gets unstable.

D denotes a derivative controller. The controller computes a rate of change of an error over the time and multiplies this slope with derivative gain constant $\mathbf{T_D}$. The derivative controller predicts the system behaviour. Consequently, the control system can quickly react to changes in the controlled system. Nonetheless, the **D** controller is sensitive to noise which causes changes in measured value with a very fast rate. Hence the **D** controller even in combination with **P** or **D** controllers is not suitable for HS cell control application because a number of interference sources are present in MT.

As a result, it is concluded that the closed loop control system is more feasible for HS cell gap height control than the open loop system. With respect to controller feasibility, the **PI controller** with fast reaction and zero steady state error is chosen. PI controller is tuned by using Ziegler-Nichol's method.

A throttling gap height closed loop control system is shown in fig. 34. This system is intended to control one HS cell hap height. The system serves to control hydraulic circuit from fig. 28. Height

set point is denoted as h_1. When actual height is subtracted from height set point and control deviation is obtained. Then PI regulator sets Voltage and Voltage-to-Current converter U/I converts it to electric current. Current thru coil of the proportional valve PV moves with its poppet and thus control flow rate. Finally, gap height of HS pocket HP is changed to set point value.

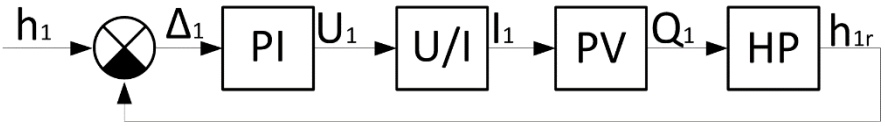

fig. 34: Single pocket control schematic

Possible improvement in control precision and dynamic could be achieved by a cascade control. Inner closed loop would control pressure in HS pocket and outer loop would control position (gap height). Similar regulation controls feed axes in MT. For controlling the working table as described in chapter 5.2 different approach is possible. It is a model based control. It allows us to describe the working table as one object. Chapter 5.2 describes that each HS cell of the working table is controlled independently. In order implement state-space representation, the controlled system must be mathematically described. A problem is description of the proportional valve and dependency of the model on mass and moment of inertia. Another issue is that the system is mathematically described by at least 12 first-order differential equations. Since both of these methods are laborious they are not further elaborated. Nevertheless, they can be addressed by future research.

Conclusion

In this chapter, a feasibility of the open loop control system and the closed loop control system were considered. For purpose of HS cell gap height control, the closed loop control system was chosen because of its advantages; namely zero steady state error, compensation of disturbance variable, no need for mathematical description of proportional valve etc. Then properties of PID controller were discussed and PI controller was chosen. Finally, HS cell closed loop control system was designed.

4.3.1 Controller

A critical part of the control system is controller hardware. The controller reads inputs from length gauges, computes height error, runs PI controller and sets voltage outputs for the voltage to current converter. When used to control multiple HS cells, another calculations are required. For purpose of experiment, temperature of oil, pocket pressure, oil flow rate are read and saved. That means 14 analog inputs. Four voltage analog 10 V outputs are need to control four proportional valves.

In order to keep high bandwidth of regulation a sampling rate of controller is required 1 ms or higher. Resolution of inputs and outputs should be at least 16 bits. The controller must be reliable and rugged. Five controllers were considered.

fig. 35: Arduino Mega 2560 [38]

fig. 36: Raspberry PI [39]

The first considered controller is Arduino MEGA 2560 depicted in fig. 35. It is recommended for 3D printers and robotic projects. It has 16 analogue inputs and 15 PWM outputs. PWM outputs could be used with other electronics as analogue outputs. Nevertheless, PWM ports are 8 bits and frequency of generated pulses is 100 Hz which is lower than required 1000 Hz. Moreover, its computing power is not sufficient. [40] Arduino is for hobby use and therefore not suitable for industrial application where high reliability is essential. Therefore, Arduino is not suitable for this application. A similar board, Raspberry PI has higher computing power. It is illustrated in fig. 36. However, other drawbacks are similar and therefore it is not suitable as well. [41]

fig. 37: PLC Tecomat FOXTROT CP-1000 [42]

fig. 38: PLC Tecomat TC700 [43]

The second possibility is to use PLC controller. PLC commonly used in the field of MT has a tact around 20 ms which is not sufficient. Such PLC is shown in fig. 37. Nevertheless, PLCs with tact around 250 μs are available. It is shown in fig. 38. Such PLC is more expensive. It costs around

40 000 CZK. As advantage is considered resilient case and input output protection circuitry since PLC is intended for industrial use. PLC can be connected to different modules and ensure sufficient amount of inputs and outputs. When more modules are used, time between input read and output write can extent up to 1000 μs because of communication BUS delay (fig. 39). As a drawback for this application is considered challenging coding, tuning and debugging. [42] [43]

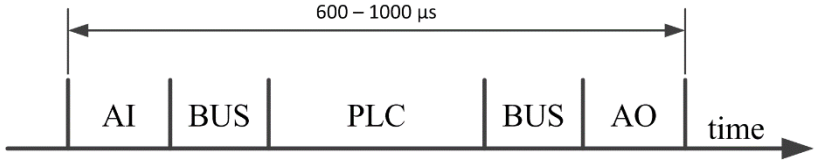

fig. 39: BUS communication schematics

Another suitable controller is a CompactRIO Platform and a Single-Board RIO from National Instruments. They contain two embedded processing units as shown in fig. 40. The first unit is a real time processor for communication, computation and processing of a signal. Second unit is a field programmable gate array (FPGA) for high-speed control, computation and data acquisition. This brings high computing power and quick response in real time. In comparison with PLC modular system, there is no delay caused by BUS communication. CompactRIO chassis also allows user to connect four or eight modules with analog/digital inputs/outputs that is more than sufficient for this application. [44]

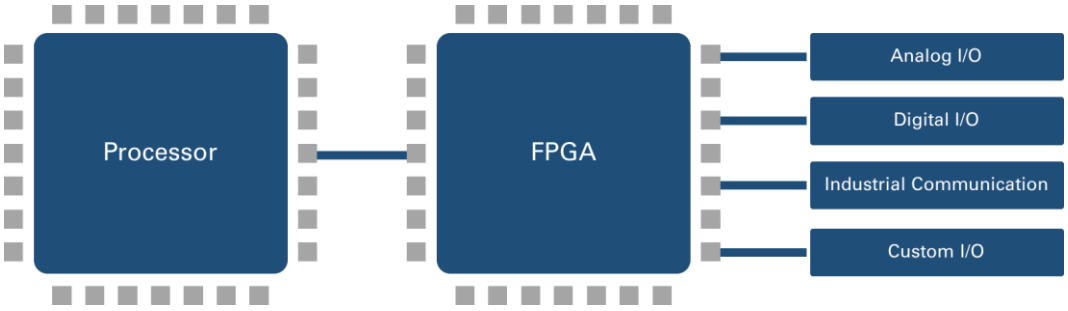

fig. 40: An architecture of the CompactRIO and Single-Board RIO [44]

An advantage is easy graphical programing by LabVIEW from National Instruments. A graphical coding is intuitive and fast and enables user to create programs with parallel execution which is beneficial for controlling multiple HS pockets simultaneously. The code is easy to modify and debug. The controller enables data acquisition and saving data to memory of a personal computer. Consequently, data analysis is faster and less laborious. LabVIEW provides user with possibly to create a front panel for real time data display and control. Data are displayed on the screen of the personal computer.

CompactRIO platform is rugged, multipurpose, providing a number of inputs and outputs as can be seen in fig. 41. This allows industrial use. Nevertheless, its cost 134 000 CZK plus chassis 123 200 CZK is high because of its versatility. A total price with peripherals and measuring modules is approximately 335 000 CZK. [45] Therefore, it is more suitable for laboratories where versatility is beneficial. For this reason and its availability in the laboratory, CompactRIO was chosen as the controller for control system development for the experiment.

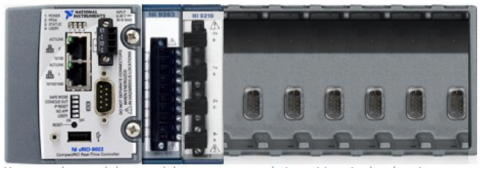

fig. 41: CompactRIO – 9025 [45]

fig. 42: Single-board RIO – 9637 [46]

Single-Board RIO possess similar advantages as CompactRIO. It is depicted in fig. 42. Code written for CompactRIO can be compiled with minor changes for Single-Board RIO. However, Single-Board RIO (sbRIO) is not the controller that can be directly used. It is a printed circuit board and as such, it is exposed to a surrounding environment. It is intended to be embedded in OEM applications in large quantities. Consequently, the cost 37 000 CZK is significantly lower. However, controller peripherals are not ready for direct use. For example, inputs and outputs can be connected only by using a breakout board or by a similar platform or by a special cable. The Single-board RIO – 9637 controller has four 16-bit analog outputs, sixteen 16-bit analog inputs, and 28 digital inputs/outputs. These can be accessed through two 50-pin IDC headers. Thus, Single-Board RIO is equipped with sufficient amount of analog/digital inputs/outputs which are directly mounted to the board and requires the breakout board. Board power supply and case need to be designed as well. SbRIO can be beneficially used for other tasks in MT, since it computational power is sufficient. In conclusion, sbRIO has lower price but peripherals and case need to be designed or bought, which is still economically effective given the speed and computational power. Nevertheless, total price is significantly lower. For this reason, sbRIO is recommended for the industrial application. [46] Design of the breaking board is shown in fig. 43. The breaking board can be referred to as PCB. Ffig. 44 shows manufactured breaking board.

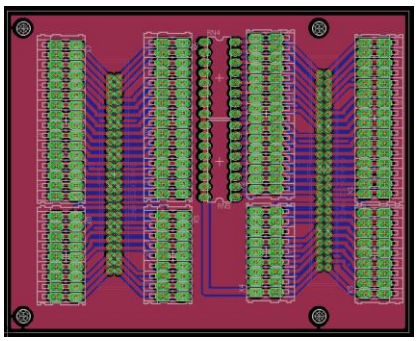

fig. 43:A design of PCB for sbRIO

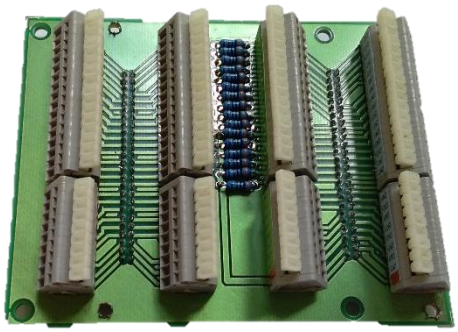

fig. 44: Physical realization of PCB

fig. 45 displays the manufactured breaking board connected to SbRIO.

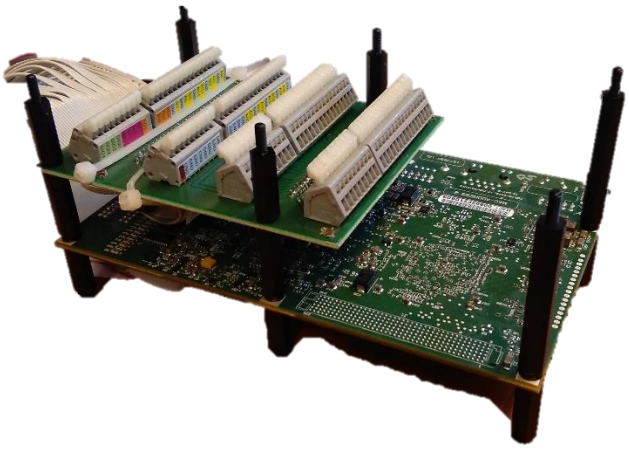

fig. 45: SbRIO connected to breaking board

Conclusion

Five different controllers were compared in order to find the most suitable solution for HS cell gap height control. Arduino MEGA 2560 and Raspberry PI are hobby controllers with low resolution of input pins and limited reliability. Therefore, they are not suitable for this application. PLC standardly used in MT are too slow or have too high communication delay of inputs/outputs. Faster PLC are fast enough but its price is higher. Its programing is challenging. CompactRIO fulfils all requirements perfectly because of its versatility. It is easy to use and program. Nevertheless, its price is high. SbRIO fulfils all requirements as CompactRIO but its cost is similar to fast PLC. Code for CompactRIO can easily be compiled for SbRIO. For this reason, CompactRIO is chosen for development of control system and experiment. Afterwards, functional system is recommended to be converted for SbRIO and implemented in MT. The breaking board was designed and manufactured for SbRIO input/output.

4.3.2 Length gauges

For proper function of the control system a suitable length gauge must be used. It is assumed that different length gages are used for an experiment and for application in machine tools (MT). For the application in MT, the length gauge is positioned in proximity of HS cell and measures relative distance between HS pocket and the guiding prism (rail). An accuracy sufficient for this application is set to 1 μm and can differ for different applications. The accuracy, a range and a price should be considered as decision factors. A gauge with continuous signal is required. Therefore binary proximity sensors are not suitable. The sensor should be robust to withstand harsh working condition. Generally, length gauges can be divided in two groups, contact free sensors and contact sensors. For purpose of an experiment that is described later a contact sensor is feasible because a testing device does not move in longitudinal direction. Therefore, a sensor will not wear out because of friction. Contrary, for application in MT there is a requirement for contact less sensor. Based on physical principle, length sensor can be divided in to: [47]

- Mechanical sensors
- Magnetic sensors
- Ultrasound sensors
- Capacitive sensors
- Optical sensors
- Inductive sensors

For purpose of the experiment a contact inductive sensor T102F from Mesing was used. A reason is economical. The sensor is equipment of a RCMT laboratory where experiments were conducted. A range of the sensor is ± 2 mm and its linearity error is 0,25 % in range ± 1 mm at a temperature 20 °C and repeatability 0,01 μm which is sufficient. [48]

For purpose of MT a mechanical sensor is not suitable because of friction and wearing off. Different sensor is required. Magnetics sensors are commonly used as binary switches which changes state (on/off) when object is at present distance. Magnetics sensors are not feasible for this application. [47]

Ultrasound sensors measure properties of acoustic waves which frequencies higher than humans can hear. They produce a high frequency sound pulses. The waves bounces of obstacles and a sensor is receiving them. An echo pulse is then evaluated and the distance determined. Usually time of flight is measured. For accuracy, a speed of sound is critical. The speed depends on material, temperature, pressure etc. Unfortunately, these parameters are varying significantly

during the operation of HS guideway. The sensor is intended to be close to HS cell. As a result, ultrasound sensors cannot be used. [47]

Capacitive sensors accuracy is sufficient. They can measure position of metallic and non-metallic parts. For this application, this characteristic is drawback since a length gauge is supposed to measure distance between a HS pocket and the guiding prism. The prism is covered with a layer of oil that flows out of the pocket. Consequently the capacitive sensor measures height of oil film covering the prism in proximity of HS pocket instead of throttling gap height. Therefore, capacitive sensors cannot be used for this application. [47]

A number of optical measuring devices with sufficient accuracy is known. For example beam triangulation and beam time of flight methods. Methods using optical sensors have similar drawbacks as capacitive sensors. A layer of oil covering the rail presents a challenge to measure the distance properly. A beam of light can be refracted or bounced off on the surface of oil and cause misinterpretation of position. [47]

Inductive sensors are non-contact position sensors. Principally, the sensor produces an alternating magnetic field that induces eddy currents in a measured part. Eddy currents induce the second magnetic field. This field counter the magnetic field of sensor. The extent of interaction depends on distance of the measured part and the sensor. As the mutual position changes, the field interaction changes and sensor electronics evaluates position. Voltage or current output of the sensor is then proportional to distance. Inductive sensors are used as binary switches or as analog distance sensors. Binary sensors are usually referred to as induction sensors while analog distance sensors are referred to as eddy-current sensors. Binary sensors are inexpensive proximity switches whereas eddy-current sensors are used for precision displacement measurements. Its major advantage for application in HS guideways are tolerance of dirty environments, insensitivity to material in gap between the sensor and the measured part and thermal stability. Based on this facts, eddy current sensors were chosen as most feasible solution for application of actively controlled HS guideways. [49] A sensor PR 6422 is suitable. [50]

A principle of measuring gap height of HS bearing is described in patent WO2008097157 and can be applied with minor changes to HS guideways. fig. 47 shows schematic of measuring system for HS bearing. A HS pocket (1) is manufactured with receiving mean (3) for distance sensor (5) that measures mutual position of HS pocket and supported structure (7). Schematics also illustrates monitoring of throttling gap height, means for displaying throttling gap height (19) and also means for storing measured data. [51]

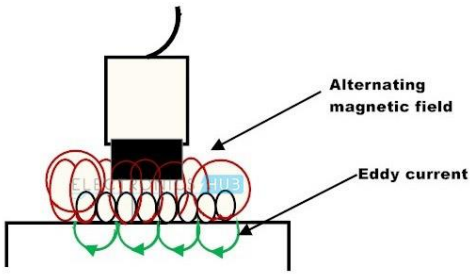

fig. 46: Eddy current sensor principle [52]

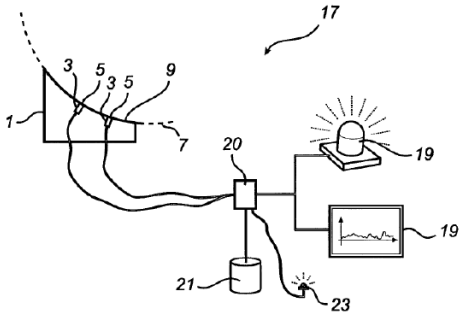

fig. 47: Schematics of HS pocket gap height measurement [51]

Conclusion

For proper function of the control system a suitable length gauge is required. The length gauge measures throttling gap height. First, specification for gauge was described. Second, a research about length measuring devices was made. Finally, length gauge was chosen. For purpose of experiment, a contact inductive sensor T102F [48] from Mesing was used because of economics. It has sufficient accuracy. For purpose of application in machine tools eddy current sensor PR 6422 [50] is suitable. Its major advantages are tolerance of dirty environments, insensitivity to material in gap between the sensor and the measured part and thermal stability.

5 Working table gap height and rotation control system

A principle of gap height control for one HS cell was described in chapter 4. To control gap height and rotation of the working table, at least three HS pocket gap heights need to be controlled simultaneously. Since the working table is usually equipped with four HS pockets in corners, in this contribution four gap height are controlled. This arrangement is also less sensitive to load caused by e.g. mass at the working table.

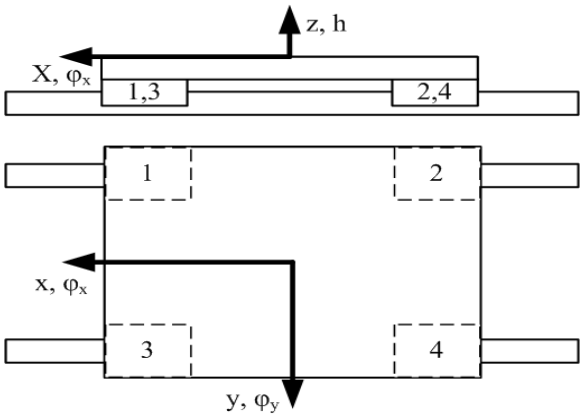

fig. 48: Working table schematics

fig. 48 shows working table of a feed drive axis that is used in an experiment. A goal is to move with the table in the direction of z axis by magnitude of h. Another goal is to rotate with the table around axis x by φ_x and around axis y by φ_y. In order to achieve this goals, a mechatronic system must be designed. Description of its critical components follows.

5.1 Hydraulic circuit design

A hydraulic circuit for gap height control of four HS cells is in fig. 49. This circuit is based on circuit in fig. 28. A part of circuit with the capillary and the proportional valve is used four times in parallel.

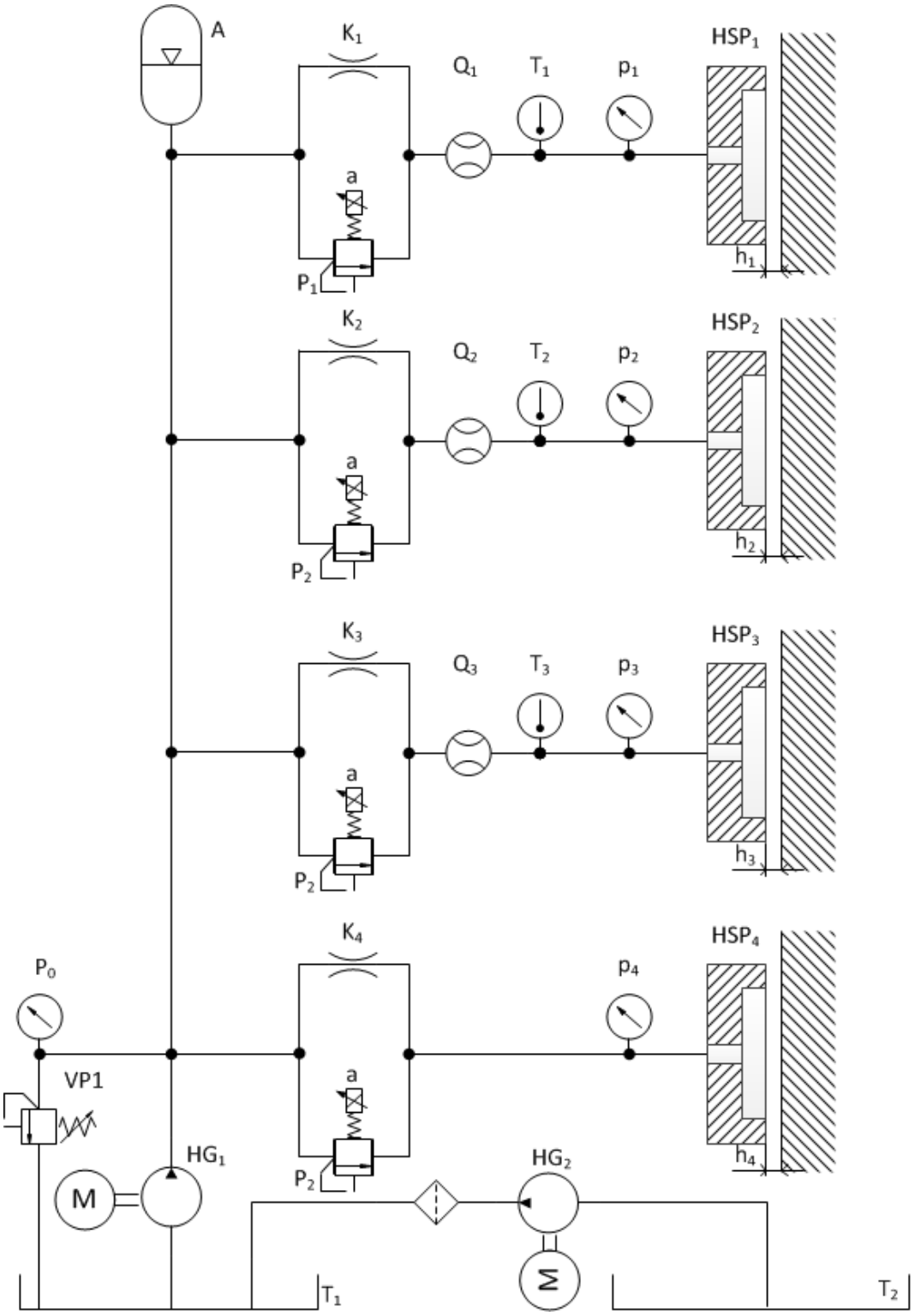

fig. 49: A hydraulic circuit for four pocket gap height control

5.2 Control system design for working table

For purpose of gap height control a control system was designed. It is closed loop control with the proportional-integral controller. The control system schematics is depicted in fig. 50. A set

value is gap height h and rotation around x axis φ_x and y axis φ_y. Gap height h refers to distance between the guiding prism and centre of the working table in a vertical direction. It is assumed that HS cells are equally distributed. If the table is rotated, h is average gap height of all four HS cells.

A description of a controller working principle follows. The gap height h and rotation around the x axis φ_x and the y axis φ_y are set and a transformation block computes set values for all four HS cells. These values are compared with actual, measured values of gap heights and error is obtained. Each closed loop consist of the PI controller, voltage to current converter U/I, proportional valve PV, HS cell HP and length gauge. First, the error is read by PI controller. Second, PI controller change output voltage in order to minimize the error. Then, a voltage to current converter converts voltage to current. This is necessary because the valve poppet is controlled by an electromagnet. The electromagnet consist of a coil and an iron core. The amount of current through the coil is proportional to a strength of magnetic field and thus magnetic force. The magnetic force counteracts pressure force on poppet and thus controls the poppet position and consequently flow rate through the valve. The flow rate flows to HS cell and is throttled over the land. As a result, the gap height is changed. Finally, the gap height is measured and subtracted from the set value. As a result the negative feedback control system is closed.

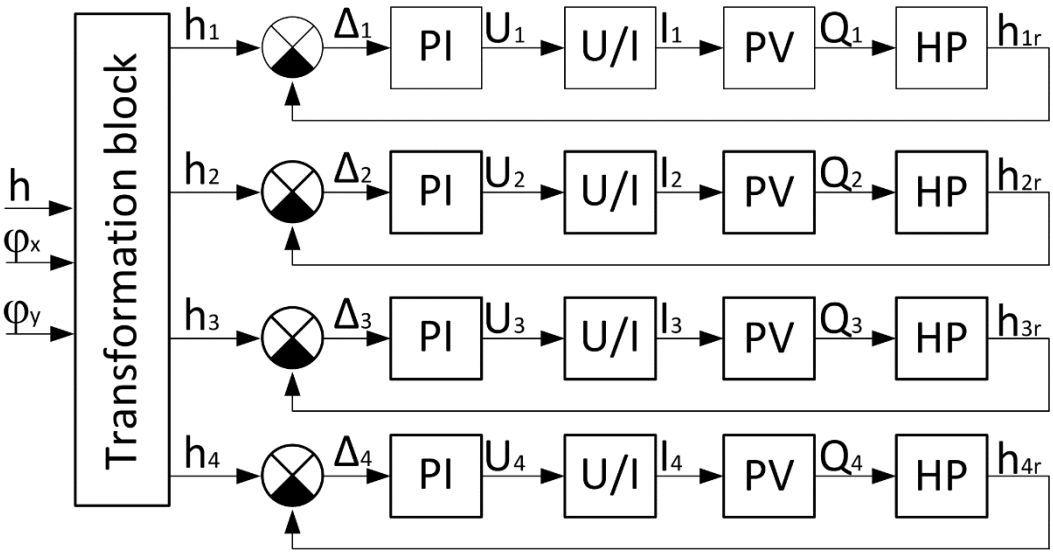

fig. 50: Control system schematics

Theoretically, only three length gauges are sufficient to determine position and orientation of the working table because a plane is fully defined by position of three non-collinear points lying in a plane. In case a height of the working table above the prism is measured in three specified points a gap height for each HS pocket can be computed. Advantage of this approach is that only three length gauges are needed. It means lower cost of gauges and also lesser amount of analog inputs

required for the controller. Nevertheless, at the basis of carried out measurements it is verified that the system with four length gauges performs better. It is because of lower stiffness of the working table. Each HS cell behaves as SISO (single-input single-output) system. In case the table is rigid then the system is MIMO (Multiple-input multiple-output). Control of MIMO system is rather difficult and control of MIMO system is not objective of this thesis.

Transformation block description

As mentioned in the previous text, the gap height for each HS pocket need to be computed from the required gap height h and rotationφ_x, φ_y. This computation is performed by transformation block as shown in fig. 50. Necessary mathematical formulas are derived by using transformation matrixes. A global coordinate system is rigidly connected with the bed. A working table coordinate system is connected to the top of the table. Transformation in vertical direction (direction of z axis) is described by matrix $T_z(h)$ where h indicates theoretical gap height in the middle of the table.

$$T_z(h) = \begin{bmatrix} 1 & 0 & 0 & 0 \\ 0 & 1 & 0 & 0 \\ 0 & 0 & 1 & h \\ 0 & 0 & 0 & 1 \end{bmatrix} \quad (22)$$

Rotation around the x axis is described by matrix $T_{\varphi_x}(\varphi_x)$ where φ_x denotes angle of rotation around the x axis.

$$T_{\varphi_x}(\varphi_x) = \begin{bmatrix} 1 & 0 & 0 & 0 \\ 0 & cos(\varphi_x) & -sin(\varphi_x) & 0 \\ 0 & sin(\varphi_x) & cos(\varphi_x) & 0 \\ 0 & 0 & 0 & 1 \end{bmatrix} \quad (23)$$

Rotation around the y axis is expressed by matrix $T_{\varphi_y}(\varphi_y)$ where φ_y denotes angle of rotation.

$$T_{\varphi_y}(\varphi_y) = \begin{bmatrix} 1 & 0 & 0 & 0 \\ 0 & cos(\varphi_y) & -sin(\varphi_y) & 0 \\ 0 & sin(\varphi_y) & cos(\varphi_y) & 0 \\ 0 & 0 & 0 & 1 \end{bmatrix} \quad (24)$$

Position of an arbitrary point in the local coordinate system of working table is expressed by a vector $X_L = [x_L \quad y_L \quad y_L \quad 1]^T$ and its position in the global coordinate system is described by a vector $X_G = [x_G \quad y_G \quad z_G \quad 1]^T$. The position of point in the global coordinate system is computed by (25) and (26). In general, position of point depends on order of rotations. If the

table is first rotated around x axis and then around y axis then the final position is different than in case when a table is first rotated around y axis and then around x axis. Consequently, two expressions are presented.

$$X_1 = T_z(h)T_{\varphi_x}(\varphi_x)T_{\varphi_y}(\varphi_y)X_L \quad (25)$$

$$X_2 = T_z(h)T_{\varphi_y}(\varphi_y)T_{\varphi_x}(\varphi_x)X_L \quad (26)$$

$X_1 \neq X_2$. After multiplying matrixes (25) the third element of vector X_1 (coordinate z) is obtained. The coordinate z expresses gap height of pocket.

$$z_G = h + y_L sin(\varphi_x) + x_L sin(\varphi_y) cos(\varphi_x) \quad (27)$$

Since angles φ_x and φ_y are minute it is possible to make substitution $sin(\varphi_x) = \varphi_x$, $sin(\varphi_y) = \varphi_y$ and $cos(\varphi_x) = 1$. The equation is obtained.

$$z_G = h + y_L sin(\varphi_x) + x_L sin(\varphi_y) = h + y_L\varphi_x + x_L\varphi_y \quad (28)$$

Analogical procedure is conducted for equation (26) and the result equals to equation (28). In conclusion can be stated that if the table is rotated by small angles the order of rotation does not matter. This was numerically verified for angles smaller than 0,5 degrees which is applicable for this application. Obtained equations are used in LabVIEW program.

5.3 LabVIEW program

A program was developed in order to run the PI controller, read and write inputs/outputs (I/O) and compute gap height for HS pocket accordingly to set gap height and angle of rotation. A developed LabVIEW program consists of two major parts. The first part is program for FPGA, which serves to read inputs and write outputs. When the program starts outputs are set to zero. Then program runs in loop until stop button is initialized. Then outputs are set to zero and program ends. I/O is performed with a frequency of 25 kHz. A measured signal is filtered by a filter of second order with a bandwidth 250 Hz. The program is shown in fig. 51. Second part of the program is a real time module. This program loop runs with a fervency of 1 kHz. Input of the program is measured voltage from FPGA. The voltage signal is converted to the gap height that is input for the PI controller. Set and actual gap height is compared and the PI controller determine output voltage in order to minimize error. The voltage is then sent to FPGA to be written to analogue outputs.

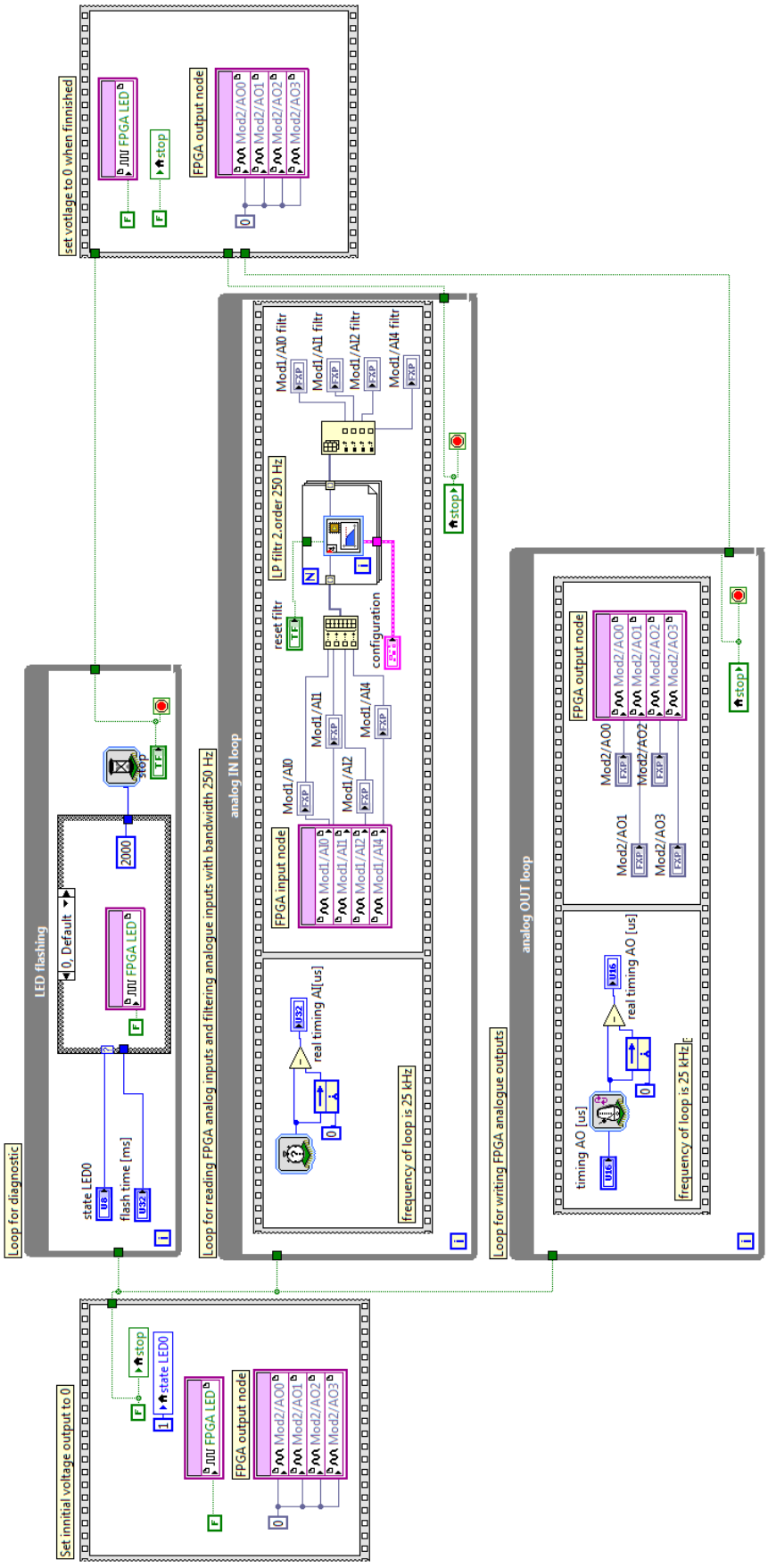

fig. 51: Program for reading input and writing output by FPGA

The second part of the program contain also graphical user interface (GUI) for displaying actual gap height and enables user to set gap height. The program writes measured gap height to a measurement file. Part of the real time module is transformation block described in chapter 5.2 and in fig. 50. Program for transformation block is shown in fig. 52. The PI controller was used from LabVIEW library and is illustrated in fig. 54. Conversion of measured voltage from length gauges to actual gap height is depicted in fig. 53. The program also enables user to zero gap height since length gauges measures relatively. The whole program is part electronic appendix.

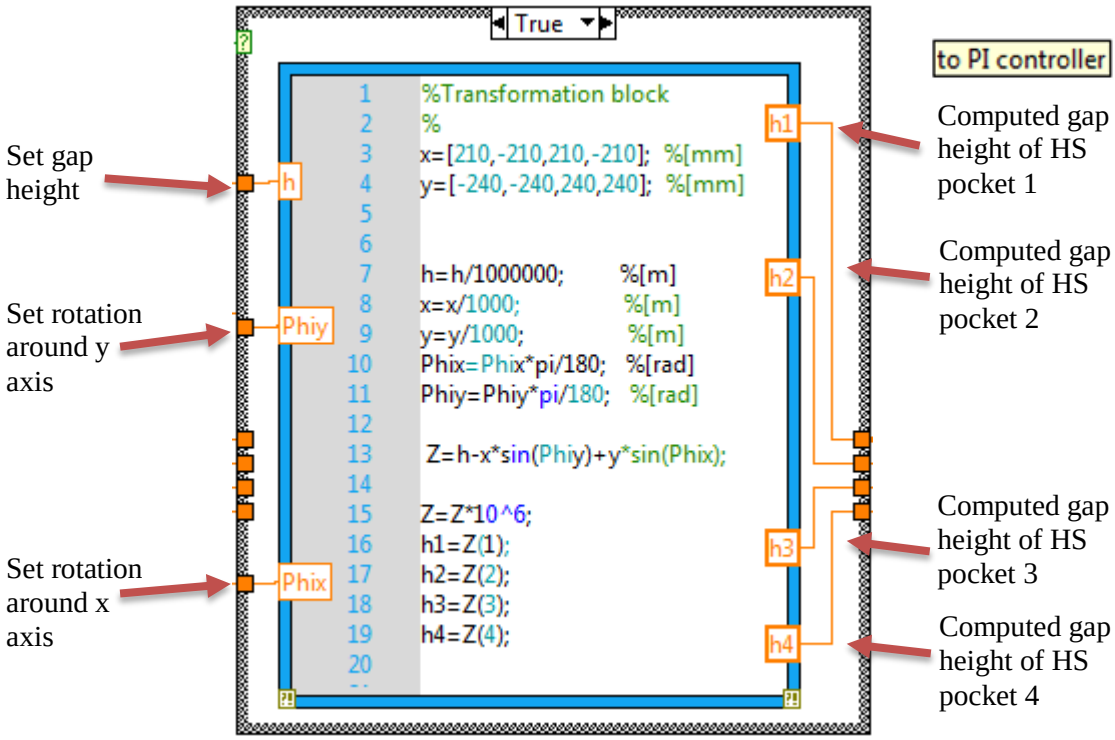

fig. 52: Transformation block in LabVIEW

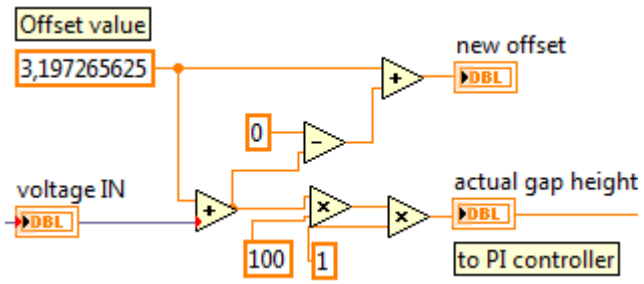

fig. 53: Measured voltage to gap height conversion

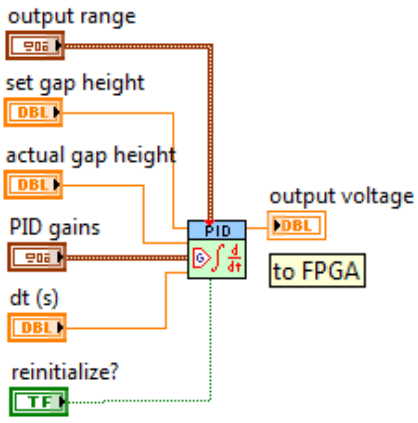

fig. 54: PI controller

5.4 Hybrid hydrostatic controller (H2C)

A hybrid hydrostatics controller consists of the proportional valve and the capillary as described in 5.1. Advantage above the simple HS circuit is its compactness and it is easy to use. Modular design consist of a several hydraulic cubes. A number of modules between first and last block can be arbitrary arranged. fig. 55 shows inlet hydraulic cube, two pieces of C+PV hydraulic cubes and end block hydraulic cube. C+PV hydraulic cube is referred to as hydraulic cube for capillary and proportional valve. In this arrangement, H2C is able to control two HS cells.

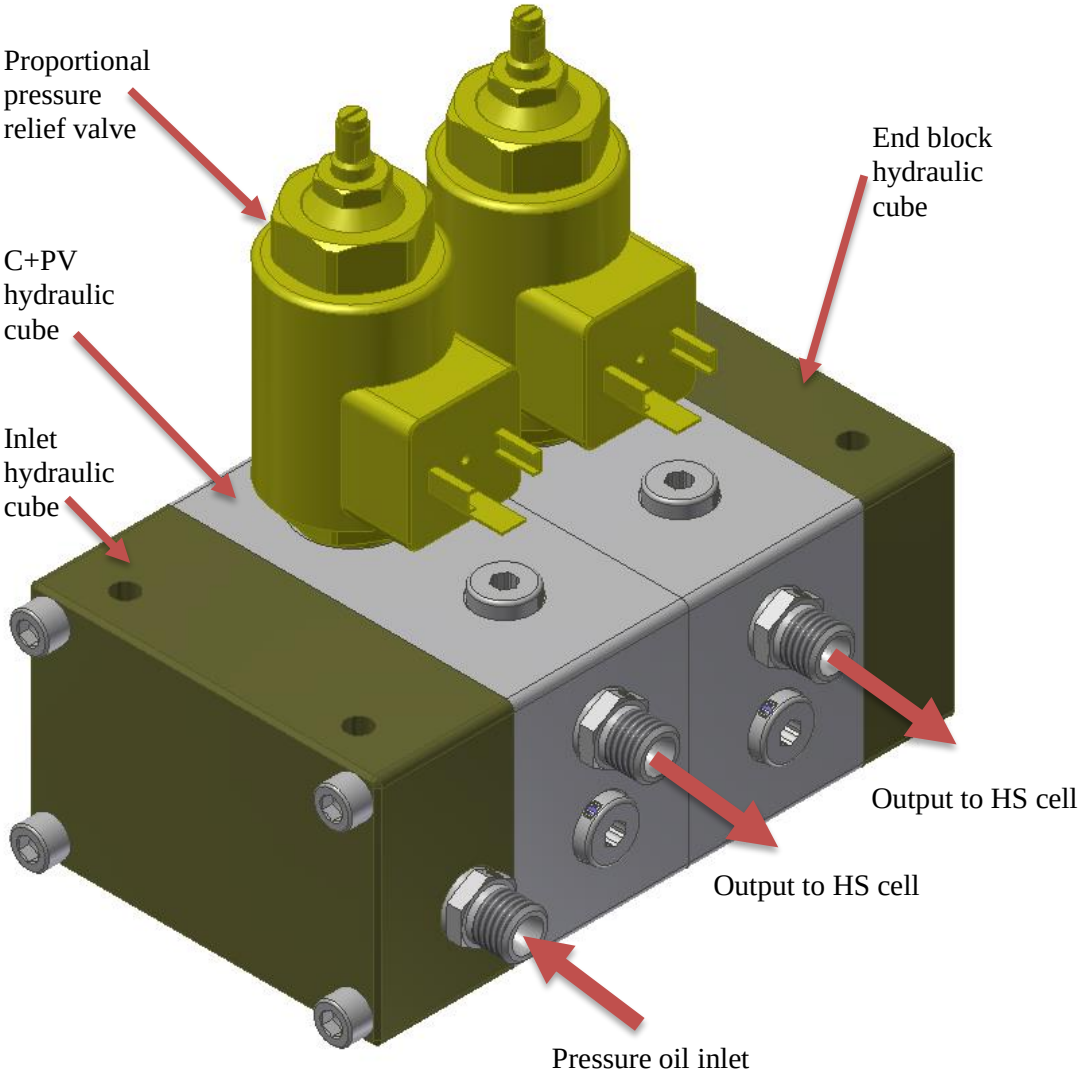

fig. 55: Hybrid hydrostatic controller (H2C)

Pressurized oil is brought thru an oil inlet and guided to C+PV hydraulic cubes through a system of channels. Oil flow is divided here in to the three streams as displayed in fig. 56. The first stream continues to the following C+PV hydraulic cube. The second stream flows thru the capillary in a

direction to the controller output. The third stream flows thru the proportional valve and afterward is merged with the stream thru the capillary.

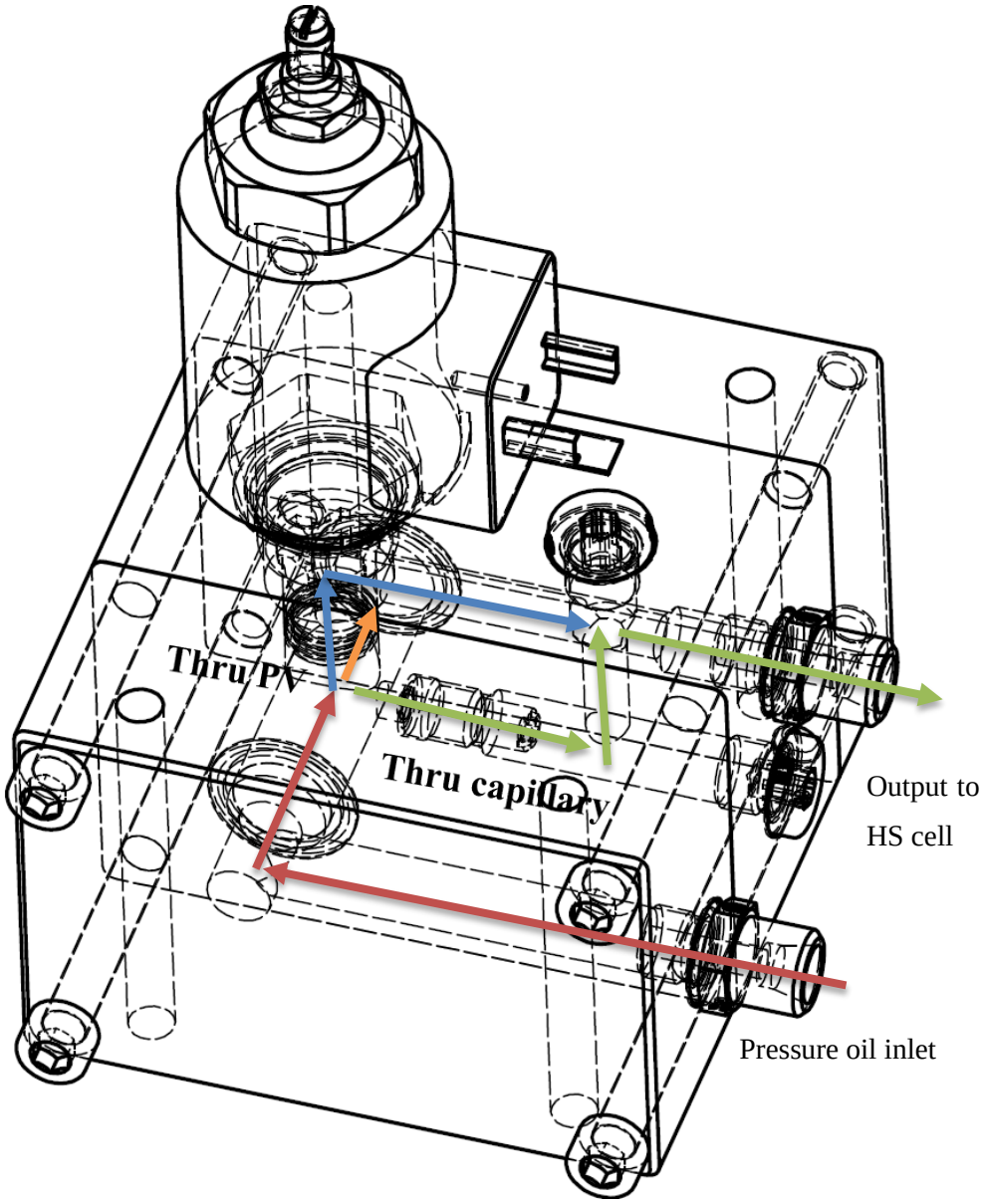

fig. 56: H2C flow schematics (red arrow – oil flow inlet, green arrow – flow thru capillary, blue arrow– flow thru proportional valve, orange arrow – flow to next hydraulic cube)

Drawings and design documentation of H2C is part on an annex. Proposed proportional valve has a designation SR1P2-A2/H12-24. Metric hollow hex plugs sealing channels are available from PARKER under the code VSTI10X1ED. Some of blinded holes can be used as a probe inlet for diagnostic. The oil inlet and outlet are designed with GE male stud connector GE06LM. A sealing between hydraulic cubes is designed by O – rings 18 x 1,5 NBR70.

6 Experiment and experiment results

A series of experiments were conducted in order to identify properties of designed system for HS cell gap height control. Experiments were performed on a testing stand STD30 depicted in fig. 57. It is a linear feed drive axis with HS guideway. Its working table is equipped with eight HS pockets. Four HS pockets are radial and supports mass of the working table and load. Radial HS guideway is the open type. Four HS pockets are lateral and prevent the working table from moving in the direction perpendicular to the feed drive axis x. Lateral HS guideway is the closed type. The difference between the open and closed type HS guideway is clear from fig. 3. The testing stand STD 30 was designed with PM controllers (chapter 3.2.1) for controlling throttling gap height. All eight HS pockets are equipped with PM controller. This testing stand was initially designed for experiments addressing new type of drive; combined linear motor and HS guideway. Therefore guiding prisms are equipped with strong permanent magnets and HS pockets are equipped with coils of the linear motor. As a consequence, there is attracting force between magnets and coils. This presents difficulty for HS cell gap height control in a form of disturbance force. Nevertheless, the designed control system minimize its effect.

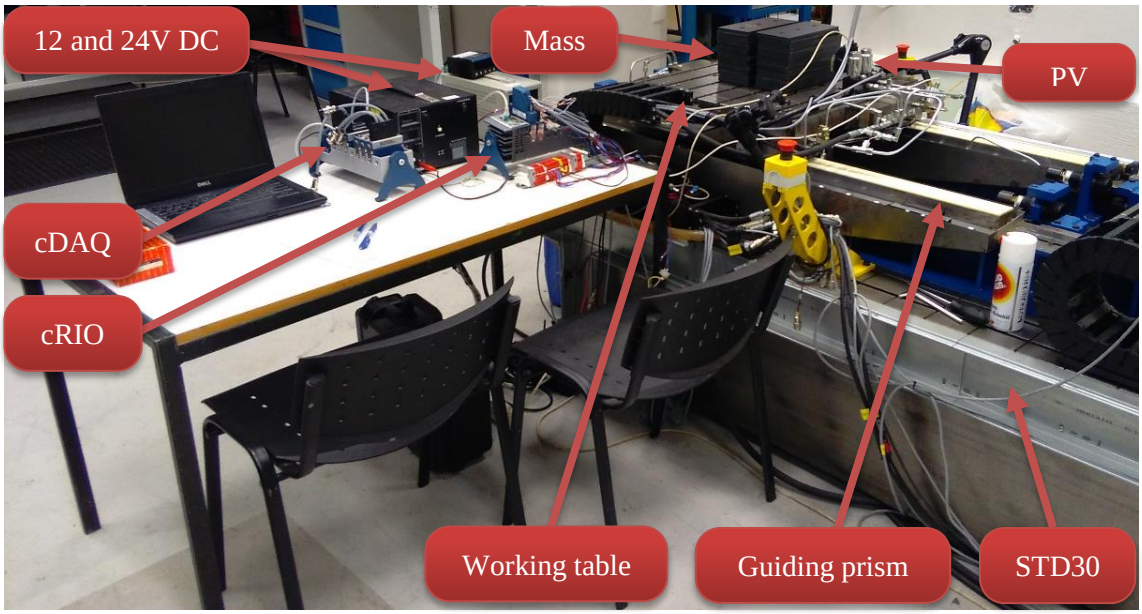

fig. 57: Testing stand STD30 and measuring devices

Magnets in guiding prisms prevent us from using eddy current length sensor because of interfering magnetic fields. Sensors should measure distance between the rail and working table. Therefore contact inductive sensor were used. Length sensors are closely described in chapter 4.3.2.

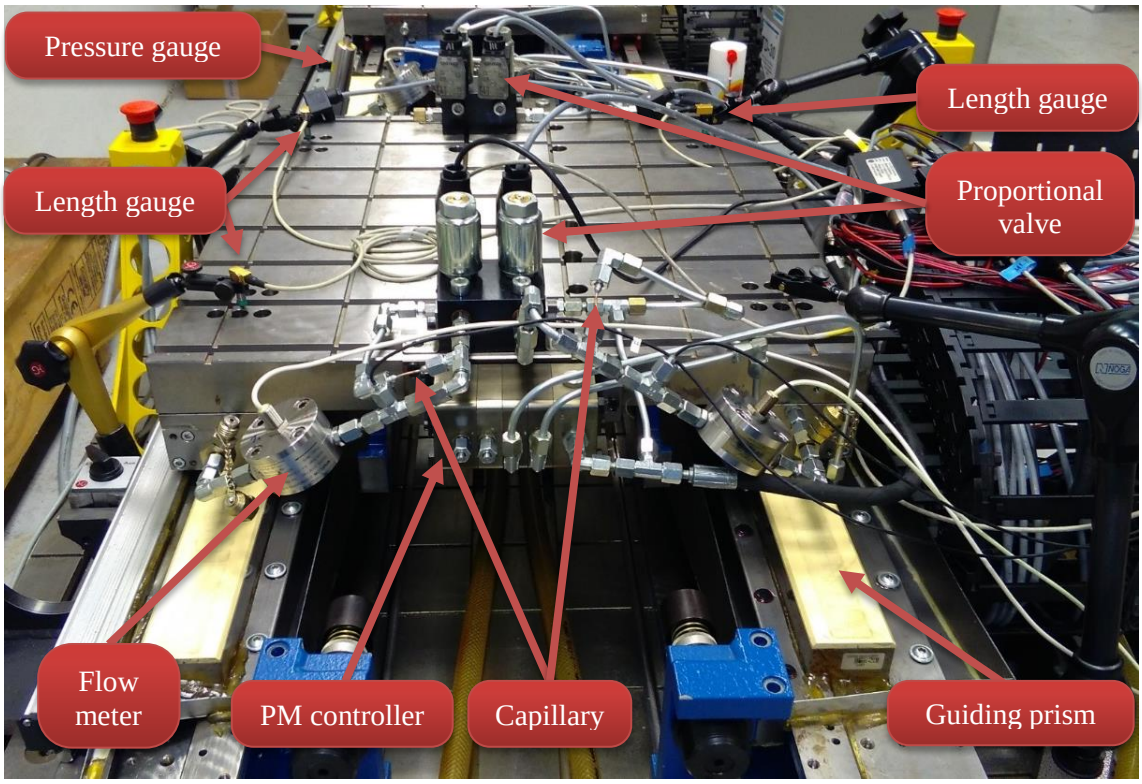

fig. 58: Experiment setup

The first measurement was performed with PM controllers in order to obtain reference values. Then two radial HS pockets were connected with proportional valves and capillaries. When control principle was verified four proportional valves were connected to hydraulic circuit.

6.1 Devices and sensors for experiment

This chapter lists used devices and sensors in tab. 3. Pressure in each of radial HS pocket cavity was measured by four pressure gauges. Gauges were located in proximity of HS pockets. Oil flow rate thru HS pockets was measured by three flow meters. Temperature of oil was measured in proximity of HS cells by three temperature gauges. Protection tube for PT 100 temperature gauge was manufactured and gauge was fixed inside using adhesive. Then the temperature gauge was placed to the oil flow through T-union. Pressure, flow rate and temperature gauges were used in order to monitor a controlling process and provide additional information about HS cells behaviour. They are not needed for closing feedback and thus to HS cell control.

Throttling gap height was measured by four length gauges located in corners of working table as shown in fig. 58. This length gauges were used for closing feedback. The gauge is supported by a magnetic base with articulating arm that is fixed to the bead of STD21. Therefore, the working table can move only in the vertical direction. It is not a problem for performing necessary experiments.

tab. 3: List of used devices and sensors

Type	Manufacturer/supplier	Designation	Measuring range	Accuracy
Temperature gauge		Pt 100	-50 + 200 °C	Class A
Pressure gauge	BHV senzory s.r.o.	DMP 333	0 - 250 bar rel.	≤±0,5%
Pressure gauge	BHV senzory s.r.o.	DMP 333	0 - 50 bar rel.	≤±0,5%
Flow meter	BOPP & REUTHER	Miniflow 015	0,1 - 1,0 l/min	≤±1% o.r.
Length gauge	Mesing	T102F	±2 mm	*
Proportional valve	Argo-Hitos	SR1P-A2/H12-24E2		
Service master Plus	Parker	SCM-500-01-00		
Real time controller	National Instruments	NI CRIO-9025		
Data acquisition system	National Instruments	Ni cDAQ-9188		
AO module	National Instruments	NI 9263		
AI module	National Instruments	NI 9219		
AI module	National Instruments	NI 9205		

*linearity error 0,25 % in range ±1mm at a temperature 20 °C, repeatability 0,01 μm

Redundant data were acquired by Ni cDAQ-9188 with three modules NI 9219. Position was measured by real time controller NI CRIO-9025 with module NI 9205. Voltage output for proportional valves was supplied by module NI 9263. Laboratory voltage sources for 24 V and 12 V powered electronic devices.

6.2 PM controller measurement

At the beginning of the experiment, the working table lies on the surface of HS guideways. The throttling gap height between prisms and HS pockets equals zero. Position sensors are reset and a position of working table gravity centre is assumed to be zero. Pump pressure is 50 bar unless different value is specified.

tab. 4: Throttling gap height measured with four PM controllers

i	x_1	x_2	x_3	x_4
[-]	[mm]	[mm]	[mm]	[mm]
1	0,028	0,027	0,029	0,026
2	0,029	0,032	0,031	0,028
3	0,029	0,032	0,031	0,028
4	0,029	0,033	0,031	0,028
5	0,029	0,033	0,031	0,028

First measurement was performed with four PM controllers in order to obtain reference values. Measured data are written in tab. 4. Measured throttling gap height with PM controllers is 30 μm. This value is too low for purpose of future experiments with active HS cells. Collisions between guiding prism and HS pocket could occur. Therefore capillaries length is computed for throttling gap height 50 μm.

6.3 Measurement to obtain the effect of pocket tilting

An experiment was carried out with two actively controlled HS cells and two PM controllers. The working table was rotated around y axis (fig. 48). Pockets number two and four were actively controlled. Throttling gap height was increased by steps up to its reachable maximum. Load of 20 and 60 kg was applied in the working table centre. HS pocket resistance was investigated and an effect of pocket tilting evaluated. fig. 59 shows HS pocket resistance computed from measured pressure and oil flow rate and also theoretical value obtained accordingly to chapter 4.1. For comparison, computed values were standardised for initial value of resistance obtained at throttling gap height 45 μm.

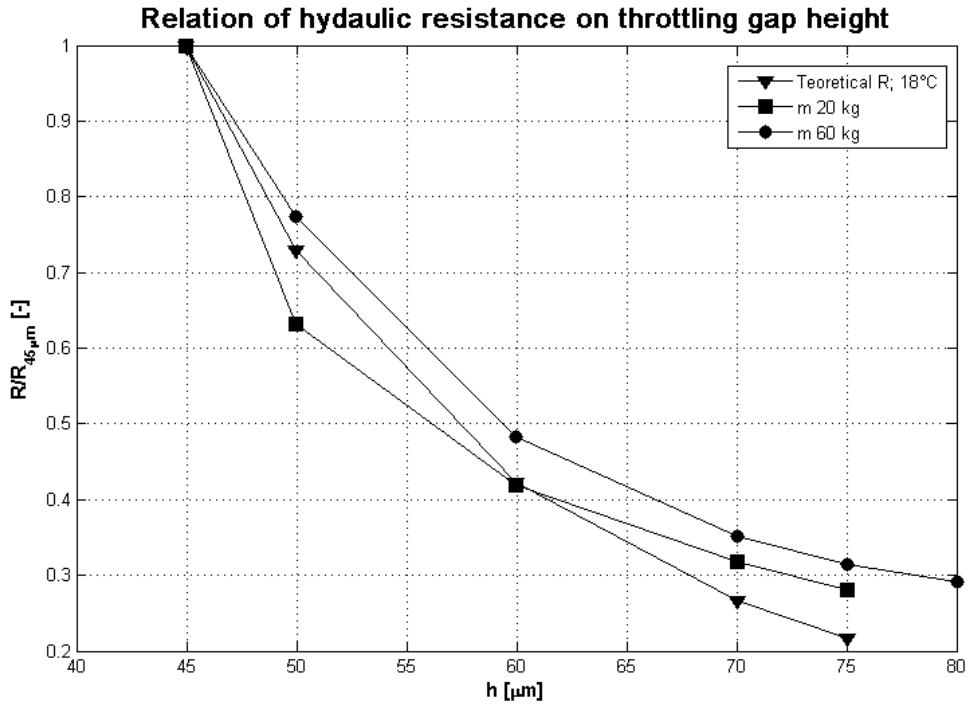

fig. 59: Hydraulic resistance of HS tilted cell

As can be seen in fig. 59, measured and theoretical values correlate closely even though that mathematical model describes HS pocket without tilting. In this case, an effect of throttling gap height change to hydraulics resistance is significantly higher than an effect of pocket tilting.

Therefore, the mathematical model is sufficient enough. HS cell behaves as was expected. Experiments with four actively controlled HS pockets can be conducted. For more information a behaviour of tilted HS pocket is described in [53], [54] and [55].

6.4 Gap height control

In this experiment steady state throttling gap height was measured. In the first stage of then experiment, throttling gap height was set to zero. It means that proportional valves are fully closed. Actual gap height is given by real dimensions of capillaries. As can be seen in fig. 60, gap height does not equal 50 μm as computed in chapter 4.1. The difference between reality and computed value is induced mainly by inaccuracy of capillary manufacturing. Then throttling gap height was set to 50 μm and the control system reached desired position. The following procedure consist of 5 μm steps until 70 μm gap height is reached. As can be seen in fig. 60, the difference between set and measured value in steady state is below 1 μm.

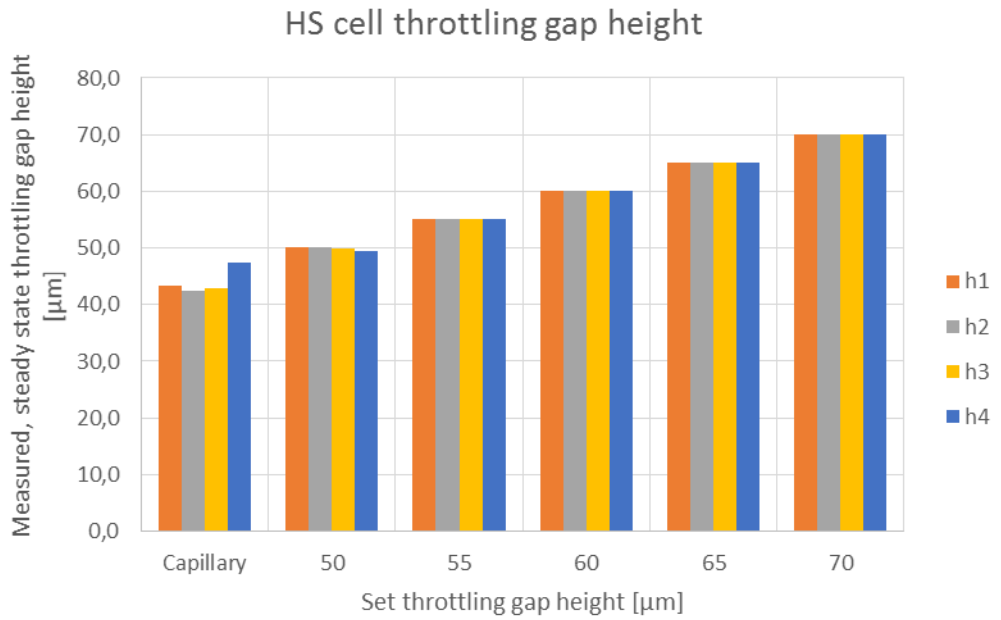

fig. 60: Measured steady state throttling gap height

During the experiment, pressure in HS pocket cavity was measured and is displayed in fig. 61. Actual gap height equals to set gap height. Pressure p_1 was measured in HS pocket number one as illustrated in fig. 48. The same rule applies to all measured pressure values. It was expected that pressure measured in all HS pockets will be similar. Nevertheless pressure differs significantly in HS pocket number two. Miss function of pressure gauges was excluded by switching them and obtaining same pressure results. Similar results were also obtained in different

positions along the feed drive axis length. Therefore, it can be assumed that guiding prism are sufficiently accurate and have negligible impact on the pressure difference. It may be caused by inaccuracy of the working table. Its HS pockets are probably not aligned in a one plane and thus load applied to the pocket two is higher than load applied to other pockets. Smaller pressure differences can be caused by difference of oil temperature depicted in fig. 62 since viscosity it dependent on oil temperature. Temperature is increasing during the experiment because the hydraulic circuit does not contain oil cooling device. The measurement was repeated two times in order to exclude possible measuring mistake.

An oil flow rate was measured during the experiment. Ffig. 63 shows measured oil flow rate. It was expected that flow rate measured in all HS pockets will be similar. Flow rate differs significantly in HS pocket two in case that gap height is high. Miss function of the flow meter was excluded by switching them and obtaining same results. The flow rate difference is probably induced by the same reason as pressure difference.

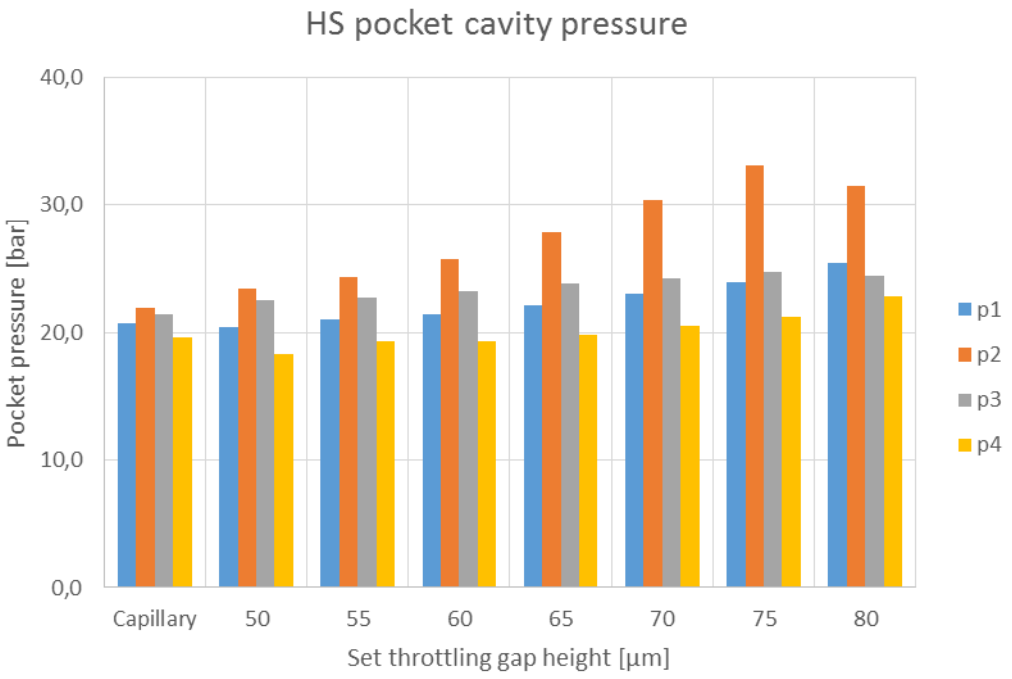

fig. 61: Pressure measured in the cavities of HS pocket

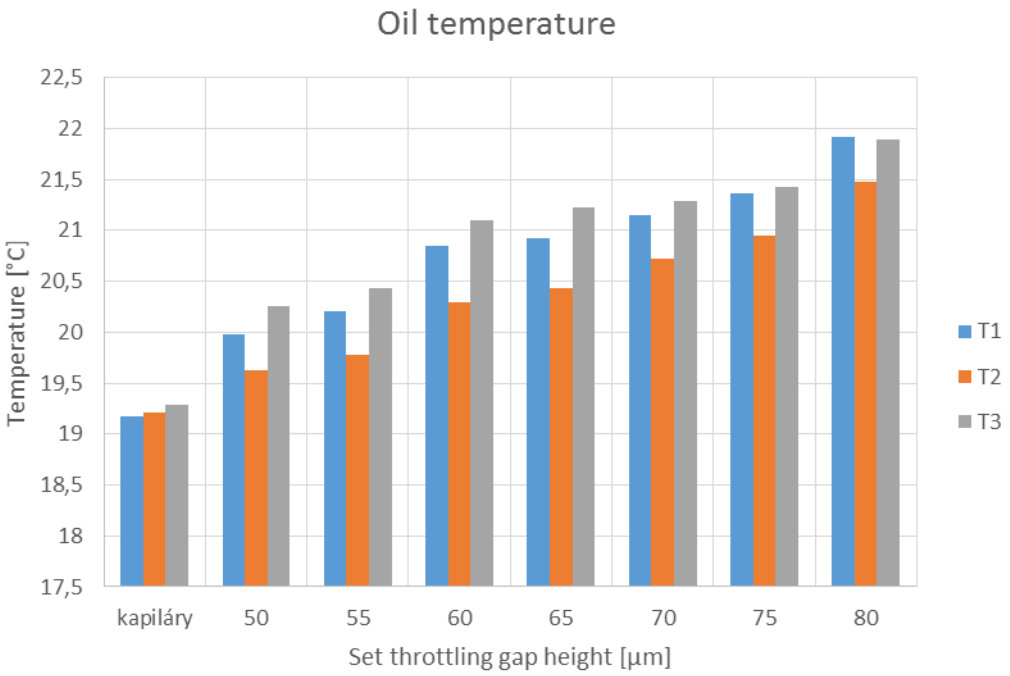

fig. 62: Measured oil temperature

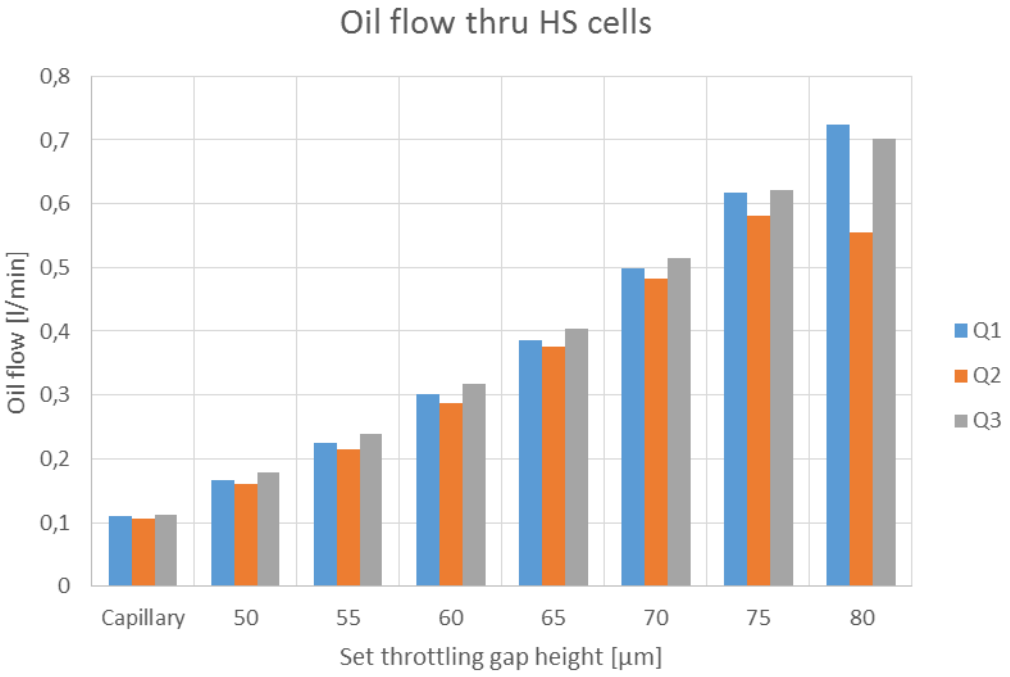

fig. 63: Measured oil flow rate thru HS cells

In this experiment a steady state throttling gap height and other specific quantities were measured. It was expected that pressure and oil flow rate thru all HS cells will be similar. However, measured values differ. It is probably caused by inaccuracy of the working table. Nevertheless, the set gap

height was reached even when disturbance influences were present. On this basis it can be stated that designed system can control throttling gap height and thus move with the working table in vertical direction.

6.5 Working table rotation around x axis

In this experiment an initial throttling gap height is set to 65 um as shown in fig. 64. That means that its centre of gravity is lifted 65 μm in the direction of the z axis above its original position. Then the table rotates around the x axis. The table rotates by steps that equals $5{,}9 \cdot 10^{-4}$degrees and the height difference per step is 5 μm. The steps are repeated until rotation $2{,}9 \cdot 10^{-3}$ degrees is achieved. That is approximately 40 $\mu m/m$. The gap height difference is 20 μm. In the next phase, rotation is set to zero. Then steps are made in opposite direction till rotation around the x axis equals $-2{,}9 \cdot 10^{-3}$ degrees.

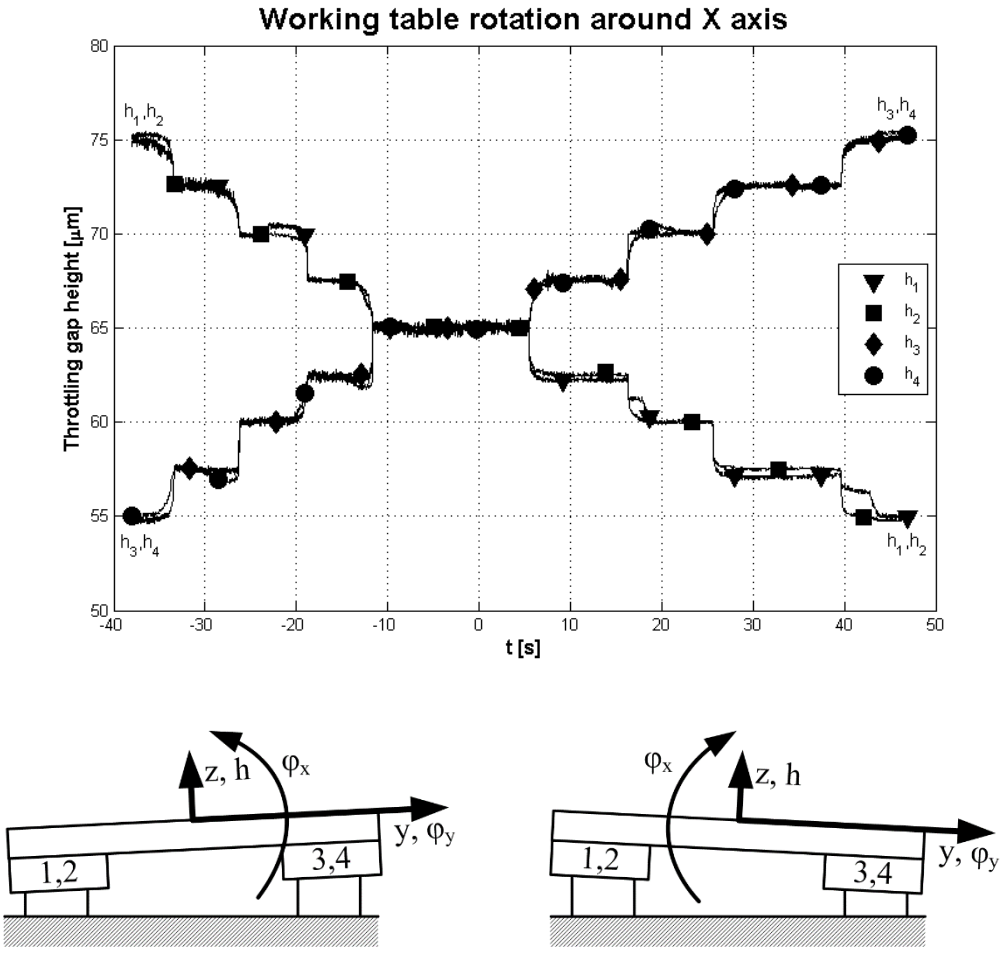

fig. 64 Measured data of working table rotation around x axis (left side schematics corresponds with left part of figure, right schematics corresponds with right part of figure)

fig. 64 is built from two measurements. In the first measurement, the working table was rotated around the x axis and φ_x in positive direction. In the second measurement, the working table was rotated around the x axis and φ_x in negative direction. The second rotation is an inverse movement. Then these two sets of data were analysed and plotted in to one figure for higher clarity. Therefore, time axis has negative values. On the basis of the conducted experiment it is possible to state the designed actively controlled HS cells can rotate with working table around the x axis.

6.6 Working table rotation around y axis

In this experiment initial throttling gap height is set to 65 μm as shown in fig. 65. That means that its centre of gravity is lifted 65 μm in the direction of the z axis above its original position.

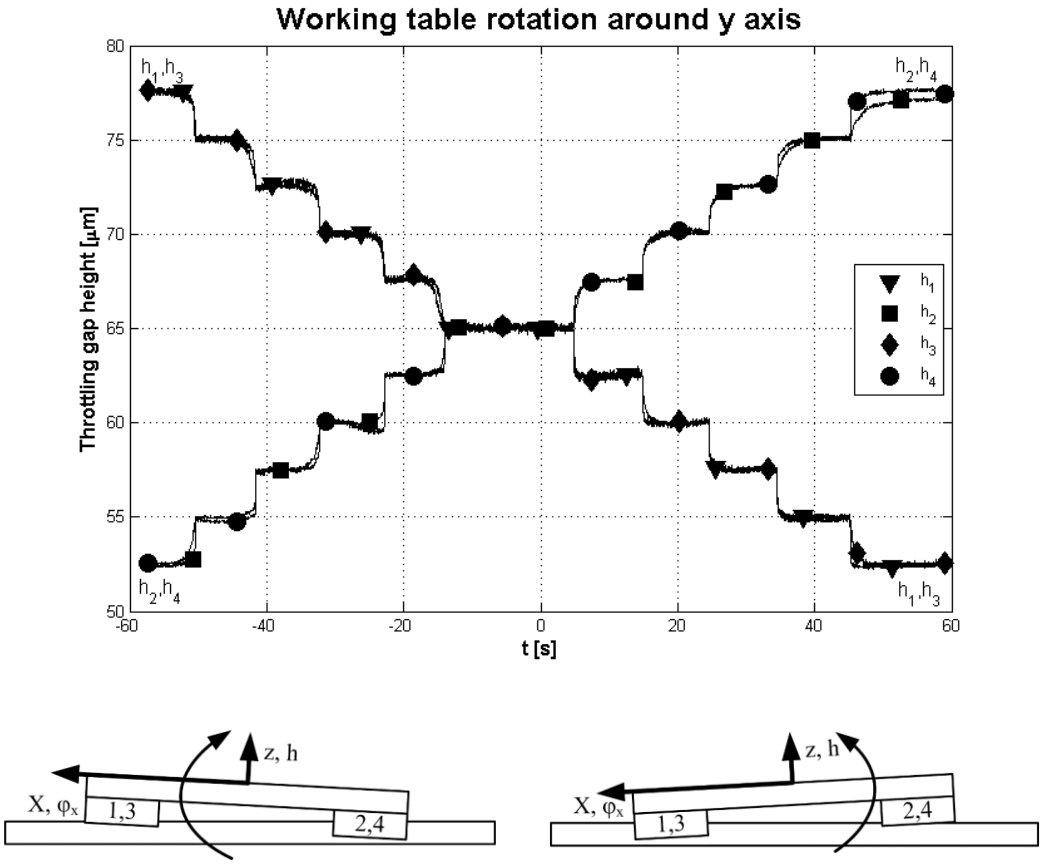

fig. 65: Measured data of working table rotation around y axis (left side schematics corresponds with left part of figure, right schematics corresponds with right part of figure)

Then the table rotates around the y axis. The table rotates by steps. Next, the worktable is rotated $6{,}8 \cdot 10^{-4}$ degrees around the y axis. It is reflected in increase 2,5 μm in gap height h_2 and h_4 of HS pocket and decrease 2,5 μm for h_1 and h_3. Thus the height difference between HS pockets

equals 5 μm.The steps are repeated until rotation $3{,}4 \cdot 10^{-3}$ degrees is achieved. That is approximately 60 μm/m. The gap height $h_{2,4}$ equal 77,5 μm and $h_{1,3}$ equal 52,5 μm. The gap height difference is 25 μm. In the next phase, rotation is set to zero. Then steps are made in opposite direction till rotation around the y axis equals $-3{,}4 \cdot 10^{-3}$ degrees. For clarity, results are also presented in a form of tab. 5. The difference in maximal angle between this and previous measurement is caused by different distance between pockets in the x and y direction. A higher number of steps is needed in case of rotating around the x axis to achieve the same angle of rotation. A range of rotation is higher in case of rotation around the y axis because of HS guideway design. It is possible to freely adjust the step size.

tab. 5: Measured data of working table rotation around y axis

Angle of rotation	Steady state throttling gap height			
φ_y	h_1	h_2	h_3	h_4
[°]	µm	µm	µm	µm
0	65	65	65	65
6,80E-04	62,5	67,5	62,5	67,6
1,36E-03	60,1	70	60,1	70
2,04E-03	57,6	72,6	57,5	72,6
2,72E-03	55	75	55	75,1
3,40E-03	52,6	77,3	52,5	77,5
0,00E+00	65	65	65	65
-6,80E-04	67,6	62,5	67,6	62,6
-1,36E-03	70,1	60	70,1	60
-2,04E-03	72,5	57,4	72,5	57,5
-2,72E-03	75,1	54,9	75,1	55
-3,40E-03	77,6	52,4	77,5	52,5

Measurements indicate that it is possible to rotate with the working table around the y axis in both directions.

6.7 Rotating around x and y axes

The working table was rotated around both x and y axes in this measurement. The schematics with axes designation is depicted in fig. 48. The step size for both axes is the same as in the previous measurements. The initial throttling gap height is set to 65 μm and the working table

first rotates around the x axis and then around the y axis. The rotations around the x and the y axis are alternating. Maximal height difference between the highest and lowest HS pocket is 25 μm.

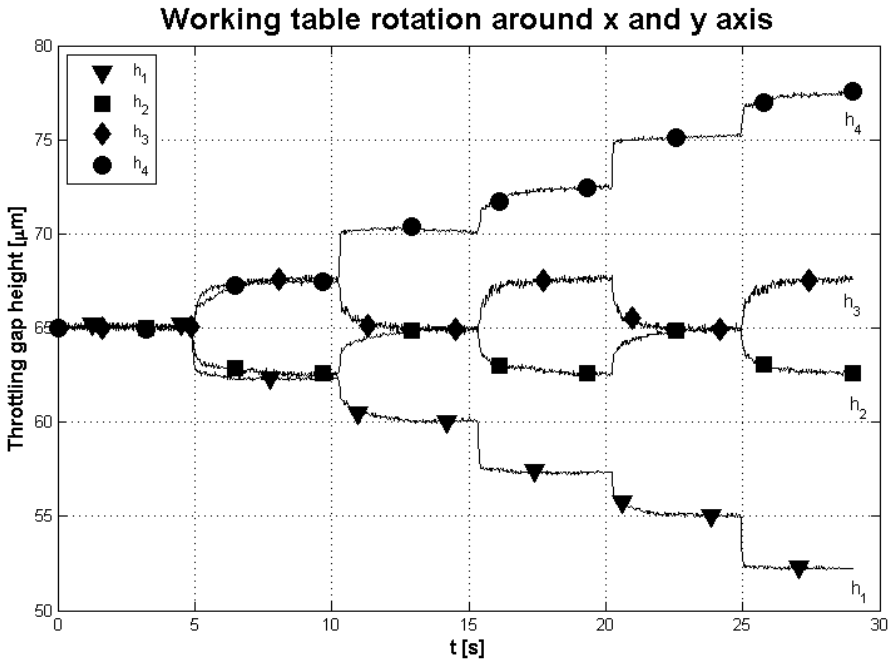

fig. 66: Measured data of working table rotation around x and y axes

The measurement proved that it is possible to rotate with working table around two axes simultaneously.

6.8 Discussion and interpretation of results

First measurement was performed with four PM controllers in order to obtain reference values. Measured throttling gap height with PM controllers is 30 μm. This value is too low for the purpose of other experiments with active HS cells. Collisions between guiding prism and HS pocket could occur. Therefore capillaries length was computed for throttling gap height 50 μm.

In the next experiment a steady state throttling gap height was measured when the working table was indexing in the vertical direction. Pressure, flow rate and temperature were measured. It was expected that pressure and oil flow rate thru all HS cells will be similar in all four HS cells. However, measured values differed. It is probably caused by inaccuracy of the working table. Nevertheless, the set gap height was reached even when disturbance influences were present. On this basis it can be stated that designed system can control throttling gap height and thus move with the working table in the vertical direction.

Next measurement addressed the effect of pocket tilting to HS cell hydraulic resistance. Measured and theoretical values correlate closely even though that mathematical model describes HS pocket without tilting. In this case, the effect of throttling gap height change to hydraulics resistance is significantly higher than the effect of pocket tilting. Therefore, the mathematical model is sufficient enough. HS cell behaves as was expected.

Next experiments deal with rotation of working table around x and y axes. On its bases it can stated that designed system can control rotation around two axes simultaneously. This can be advantageously used for MT compensations.

Results interpretation

Obtained results are interpreted by using the example of application from chapter 3.6. The chapter addresses cutting tool position compensation for the horizontal milling machine. A rigid ram is assumed. Analysis is geometrical. When the ram is extended the cutting tool position shifts in the vertical direction and the end of the ram is also tilted. Thus the cutting tool displaced is position and angular. The displacement is induced by deformation of other machine parts such as, the stand, the bed, etc. In order to compensate the displacement, the slider and the ram are rotated as depicted by arrow in fig. 25. It is assumed that the ram is extended by 2,2 m and the distance between HS cells is 0,42 m (fig. 67). Then, if the maximal rotation achieved in experiment $3{,}4 \cdot 10^{-3}$ degrees is applied to the rigid ram a possible vertical displacement compensation is 0,15 mm which is in the order of real displacements. Whether the value is sufficient depends on specific case. Rotation $3{,}4 \cdot 10^{-3}$ is also in order of real angular deformations. The compensation of angular displacement is even more significant since angular deformations are more challenging to compensate. Moreover, the vertical shift can be compensated by the drive of vertical axis of the horizontal milling machine. For the ram extension greater than three meters, reached values of rotation are not sufficient to compensate the vertical displacement. It such case it is advantageous to use compensation by HS guideways as additional compensation method to traditional compensation methods for increasing their accuracy. Suitable compensation method is for example the counterbalance system. Then active HS guideway can compensate the angular displacement.

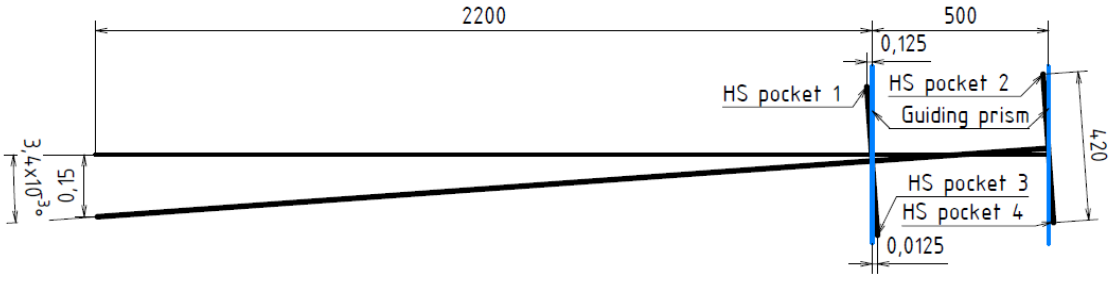

fig. 67: Sketch for compensation estimation

7 Conclusion

The aim of this thesis is to design and experimentally verify system for active control of hydrostatic (HS) cell throttling gap height of HS guideway. The system is to be used for machine tool geometrical and manufacturing error compensation.

A research addressing HS guideways and throttling gap height control systems was conducted in order to find the most feasible system for multiple HS cells control. The gap height control systems were divided into the three categories accordingly to control principle and regulation possibilities. General gap height control systems such as, flow restrictors and flow dividers, control gap height in a limited extent. More complex control systems included in the second category make use of different kinds of feedback to control constant gap height. The last category contains actively controlled systems that control gap height accordingly to an external signal. Various control systems with active control were compared and a control system with electronic feedback was chosen for further elaboration because the electronic feedback system was the most suitable for multiple HS cell control.

In the next phase the system for HS cell throttling gap height control was designed. HS cell was mathematically described and a mathematical formula was obtained. The mathematical formula provides us with information that it is beneficial to control oil flow rate thru HS cell to control the gap height. Then a hydraulic circuit for flow rate to HS cell control was designed and control system with a PI regulator was developed. The hydraulic circuit combines advantages of capillary that bypassed a proportional pressure relief valve in one device that was referred to as a hybrid hydrostatic controller (H2C). Combination of the capillary and the proportional valve had stabilising effect on the control system. The control system is a closed loop system. In order to close feedback between a chosen controller (CompactRIO) and the controlled system, a suitable length gauge (eddy current sensor) was selected. The control system was programmed in LabVIEW. In the next phase, hydraulic circuit and control system were expanded for multiple HS cell control. The designed system was then assembled and tested on testing stand STD30. The stand STD30 is a linear feed drive axis with a working table mounted on HS guideway. A series of experiments confirmed that the designed system control throttling gap height of HS cell. Moreover, the system enable us to control HS cells independently and simultaneously in real time. As a result, it is possible to rotate with working table to some extent around two axes.

Measured data were geometrically interpreted by using the example of the horizontal milling machine and a cutting toll position compensation. HS guideway that can reach similar maximal values as tested HS guideway could compensate the cutting toll position displacement of smaller

horizontal milling machines. Furthermore, HS guideway with actively controlled HS cells can be used as additional compensation system for large machine tools. Then it is advantageous to compensate the angular displacement of cutting tool by the HS guideway with actively controlled HS cells. Moreover, the system can compensate machine tool geometrical errors and known manufacturing errors.

On the basis of conducted experiments can be concluded that proposed compensation principle is feasible for use in machine tool industry, nevertheless further research should address dynamical behaviour, positioning accuracy and possibly an increase of rotation range.

8 Bibliography

1. PENTON MEDIA, I. *Machine Design* [online]. 2016. Dostupné také z: http://machinedesign.com/bearings/new-ways-damp-vibration-linear-axes
2. WECK, M. a C. BRECHER. *Werkzeugmaschinen - Konstruktion und Berechnung*. Berlín: Springer-Verlag, 2006. ISBN 10 3-540-22502-1.
3. *Advantages over rolling-element bearings* [online]. HYPROSTATIK SCHÖNFELD GMBH, ed. [cit. 2015]. Dostupné z: http://hyprostatik.de/vorteilegegenuberwaelzsystemen/?L=2
4. MAREŠ, M. E. STACH a T. HOLKUP. A general method for design optimization of hydrostatic bearings for machine tools. In: *Proceedings of the 15th International Conference on Machine Design and Production*. Denizli: 2012.
5. XUE, F. et al. Research on error averaging effect of hydrostatic guideways. Elsevier Inc. 2012 roč. XXXVI, s. 84-92.
6. ZELENÝ, J. Servostatics guideways - a new kind of hydraulically operating guideways for machine tools. In: *Advances in Machine Tool Design and Research 1969: Proceedings of the 10th International M.T.D.R. Conference, University of Manchester Institute of Science and Technology*. Oxford: Pergamon Press, 1970, s. 193-201.
7. ROWE, B. W. *Hydrostatic, Aerostatic and Hybrid Bearing Design*. Elsevier, 2012. ISBN 978-0-12-396994-1.
8. STACH, E. M. MAREŠ a M. SULITKA. Comparison of hydrostatic regulation system of thrust bearing of turntable. In: *Proceedings of the 22nd International Conference on Hydraulics and Pneumatics,* sv. 22. 2013, s. 151-58. ISBN 978-80-248-3136-7.
9. BASSANI, R. Hydrostatic systems supplied throught flow dividers. Elsevier Science Ltd. 2001 roč. XXXIV, s. 25-38.
10. STACH, E. *Regulace průtoku, řízení*. Prague: CTU in Prague, Faculty of machanical engineering, RCMT, 2012. Research report number V-12-012.
11. HYPROSTATIK SCHONFELD GMBH. *PM controller and jet pump*. 2015. Technické informace [cit. 2015].
12. YANG, S. et al. Hydrostatic worktable performance of an ultra-precision optical aspheric machine tool. In: *Procedings of 13th CIRP conference on Computer Aided Tolerancing*. Elsevier B.V. 2015, s. 187-91.
13. ZOLLERN GMBH & CO. KG. *Hydrostatic Bearing Systems*. 2015. Katalog [cit. 2015].
14. HUANG, H.C. a P.C. YAUNG. *Self-compensating hydrostatic journal bearing*. United states patent, US 20120141055 A1. 2010-12-03.
15. SLOCUM, A. H. *Precision Machine Design*. Prentice Hall, 1992. ISBN 0136909183.
16. SLOCUM, A. H. a E. WASH. *Self-Compensating hydrostatic linear motion bearing*. United States Patent, US005104237. 1990-11-08.

17. YOSHIMOTO, S. Y. ANNO a T. TANAKA. Hydrostatic thrust bearing with a self-controlled restrictor using a floating disk. (Step response …. Japan Society of Mechanical Engineers, 1991 roč. LVII, s. 3386-92. ISSN 0387-5024.

18. NOT, K. *FLOW LIMITERS AND TO HYDROSTATIC BEARING ARRANGEMENTS INCORPORATING FLOW LIMITERS*. Invalid patent, GB1487080 (A). 1977-09-28.

19. KANE, N. R. J. SIHLER a A. H. SLOCUM. A hydrostatic rotary bearing with angled surface self-compensation. Elsevier Science Inc. 2003 roč. MMMMMCCCXXI, s. 1-15.

20. ZUO, X. et al. Comparative performance analysis of conical hydrostatic bearings compensated by variable slot and …. Elsevier Ltd. 2013 roč. LXVI, s. 83-92.

21. ZELENÝ, J. *Control system for machine tool members*. United States Patent, US 3720134 A. 1970-03-03.

22. PARK, C. H. et al. Compensation for five DOF motion errors of hydrostatic feed table by utilizing actively controlled …. In: *Precision Engineering*, sv. 30. Elsevier Inc. 2006, s. 299-305.

23. PARK, C.H. a H.S. LEE. *Variable capillary apparatus for hydrostatic bearing and motion error compensating method using same*. United States Patent, US006120004. 1998-01-16.

24. HESSELBACH J. A.K. C. Active hydrostatic bearing with magnetorheological fluid. AMER INST PHYSICS, 2003 roč. XCIII, s. 8441-43. ISSN 0021-8979.

25. GULDBAKKE, J. M. a J. HESSELBACH. Development of bearings and a damper based on magnetically controllable fluids. Bristol: IOP PUBLISHING LTD, 2016 roč. XVIII, s. S2959-72. ISSN 0953-8984.

26. Magnetorheological fluid. *Wikipedia, free enciklopeida* [online]. 2016. Dostupné také z: https://en.wikipedia.org/wiki/Magnetorheological_fluid

27. GLEICHNER, A. *Aktive hydrostatische Führungen mit elektrorheologischen Flüssigkeiten*. Technische Universität Braunschweig, 2000. Doctoral thesis. ISBN 978-3-8027-8647-1. Institut für Werkzeugmaschinen und Fertigungstechnik.

28. ABEL-KEILHACK, C. *Magnetische Flüssigkeiten als medium in hydrostatischen Lagern*. Braunschweig: Technische Universität Braunschweig, Vulkan-Verlag, Essen, 2004. Doctoral thesis. ISBN 978-3-8027-8678-5. Institut für Werkzeugmaschinen und Fertigungstechnik.

29. HASHIZUME, , et al. Characteristic Control of Table System Using Electrorheological Fluid : Comparison of Colloidal ERF …. Japan Society of Mechanical Engineers, 1995 roč. LXI, s. 4105-10. ISSN 03875024.

30. PATZWALD, R. *Magnetische Flüssigkeiten als Schmierstoff in hydrodynamischen Gleitlagern*. Berlin: Technische Universität Berlin, Fakultät V - Verkehrs- und Maschinensysteme, 2001. Doctoral thesis.

31. YOHICHI, N. et al. Displacement control of water hydrostatic thrust bearing by hybrid use of constant resistance …. Leuven: euspen, 2015, s. 263- 64. 14: 978-0-9566790-7-9.

32. BENTLY, D. E. a J. W. GRANT. *Hydrostatic bearing for supporting rotating equipment, a fluid handling system associated …*. Invalid patent, US 5769545 A. 1998-12-04.

33. LAZÁK, T. E. STACH a M. SULITKA. *Patentová rešerše systémů pro kompenzace svěšování smykadel horizontálních frézovacích strojů*. Praha: ČVUT v Praze, Fakulta strojní, RCMT, 2016. Výzkumná zpráva V-16-008.

34. *2-Way Proportional Flow Control Valve Series DUR*L06* [online]. PARKER, ed. 2016. Dostupné také z: http://ph.parker.com/us/en/dur-l06-2-way-proportional-flow-control-valve

35. *Proportional Directly Operated Pressure Relief Valve* [online]. HYTOS, A. ed. 2016. Dostupné také z: http://www.argo-hytos.com/products/valves/proportional-valves/sr1p2-a2.html

36. *Control System | Closed Loop Open Loop Control System* [online]. ELETRICAL4U, ed. 2016. Dostupné také z: http://www.electrical4u.com/control-system-closed-loop-open-loop-control-system/

37. MAIXNER, L. *Mechatronika*. Brno: Computer Press, 2006. ISBN 80-251-1299-3.

38. *Arduino Mega 2560* [online]. AFRICA, R. E. S. , ed. 2016. Dostupné také z: https://www.riecktron.co.za/en/product/211

39. *Raspberry PI* [online]. ADAFRUIT, ed. 2016. Dostupné také z: https://www.adafruit.com/category/105

40. *Arduino - ArduinoBoardMega2560* [online]. ARDUINO, ed. 2016. Dostupné také z: https://www.arduino.cc/en/Main/ArduinoBoardMega2560

41. *Raspberry Pi 3 Model B - Raspberry Pi* [online]. PI, R. ed. 2016. Dostupné také z: https://www.raspberrypi.org/products/raspberry-pi-3-model-b/

42. *PROGRAMOVATELNÉ AUTOMATY* [online]. TECO, ed. 2016. Dostupné také z: http://www.tecomat.com/wpimages/other/DOCS/cze/TXV00430_01_Foxtrot_CP_1000.pdf

43. *Co je Tecomat TC700?* [online]. TECO, ed. 2016. Dostupné také z: http://www.tecomat.com/clanek-857-co-je-tecomat-tc700_.html

44. *CompactRIO Controller* [online]. CORPORATION, N. I. ed. 2016. Dostupné také z: http://www.ni.com/white-paper/52251/en/#toc2

45. *NI CompactRIO Advisor - National Instruments* [online]. CORPORATION, N. I. ed. 2016. Dostupné také z: http://ohm.ni.com/advisors/crio/pages/common/classic/summary.xhtml?conversationContext=1

46. *sbRIO-9637* [online]. CORPORATION, N. I. ed. 2016. Dostupné také z: http://sine.ni.com/nips/cds/view/p/lang/cs/nid/213224

47. MARTINEK, R. *Senzory v průmyslové praxi*.. Praha: nakladatelství BEN - technická literatura, 2014. ISBN 80-7300-114-4.

48. *Délková měřicí technika MESING* [online]. KYSELÁK, M. ed. 2016. Dostupné také z: http://www.mesing.cz/index.php?s=snimace&o=15

49. *Eddy-Current Linear Displacement Sensors* [online]. PRECISION, L. ed. [cit. 2016]. Dostupné z: http://www.lionprecision.com/eddy-current-sensors/

50. *Snímače dráhy na principu vířivých proudů* [online]. PROFESS, ed. 2016. Dostupné také z: http://www.profess.cz/mms/cs/produkty/snimace-drahy-na-principu-virivych-proudu

51. LARSSON, a A. LIND. *DEVICES FOR MEASURING AND CONTROLLING FLUID FILM THICKNESS OF A HYDROSTATIC OR HYDRODYNAMIC BEARING*. Patent, WO2008097157 (A1). 2009-08-06.

52. *Position Sensors* [online]. ELETRONICSHUB, ed. 2016. Dostupné také z: http://www.electronicshub.org/position-sensors/

53. STACH, E. J. FALTA a M. SULITKA. Analytical Solution of Hydrostatic Pocket Tilting. In: *Proceedings of the 21st International Conference Engineering Mechanics 2015*. Praha: 2015, s. 288-89. ISBN 978-80-86246-42-0.

54. STACH, E. J. FALTA a M. SULITKA. Analytical Solution of Hydrostatic Pocket Tilting. Trans Tech Publications, 2016 roč. DCCCXXI, s. 113-19. ISBN 978-3-03859-503-8.

55. VAN BEEK, A. a R. A. J. VAN OSTAYEN. Analytical solution for tilted hydrostatic multi-pad thrust bearings of infinite length. In: *Tribology International*, sv. 30. Elsevier Ltd. 1997, s. 33-39.

9 Lists

9.1 List of tables

9.2 List of figures

9.3 List of software

- MS Office
- Autodesk Inventor professional 2013
- LabVIEW 2014 and Measurement & Automation Explorer (MAX)
- Eagle 7.5
- Matlab 2011b

9.4 Appendices list

9.4.1 Text appendices

- Six measurement protocols
- Proportional Directly Operated Pressure Relief Valve SR1P2-A2/H12-24 – catalogue list
- List of patents addressing horizontal milling machine compensations
- Male connector 24° flareless GE06LM – catalogue list
- Metric hollow hex plugs VSTI10X1ED – catalogue list

9.4.2 Technical drawings

- HYBRID HYDROSTAIC CONTROLLER (H2C) H2C-01-01-A
- C+PV HYDRULIC CUBE H2C-01-01
- INLET HYDROULIC CUBE H2C -01-02
- EB HYDRAULIC CUBE H2C -01-03
- CAPILLARY H2C -01-04
- BILL OF MATERIAL H2C-01-01-K

9.4.3 Electronic appendices

Electronic appendices includes everything from chapter 9.4.1 and 9.4.2. Moreover, it electronic appendices contain following:

- Electronic version of the thesis
- Measured data
- LabVIEW program for active control of multiple HS cells

FACULTY OF MECHANICAL ENGINEERING

Department of production machines and equipment

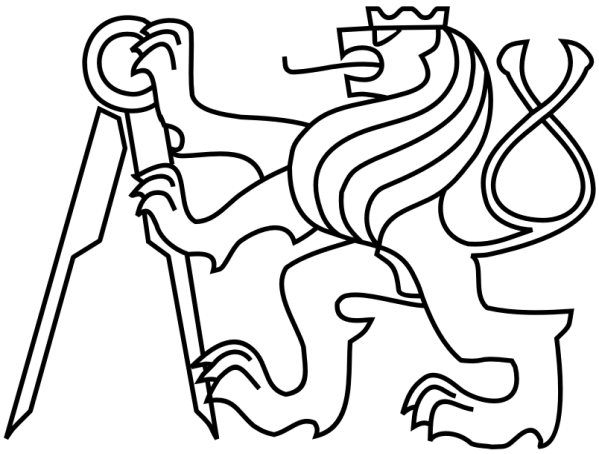

Master thesis

Active control of hydrostatic pocket throttling gap height

Text appendices

2016 **Bc. Tomáš Lazák**

THE CZECH TECHNICAL UNIVERSITY IN PRAGUE

Measurement protocol

Department of Production Machines and Equipment

Date	Number	Place of measurement	Testing stand	Author
18.11.2015	1	U12135 - Horská, Praha	STD 30	Tomáš Lazák

List of used devices and sensors

Type	Manufacturer/ supplier	Designation	Measuring range	Accuracy	Placement
Temperature gauge		Pt 100	-50 + 200 °C	Třída A	-
Pressure gauge	BHV senzory s.r.o.	DMP 333	0 - 250 bar rel	≤±0,5%	-
Pressure gauge	BHV senzory s.r.o.	DMP 333	0 - 50 bar rel	≤±0,5%	-
Flow meter	BOPP & REUTHER	Miniflow 015	0,1 - 1,0 l/min	≤±1% o.r.	-
Length gauge	Mesing	T102F	-2÷2 mm		one for 1,2,3,4
Proportional valve	Argo-hitos	SR1P-A2/H12-24E2			-
Service master Plus	Parker	SCM-500-01-00			-
Real time controller	National Instruments	NI CRIO-9025			-
Real time controller	National Instruments	Ni sbRiio-9637			-
Data acquisition system	National Instruments	Ni cDAQ-9188			yes
AO module	National Instruments	NI 9263			-
AI module	National Instruments	NI 9219			yes
AI module	National Instruments	NI 9205			-

*linearity error 0,25 % in range ±1mm at a temperature 20 °C, repeatability 0,01 μm

Measurement conditions			**Schematics**
Hydrostatic pockets	4 * 40 x 40, land 8		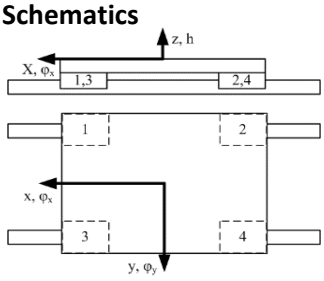
Control system program	RT_mainVI_hydrolinear_v1		
Oil type	ISO VG 46, VI 149		
Pump pressure	50	bar	
Room temperature	19	°C	
Oil temperature-measurement start	21	°C	
Oil temperature-measurement end	22	°C	
Applied mass (m - x -y)	20and60 - 0 - 0	kg - mm - mm	

Designation:	**PM controller - gap height measurement**

Measurement description:

Gap heiht of all HS pockets was measured 5 times. One gap height was measured at a time

Average gap height controlled by PM controller is 30 um

Measured data

i	h_1	h_2	h_3	h_4
[-]	[mm]	[mm]	[mm]	[mm]
1	0,028	0,027	0,029	0,026
2	0,029	0,032	0,031	0,028
3	0,029	0,032	0,031	0,028
4	0,029	0,033	0,031	0,028
5	0,029	0,033	0,031	0,028

THE CZECH TECHNICAL UNIVERSITY IN PRAGUE

Measurement protocol

Department of Production Machines and Equipment

Date	Number	Place of measurement	Testing stand	Author
24.3.2016	2	U12135 - Horská, Praha	STD 30	Tomáš Lazák

List of used devices and sensors

Type	Manufacturer/ supplier	Designation	Measuring range	Accuracy	Placement
Temperature gauge		Pt 100	-50 + 200 °C	Třída A	-
Pressure gauge	BHV senzory s.r.o.	DMP 333	0 - 250 bar rel	≤±0,5%	-
Pressure gauge	BHV senzory s.r.o.	DMP 333	0 - 50 bar rel	≤±0,5%	2
Flow meter	BOPP & REUTHER	Miniflow 015	0,1 - 1,0 l/min	≤±1% o.r.	2
Length gauge	Mesing	T102F	-2÷2 mm		2, 4
Proportional valve	Argo-hitos	SR1P-A2/H12-24E2			2, 4
Service master Plus	Parker	SCM-500-01-00			-
Real time controller	National Instruments	NI CRIO-9025			yes
Real time controller	National Instruments	Ni sbRiio-9637			-
Data acquisition system	National Instruments	Ni cDAQ-9188			yes
AO module	National Instruments	NI 9263			yes
AI module	National Instruments	NI 9219			yes
AI module	National Instruments	NI 9205			yes

*linearity error 0,25 % in range ±1mm at a temperature 20 °C, repeatability 0,01 μm

Measurement conditions			**Schematics**
Hydrostatic pockets	4 * 40 x 40, land 8		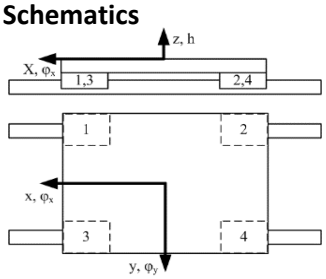
Control system program	RT_mainVI_hydrolinear_v6		
Oil type	ISO VG 46, VI 149		
Pump pressure	50	bar	
Room temperature	19	°C	
Oil temperature-measurement start	19	°C	
Oil temperature-measurement end	20	°C	
Applied mass (m - x -y)	60 - 0 - 0	kg - mm - mm	

Designation:	**Hydraulic resistance - efect of HS pocket tilting**

Measurement description:

HS pockets (2, 4) are astively controlled

HS pockets (1, 3) are controlled by PM controller and keep gap height 30 um

Working table is loaded by 20 kg

Working table is rotated by steps aroun y axis

Working table is loaded by 60 kg

Working table is rotated by steps aroun y axis

Values of hydraulic resistance are computed and compared with theoretical values

Measured and theoretical values correlate closely even though that mathematical model describes HS pocket without tilting. In this case, an effect of throttling gap height change to hydraulics resistance is significantly higher than effect of pocket tilting

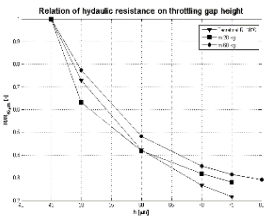

THE CZECH TECHNICAL UNIVERSITY IN PRAGUE

Measurement protocol

Department of Production Machines and Equipment

Date	Number	Place of measurement	Testing stand	Author
24.3.2016	3	U12135 - Horská, Praha	STD 30	Tomáš Lazák

List of used devices and sensors

Type	Manufacturer/ supplier	Designation	Measuring range	Accuracy	Placement
Temperature gauge		Pt 100	-50 + 200 °C	Třída A	1,2,3
Pressure gauge	BHV senzory s.r.o.	DMP 333	0 - 250 bar rel	≤±0,5%	4
Pressure gauge	BHV senzory s.r.o.	DMP 333	0 - 50 bar rel	≤±0,5%	1,2,3
Flow meter	BOPP & REUTHER	Miniflow 015	0,1 - 1,0 l/min	≤±1% o.r.	1,2,3
Length gauge	Mesing	T102F	-2÷2 mm	*	1,2,3,4
Proportional valve	Argo-hitos	SR1P-A2/H12-24E2			1,2,3,4
Service master Plus	Parker	SCM-500-01-00			-
Real time controller	National Instruments	NI CRIO-9025			yes
Real time controller	National Instruments	Ni sbRiio-9637			-
Data acquisition system	National Instruments	Ni cDAQ-9188			yes
AO module	National Instruments	NI 9263			yes
AI module	National Instruments	NI 9219			yes
AI module	National Instruments	NI 9205			yes

*linearity error 0,25 % in range ±1mm at a temperature 20 °C, repeatability 0,01 μm

Measurement conditions			
Hydrostatic pockets	4 * 40 x 40, land 8		**Schematics**
Control system program	RT_mainVI_hydrolinear_v13		
Oil type	ISO VG 46, VI 149		
Pump pressure	50	bar	
Room temperature	18	°C	
Oil temperature-measurement start	19	°C	
Oil temperature-measurement end	22	°C	
Applied mass (m - x -y)	0 - 0 - 0	kg - mm - mm	

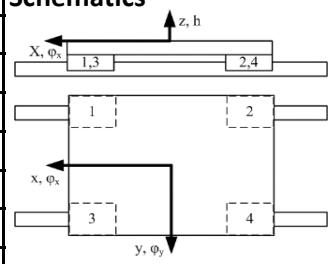

Designation:	**Hap height control**

Measurement description:

In this measuremen a steady state throttling gap height is measured
Firstly, proportonal valve is closed and gap height is given by capillaries
Then gap height is set to 50 um
The gap height is increased by 5 um steps up to 70 um
Pocket cavity pressure, oil flow rate and oil temperature is measured

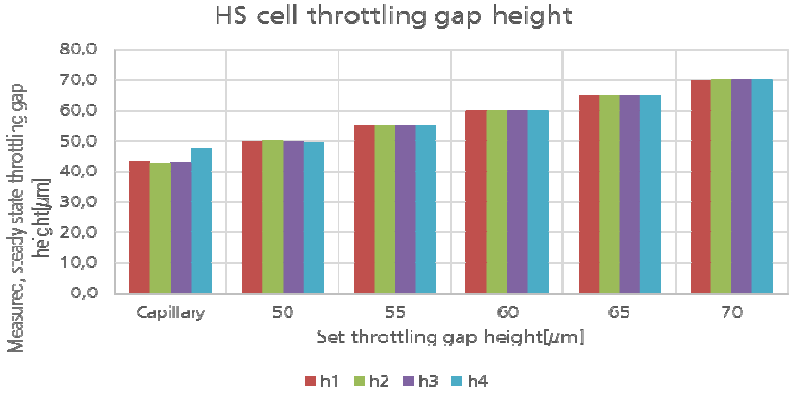

THE CZECH TECHNICAL UNIVERSITY IN PRAGUE

Measurement protocol

Department of Production Machines and Equipment

Date	Number	Place of measurement	Testing stand	Author
28.3.2016	4	U12135 - Horská, Praha	STD 30	Tomáš Lazák

List of used devices and sensors

Type	Manufacturer/ supplier	Designation	Measuring range	Accuracy	Placement
Temperature gauge		Pt 100	-50 + 200 °C	Třída A	1,2,3
Pressure gauge	BHV senzory s.r.o.	DMP 333	0 - 250 bar rel	≤±0,5%	4
Pressure gauge	BHV senzory s.r.o.	DMP 333	0 - 50 bar rel	≤±0,5%	1,2,3
Flow meter	BOPP & REUTHER	Miniflow 015	0,1 - 1,0 l/min	≤±1% o.r.	1,2,3
Length gauge	Mesing	T102F	-2÷2 mm	*	1,2,3,4
Proportional valve	Argo-hitos	SR1P-A2/H12-24E2			1,2,3,4
Service master Plus	Parker	SCM-500-01-00			-
Real time controller	National Instruments	NI CRIO-9025			yes
Real time controller	National Instruments	Ni sbRiio-9637			-
Data acquisition system	National Instruments	Ni cDAQ-9188			yes
AO module	National Instruments	NI 9263			yes
AI module	National Instruments	NI 9219			yes
AI module	National Instruments	NI 9205			yes

*linearity error 0,25 % in range ±1mm at a temperature 20 °C, repeatability 0,01 μm

Measurement conditions		
Hydrostatic pockets	4 * 40 x 40, land 8	
Control system program	RT_mainVI_hydrolinear_v13	
Oil type	ISO VG 46, VI 149	
Pump pressure	50	bar
Room temperature	18	°C
Oil temperature-measurement start	19	°C
Oil temperature-measurement end	21	°C
Applied mass (m - x -y)	0 - 0 - 0	kg - mm - mm

Schematics

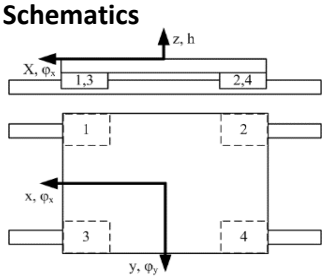

Designation:	**Working table rotation around X axis**

Measurement description:

Throttling gap height is set to 65 um

Working table is rotated by steps around x axis and rotation is positive

Throttling gap height is set to 65 um

Working table is rotated by steps around x axis and rotation is negative

Maximal measured gap heiht difference is 20 um

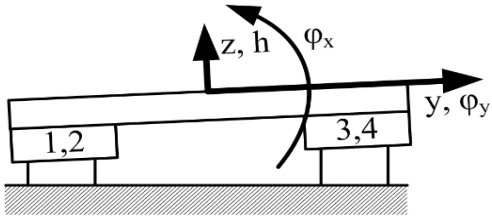

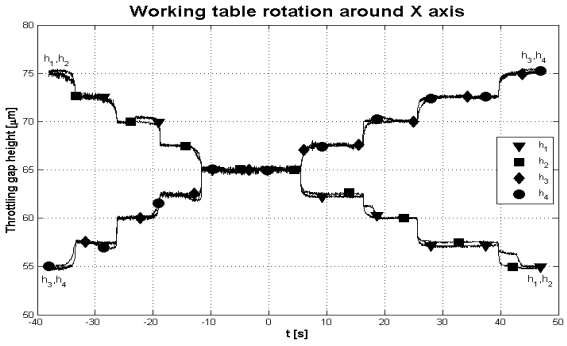

THE CZECH TECHNICAL UNIVERSITY IN PRAGUE

Measurement protocol

Department of Production Machines and Equipment

Date	Number	Place of measurement	Testing stand	Author
28.3.2016	5	U12135 - Horská, Praha	STD 30	Tomáš Lazák

List of used devices and sensors

Type	Manufacturer/ supplier	Designation	Measuring range	Accuracy	Placement
Temperature gauge		Pt 100	-50 + 200 °C	Třída A	1,2,3
Pressure gauge	BHV senzory s.r.o.	DMP 333	0 - 250 bar rel	≤±0,5%	4
Pressure gauge	BHV senzory s.r.o.	DMP 333	0 - 50 bar rel	≤±0,5%	1,2,3
Flow meter	BOPP & REUTHER	Miniflow 015	0,1 - 1,0 l/min	≤±1% o.r.	1,2,3
Length gauge	Mesing	T102F	-2÷2 mm	*	1,2,3,4
Proportional valve	Argo-hitos	SR1P-A2/H12-24E2			1,2,3,4
Service master Plus	Parker	SCM-500-01-00			-
Real time controller	National Instruments	NI CRIO-9025			yes
Real time controller	National Instruments	Ni sbRiio-9637			-
Data acquisition system	National Instruments	Ni cDAQ-9188			yes
AO module	National Instruments	NI 9263			yes
AI module	National Instruments	NI 9219			yes
AI module	National Instruments	NI 9205			yes

*linearity error 0,25 % in range ±1mm at a temperature 20 °C, repeatability 0,01 μm

Measurement conditions		
Hydrostatic pockets	4 * 40 x 40, land 8	
Control system program	RT_mainVI_hydrolinear_v13	
Oil type	ISO VG 46, VI 149	
Pump pressure	50	bar
Room temperature	18	°C
Oil temperature-measurement start	19	°C
Oil temperature-measurement end	21	°C
Applied mass (m - x -y)	0 - 0 - 0	kg - mm - mm

Schematics

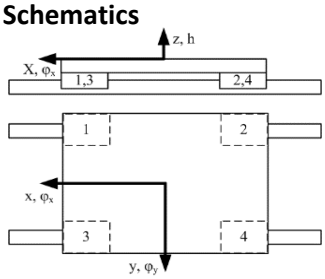

Designation:	**Working table rotation around Y axis**

Measurement description:

Throttling gap height is set to 65 um

Working table is rotated by steps around y axis and rotation is positive

Throttling gap height is set to 65 um

Working table is rotated by steps around y axis and rotation is negative

Maximal measured gap heiht difference is 25 um.

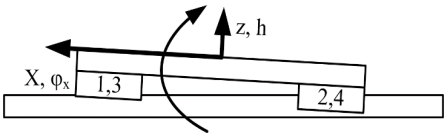

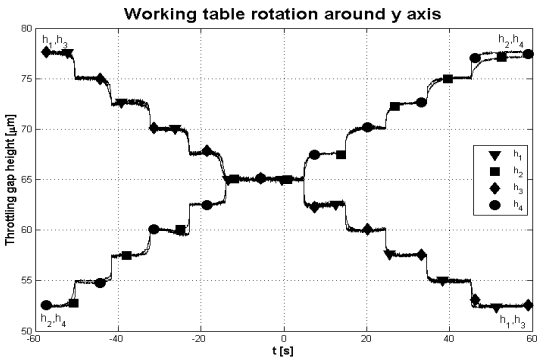

THE CZECH TECHNICAL UNIVERSITY IN PRAGUE

Measurement protocol

Department of Production Machines and Equipment

Date	Number	Place of measurement	Testing stand	Author
28.3.2016	6	U12135 - Horská, Praha	STD 30	Tomáš Lazák

List of used devices and sensors

Type	Manufacturer/ supplier	Designation	Measuring range	Accuracy	Placement
Temperature gauge		Pt 100	-50 + 200 °C	Třída A	1,2,3
Pressure gauge	BHV senzory s.r.o.	DMP 333	0 - 250 bar rel	≤±0,5%	4
Pressure gauge	BHV senzory s.r.o.	DMP 333	0 - 50 bar rel	≤±0,5%	1,2,3
Flow meter	BOPP & REUTHER	Miniflow 015	0,1 - 1,0 l/min	≤±1% o.r.	1,2,3
Length gauge	Mesing	T102F	-2÷2 mm	*	1,2,3,4
Proportional valve	Argo-hitos	SR1P-A2/H12-24E2			1,2,3,4
Service master Plus	Parker	SCM-500-01-00			-
Real time controller	National Instruments	NI CRIO-9025			yes
Real time controller	National Instruments	Ni sbRiio-9637			-
Data acquisition system	National Instruments	Ni cDAQ-9188			yes
AO module	National Instruments	NI 9263			yes
AI module	National Instruments	NI 9219			yes
AI module	National Instruments	NI 9205			yes

*linearity error 0,25 % in range ±1mm at a temperature 20 °C, repeatability 0,01 μm

Measurement conditions		
Hydrostatic pockets	4 * 40 x 40, land 8	
Control system program	RT_mainVI_hydrolinear_v13	
Oil type	ISO VG 46, VI 149	
Pump pressure	50	bar
Room temperature	18	°C
Oil temperature-measurement start	21	°C
Oil temperature-measurement end	22	°C
Applied mass (m - x -y)	0 - 0 - 0	kg - mm - mm

Schematics

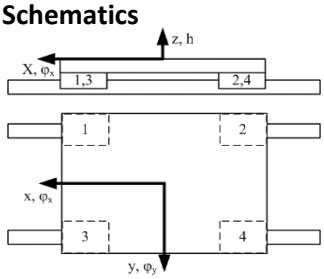

Designation:	**Working table rotation around X and Y axis**

Measurement description:

Throttling gap height is set to 65 um
Working table is rotated by one step around x axis and rotation is positive
Working table is rotated by one step around y axis and rotation is positive
Working table is rotated by one step around x axis and rotation is positive
Working table is rotated by one step around y axis and rotation is positive
Step are repeated untim aximum rotation is achieved

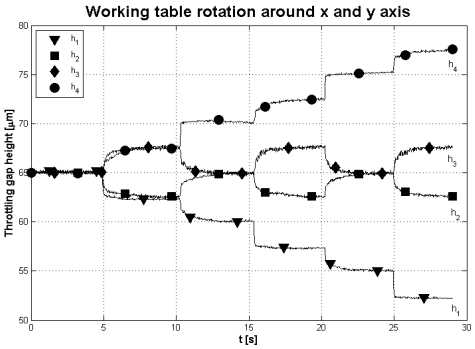

List of patents addressing horizontal milling machine compensations

Nmbr.	Title	Publication number	Inventor(s)	Applicant(s)	International classification	Date of application
1	DEFLECTION CORRECTION SYSTEM FOR A MILLING MACHINE	**US8764357 (B2); US2012321406 (A1)**	HUANG KUN-FANG [TW] CHEN TSAIR-RONG [TW] TANG CHIA-HUI [TW] YANG WEN-REN [TW] CHANG PAUL [TW]	HUANG KUN-FANG [TW] CHEN TSAIR-RONG [TW] TANG CHIA-HUI [TW] YANG WEN-REN [TW] CHANG PAUL [TW] DEPT OF ELECTRICAL ENGINEERING NAT CHANG HUA UNIVERSITY OF EDUCATION [TW] BUFFALO MACHINERY COMPANY LTD [TW]	B23C9/00	20110614
2	Compensation device for dead-weight deformation of ram of numerical control floor boring and milling machining center	**CN103465109 (A)**	CUI YONGCHAO ZHANG MINGLI MA GUOCHENG	SUZHOU JIANG YUAN PREC MACHINERY CO LTD	B23Q23/00 B23Q11/00	20130923
3	Ram deflection deformation compensation device	**CN102380802 (A)**	ZIJUN HU KANGJIAN PAN YUEHUA SUN	WUHU HENGSHENG HEAVY MACHINE TOOL CO LTD	B23Q23/00 B23Q1/25	20111103
4	Ram bending deformation two-way compensating device	**CN101913106 (A)**	BO QU FENGHE WU YUEHONG WANG	QIER MACHINE TOOL GROUP CO LTD	B23Q23/00 B23P23/02 B23Q1/01	20100805
5	Anti-sag underarm for horizontal boring, drilling and milling machines and the like	**US3227047 (A)**	JONES GORDON H FRITZ SCHULTHEISS	GIDDINGS & LEWIS	B23Q11/00	19630220
6	HORIZONTAL MACHINE TOOL	**US9058030 (B2); US2013264989 (A1)**	TAUCHI HIROYUKI [JP]	TAUCHI HIROYUKI [JP] MITSUBISHI HEAVY IND LTD [JP]	G05B19/404	20111208
7	Hydraulic servo compensating device of spindle system of floor boring-milling machine	**CN201900505 (U)**	MINGLI ZHANG HONGKUI CUI WENZHENG JI ZHIBIN YU	SUZHOU JIANGYUAN PREC MACHINERY CO LTD	B23Q11/00	20101215
8	Ram gravity center supporting mechanism for numerically controlled floor type boring and milling machines	**CN201922304 (U)**	RUOFEI ZHANG	ANHUI GUORUITE HEAVY CNC MACHINE TOOL MFG CO LTD	B23Q11/00 B23Q1/01	20101203
9	SYSTEM FOR COMPENSATING FOR THE RAM DROP IN A MACHINE-TOOL	**US9033627 (B2); US2011255933 (A1)**	MENDIA OLABARRIA ANGEL MARIA [ES]	SORALUCE S COOP [ES]	B23Q11/00	20091015
10	Method of error compensation for angular errors in machining (droop compensation)	**US6325578 (B1)**	SZUBA PHILIP S [US] PASEK ZBIGNIEW JAN [US]	UNOVA IND AUTOMATION SYS INC [US]	B23Q15/18 B23Q1/00 B23Q1/48 B23Q1/56 B23Q1/60 B23Q1/70 B23Q5/40 B23Q11/00 B23Q17/22 G05B19/404 B23Q5/36	20010216
11	Spindle box double-screw compensation device of large numerically-controlled floor type boring and milling machine	**CN202292289 (U)**	XIANG ZHU	SHENJI GROUP KUNMING MACHINE TOOL CO LTD	B23Q23/00 B23B19/00	20111012
12	Apparatus for compensating position errors of spindle head and machine tool provided with same	**US2003063957 (A1); US6821064 (B2)**	HIRABAYASHI KATSUMI [JP]	HIRABAYASHI KATSUMI, TOSHIBA KIKAI KABUSHIKI KAISHA	B23Q15/18 B23C1/00 B23Q1/00 B23Q1/72 G05B19/404 B23Q1/46 B23C1/00	20020926
13	Spindle box gravity center balancing device of boring-milling machine	**CN104325351 (A)**	LIU XIAOFENG DONG YAN LIAO KAINING	LIUZHOU ZHENGLING HEAVY CNC MACHINE TOOL CO LTD	B23Q11/00 B23B19/00	20131112
14	Balance compensation structure and mode for three hanging points of spindle box	**CN102248183 (A); CN102248183 (B)**	LIN GUI RONG LI QINGGUO GAO ZHONGPING QI XING ZHANG	WUHAN HEAVY MACHINE TOOL GROUP CO LTD	B23B19/00 B23B47/00 B23Q23/00	20110426
15	Main spindle box gravity center shift compensating device	**CN102380803 (A)**	ZIJUN HU KANGJIAN PAN YUEMIN SHI HEMEI YANG	WUHU HENGSHENG HEAVY MACHINE TOOL CO LTD	B23Q23/00	20111103
16	Gravity centre compensation apparatus for electric bridge type main spindle box	**CN201154403 (Y)**	DAGUANG ZHU [CN] HONGCAI WANG [CN] XIAO SONG [CN]	QIQIHAR NO 2 MACHINE TOOL GROU [CN]	B23B47/26 B23B39/02	20080128
17	Numerical control floor type boring and milling machine main spindle box balancing compensation system	**CN202045535 (U)**	JINSUO MU	TONTEC INVESTEMENT GROUP CO LTD	B23Q11/00	20110428
18	Headstock balancing arrangement for machine tools	**US4149822 (A)**	LEHMKUHL ROBERT A	CARLTON MACHINE TOOL CO	B23Q11/00 B23B47/26	19771121
19	Balance compensating devices	**US3168000 (A)**	RENE DEFLANDRE	DEREFA ETS [LI]	B23Q11/00 F16F15/28	19630401

20	BALANCE COMPENSATED MACHINE TOOLS	**US3671133 (A)**	GALBARINI MASO RAMUSINO FRANCESCO COTTA	INNOCENTI SOC GENERALE	B23Q11/00 B23B47/26	19701102
21	HORIZONTAL DRILLING AND MILLING MACHINE WITH A HEADSTOCK MOVABLE UPWARDLY AND DOWNWARDLY ON GUIDING MEANS	**US3853423 (A)**	QUACK P	SCHARMANN & CO	B23Q11/00 B23B47/26	19720925
22	Gravity center follow-up balance compensating device of floor type boring and milling machine	**CN102039542 (B);** **CN102039542 (A)**	MO WANG JINGHONG SU KUN CHENG MINREN YU	TDG MACHINERY TECHNOLOGY CO LTD	B23Q11/00	20101125
23	HEADSTOCK BALANCING CONSTRUCTION FOR MACHINE TOOLS	**US3684395 (A)**	NURAKAMI AKIRA	MITSUBISHI HEAVY IND LTD	B23Q11/00 B23B47/26	19701214
24	HEADSTOCK BALANCING CONSTRUCTION FOR MACHINE TOOLS	**US3707333 (A)**	KITAMURA TETSUO TAMAI AKIRA	MITSUBISHI HEAVY IND LTD	B23Q11/00 B23B47/26	19700713
25	A milling and/or boring machine	**GB885426 (A)**		SCHIESS AG	B23Q11/00	19600601
26	BALANCE COMPENSATING DEVICE	**US3580133 (A)**	BERTHIEZ CHARLES WILLIAM	BERTHIEZ CHARLES WILLIAM	B23Q11/00 B23C1/02	19690501
27	Balancing and compensating arrangement	**US4048902 (A)**	DEFLANDRE RENE	DEFLANDRE RENE	B23B47/26 B23Q11/00 B23Q5/22 B23C1/027	19750120
28	Precision compensating device for spindle box of boring machine	**CN102581688 (A)**	YONGXING WANG XUEMEI CHANG	SHANGHAI SANY PREC MACHINERY	B23Q11/00	20111229
29	Ram hydrostatic guideway hydrostatic compensation mechanism	**CN204209514 (U)**	HAO YUQIN QIU YULIANG QIN ZHIXU QU TONG XUE KAI SHAO JIANGTAO	WEIHAI HUADONG AUTOM CO LTD	B23Q23/00	20141106
30	Deflection compensation device of numerical-control boring and milling machine	**CN203843602 (U)**	CHENG KUN REN JIEHUI HE ZHENWEI	TDG MACHINERY TECHNOLOGY CO LTD	B23Q23/00 B23Q17/00	20140523
31	Overhanging deformation real-time compensation method of numerical control machine ram	**CN102063090 (A);** **CN102063090 (B)**	YONGQING WANG YANFENG LU YE TAO XIANJUN SHENG HAIBO LIU ZHIQIANG JIAO SONG CHEN	UNIV DALIAN TECH	G05B19/404	20101230
32	MACHINE TOOL	**WO2009098931 (A1)**	DOMARU HIROYUKI [JP] MIZUTA KEIJI [JP]	MITSUBISHI HEAVY IND LTD [JP] DOMARU HIROYUKI [JP] MIZUTA KEIJI [JP]	B23Q15/18 B23Q1/72 B23Q17/22 G05B19/404	20090120
33	Method and apparatus for correcting deflection of a movable member	**US5053973 (A)**	FUJII SHIGEHARU [JP] OCHIAI AKIRA [JP] FUJII AKIO [JP]	TOSHIBA MACHINE CO LTD [JP]	B23Q15/24 B23Q1/00 B23Q1/72 G05B19/404 G06F15/46	19890724

Proportional Directly Operated Pressure Relief Valve

SR1P2-A2

HA 5122
5/2012

3/4-16 UNF • pmax 350 bar (5076 PSI) • Qmax 1,5 L/min (0.396 GPM)

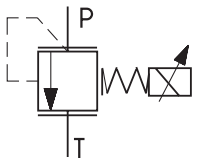

- ❑ **Screw-in cartridge design**
- ❑ **Direct acting, poppet type**
- ❑ **Three pressure ranges**
- ❑ **Pressure output proportional to DC current input**

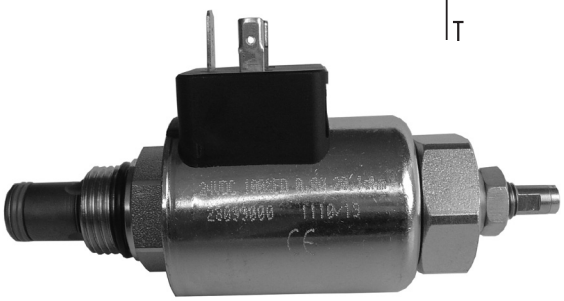

Functional Description

The valve is designed for continuous regulation of pressure in the circuit. The valve consists of the seat (1), poppet (3), return spring (2), main spring (4), spring support ring (5) and control proportional solenoid (6).

In the basic position (with the coil deenergized) the port P is fully open to port T. Proportional increase of DC current at solenoid (6) increase force to valve poppet (3) through preload spring (4).
This blocks flow in direction P – T until sufficient pressure is pre-sent to offset electrically induced solenoid force.

The minimum value of the cracking pressure can be adjusted using the screw (7), position of which is secured with the nut (8). The adjusting screw (7) can also be used as the emergency control. Screw (9) is used to air bleed the solenoid control system. To ensure self-bleeding of the valve it is recommended to install it in a vertical position with the solenoid facing downwards. Bleeding process is necessary for the proper functioning of the valve.

The valve can be used alone or as a built-in, pilot operated pressure relief valve SR4P2-B2 (datasheet No. HC 5117), or as a control valve of a built-in indirectly controlled pilot operated pressure reducing valve SP4P2-B3 (datasheet No. HA 5123).

The valve body and the adjustment screw are zinc coated.

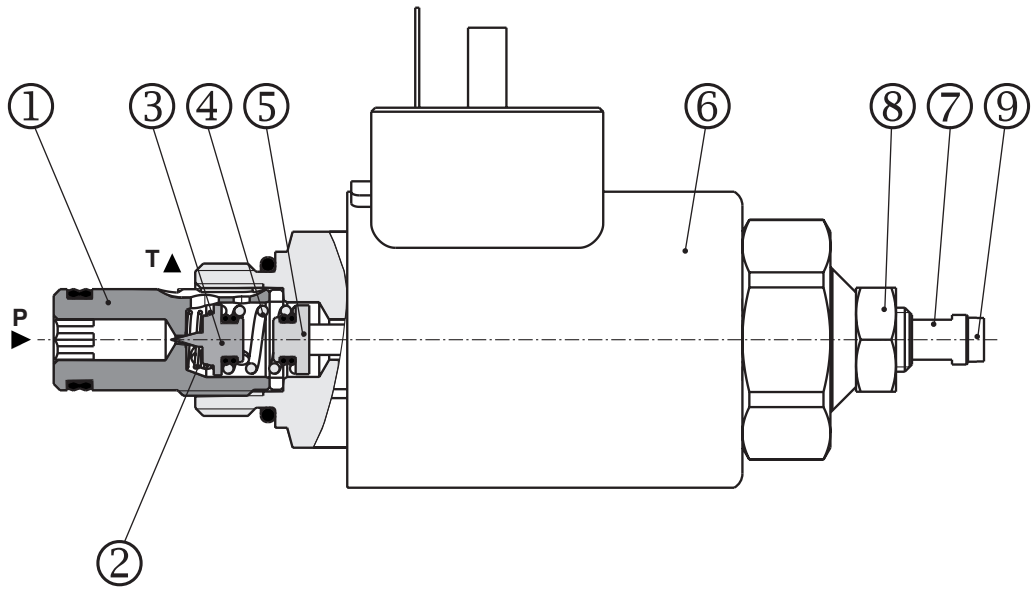

Ordering Code

SR1P2-A2 / □ □ - □ □ □

Proportional Directly Operated Pressure Relief Valve 3/4-16UNF

High performance — **H**

Pressure range

up to 120 bar (1740 PSI)	**12**
up to 210 bar (3046 PSI)	**21**
up to 350 bar (5076 PSI)	**35**

Nominal solenoid supply voltage

12 V DC	**12**
24 V DC	**24**

Seals

V	Viton (FPM)

Type of solenoid coil

E2	Connector EN 175301-803-A with quenching diode
E4	Connector AMP Junior Timer with quenching diode
E13	Connector Deutsch DT04-2P with quenching diode

Other coils on demand see catalog HA8007.

Technical Data

Valve size		A2
Cartridge Cavity		3/4-16 UNF-2A
Maximum operating pressure at ports P	bar (PSI)	350 (5076)
Maximum operating pressure at ports T*	bar (PSI)	100 (1450)
Flow range	L/min (GPM)	1,5 (0.396)
Hydraulic fluid		Hydraulic oils of power classes (HL, HLP) to DIN 51524
Fluid temperature range (FPM)	°C (°F)	-20 ...120 (-4 ... 248)
Ambient temperature, range	°C (°F)	-20 ... 80 (-4 ...176)
Viscosity range	mm^2/s (SUS)	10 ... 500 (49 ... 2450)
Duty cycle	%	100
Enclosure type to EN 60 529		IP 67 (IP 65)
Maximum valve tightening torque	Nm (lbf.ft)	30+2 (22.12+1.47)
Optimum dither control	Hz	200
Maximum degree of fluid contamination		Class 21/18/15 according to ISO 4406
Minimum reachable pressure for Q=1,5 L/min (0.396 GPM)	bar (PSI)	~ 20 (290)
Valve hysteresis	%	< 5
Weight	kg (lb)	0,440 (0.97)
Mounting position		When possible, the valve should be mounted with solenoid faced down.
Valve body (data shee HA 0018)		SB-A2

*Pressure in T influences p = f(I) a p = f(Q) valve performance

Solenoid Technical Data

Type of coil	V	12 DC	24 DC
Limit current	A	1	0,6
Resistance at 20 °C (68 °F)	Ω	6,5	20,8
Quenching diode (E2, E4, E13)		BZW06-19B	BZW06-33B

p-I Characteristics

Measured at ν = 32 mm^2/s (156 SUS)

p = f (I), Q = 0,2 L/lmin (0.053 GPM)

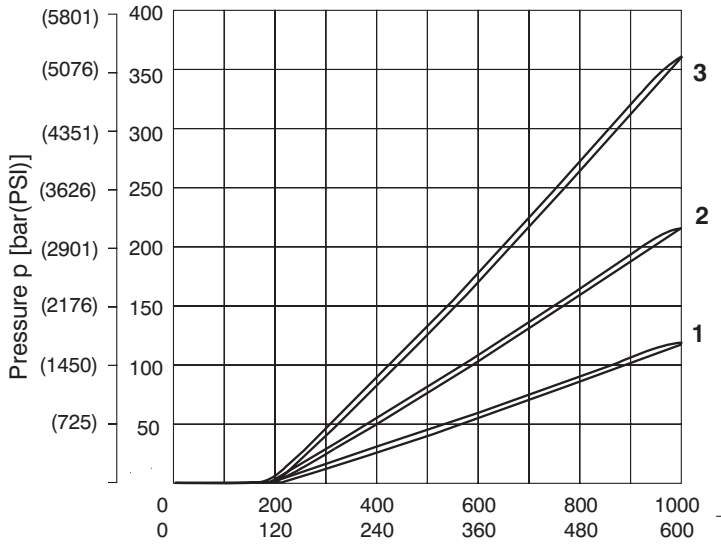

Attention:
The proportional pressure relief valve is not mechanically protected and it does not perform the relief valve function.

3	Pressure range 35
2	Pressure range 21
1	Pressure range 12

Type of the Solenoid Coil

Note:
Example of most frequent coil types.
For complete range valve coils with technical informatik about voltage, enclosure type, terminal box please afer to coil data sheet HA 8007.

Coil example	Solenoid	Connector	Type code
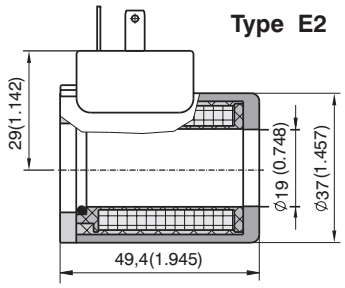	12 VDC	Connector EN 175301-803-A with quenching diode	C19B-01200E2-6,5NA
	24 VDC	Connector EN 175301-803-A with quenching diode	C19B-02400E2-20,6NA
	12 VDC	Connector AMP Junior Timer with quenching diode	C19B-01200E4-6,5NA
	24 VDC	Connector AMP Junior Timer with quenching diode	C19B-02400E4-20,6NA
	12 VDC	Connector Deutsch DT04-2P with quenching diode	C19B-01200E13-6,5NA
	24 VDC	Connector Deutsch DT04-2P with quenching diode	C19B-02400E13-20,6NA

Valve Dimensions

Dimensions in millimeters and (inches)

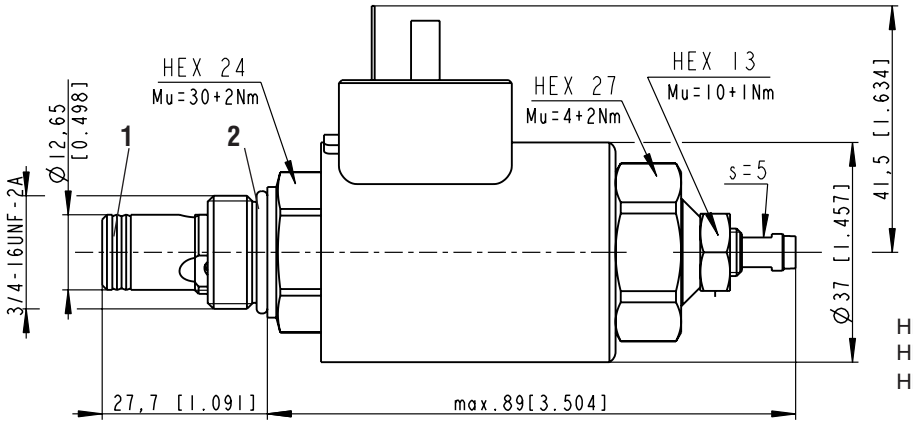

Seal kit
- see Spare Parts
1. Dualseal - PU
2. O-ring - Viton

HEX 24 Mu=[30+2 Nm (22+1.47 lb.ft)]
HEX 27 Mu=[4+2 Nm (2.95+1.47 lb.ft)]
HEX 13 Mu=[10+1 Nm (7.37+0.73 lb.ft)]

Cavity

Dimensions in millimeters and (inches)

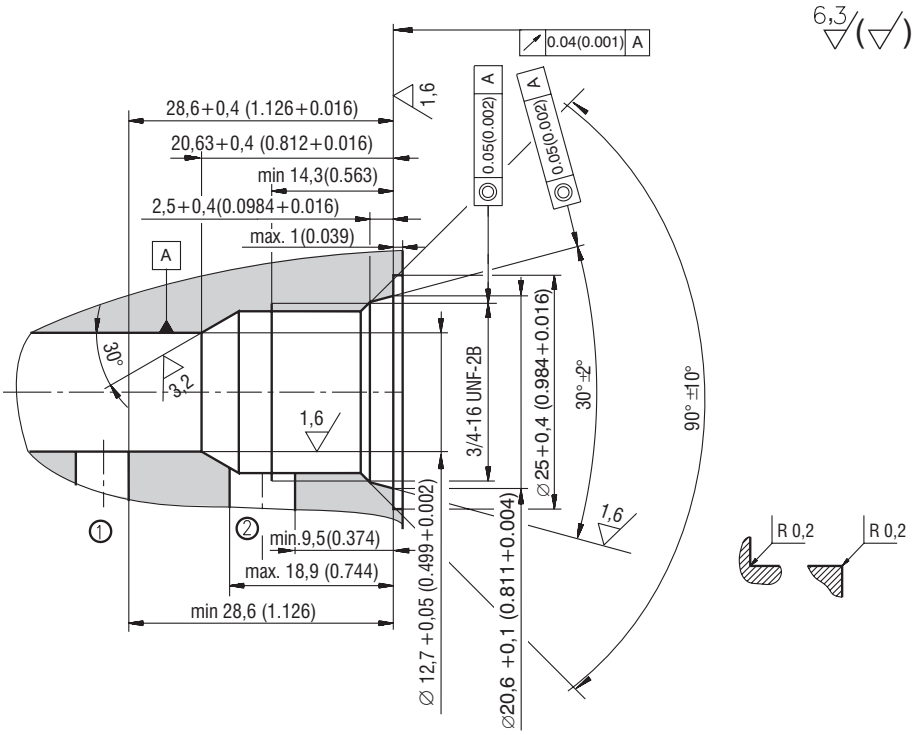

Spare Parts

Solenoid coil	Type of the coil		
	E2	E4	E13
Nominal voltage coil	Ordering number		
12 V DC	28145600	28145800	29867600
24 V DC	27824300	27824400	29868600
Seal kit	Dimensions, quantity		Ordering number
	Dualseal - PU	O-ring	
	10,3 x 12,7 x 3,1 (1pc)	17,17 x 1,78 (1pc)	17014300

Caution!

- The packing foil is recyclable.
- The technical information regarding the product presented in this catalogue is for descriptive purposes only. It should not be construed in any case as a guaranteed representation of the product properties in the sense of the law.

ARGO-HYTOS s.r.o. CZ - 543 15 Vrchlabí
tel.: +420-499-403 111
e-mail: info.cz@argo-hytos.com
www.argo-hytos.com

GE-M

Male Connector
24° Flareless / Metric

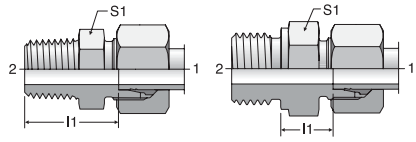

Metric taper thread

Cutting face DIN 3852, form B, Metric thread

TUBE FITTING PART #	END SIZE 1 (mm)	END SIZE 2 Metric	l 1 (mm)	S1 (mm)	Pressure Rating (bar) EO CF	EO 71	EO MS
GE04LLM6X1KEG	4	M6 x 1 keg.	16.0	9	100	100	63
GE04LLM	4	M8 x 1 keg.	16.0	10	100	100	63
GE06LLM	6	M10 x 1 keg.	14.5	11	100	100	63
GE08LLM	8	M10 x 1 keg.	16.5	12	100	100	63
GE06LM	6	M10 x 1	8.5	14	315	315	200
GE08LM	8	M12 x 1.5	10.0	17	315	315	200
GE10LM	10	M14 x 1.5	11.0	19	315	315	200
GE10LM16X1.5	10	M16 x 1.5	12.0	22	315	315	200
GE10LM18X1.5	10	M18 x 1.5	12.5	24	315	315	200
GE10LM22X1.5	10	M22 x 1.5	14.0	27	315	315	200
GE12LM14X1.5	12	M14 x 1.5	11.0	19	315	315	200
GE12LM	12	M16 x 1.5	12.5	22	315	315	200
GE12LM18X1.5	12	M18 x 1.5	12.5	24	315	315	200
GE12LM22X1.5	12	M22 x 1.5	14.0	27	315	315	200
GE15LM16X1.5	15	M16 x 1.5	13.0	24	250	250	160
GE15LM	15	M18 x 1.5	13.5	24	250	250	160
GE15LM22X1.5	15	M22 x 1.5	15.0	27	250	250	160
GE18LM18X1.5	18	M18 x 1.5	14.0	27	250	250	160
GE18LM	18	M22 x 1.5	14.5	27	250	250	160
GE22LM22X1.5	22	M22 x 1.5	16.5	32	160	160	100
GE22LM	22	M26 x 1.5	16.5	32	160	160	100
GE28LM	28	M33 x 2	17.5	41	160	160	100
GE35LM	35	M42 x 2	17.5	50	160	160	100
GE42LM	42	M48 x 2	19.0	55	160	160	100
GE06SM	6	M12 x 1.5	13.0	17	400	400	250
GE08SM	8	M14 x 1.5	15.0	19	400	400	250
GE10SM	10	M16 x 1.5	15.0	22	400	400	250
GE12SM	12	M18 x 1.5	17.0	24	400	400	250
GE12SM22X1.5	12	M22 x 1.5	17.5	27	400	400	250
GE14SM	14	M20 x 1.5	19.0	27	400	400	250
GE16SM18X1.5	16	M18 x 1.5	18.0	27	400	400	250
GE16SM	16	M22 x 1.5	18.5	27	400	400	250
GE20SM	20	M27 x 2	20.5	32	400	400	250
GE25SM	25	M33 x 2	23.0	41	250	250	160
GE30SM	30	M42 x 2	23.5	50	160	160	100
GE38SM	38	M48 x 2	26.0	55	160	160	100

Note: "keg." refers to taper threads.
Not sold with EO-2 Functional Nut.

GAI-R

Female Connector
24° Flareless / BSPP

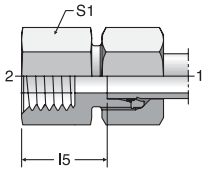

TUBE FITTING PART #	END SIZE 1 (mm)	END SIZE 2 BSPP	l 5 (mm)	S1 (mm)	Pressure Rating (bar) EO CF	EO 71	EO MS	EO-2 CF	EO-2 71
GAI06LR	6	G 1/8	19.0	14	315	315	200	315	315
GAI08LR	8	G 1/4	24.0	19	315	315	200	315	315
GAI08LR3/8	8	G 3/8	25.0	24	315	315	200	315	315
GAI08LR1/2	8	G 1/2	29.0	27	315	315	200	315	315
GAI10LR	10	G 1/4	25.0	19	315	315	200	315	315
GAI10LR3/8	10	G 3/8	26.0	24	315	315	200	315	315
GAI10LR1/2	10	G 1/2	30.0	27	315	315	200	315	315
GAI12LR	12	G 3/8	26.0	24	315	315	200	315	315
GAI12LR1/2	12	G 1/2	30.0	27	315	315	200	315	315
GAI15LR	15	G 1/2	31.0	27	315	315	200	315	315
GAI18LR	18	G 1/2	30.5	27	315	315	200	315	315
GAI22LR	22	G 3/4	35.5	36	160	160	100	160	160
GAI28LR	28	G 1	38.0	41	160	160	100	160	160
GAI35LR	35	G 1 1/4	41.0	55	160	160	100	160	160
GAI42LR	42	G 1 1/2	42.5	60	160	160	100	160	160
GAI06SR	6	G 1/4	26.0	19	400	400	250	400	400
GAI08SR	8	G 1/4	26.0	19	400	400	250	400	400
GAI10SR	10	G 3/8	26.5	24	400	400	250	400	400
GAI12SR	12	G 3/8	26.5	24	400	400	250	400	400
GAI14SR	14	G 1/2	32.0	30	400	400	250	400	400
GAI16SR	16	G 1/2	31.5	30	400	400	250	400	400
GAI20SR	20	G 3/4	34.5	36	315	315	200	315	315
GAI25SR	25	G 1	37.5	41	315	315	200	315	315
GAI30SR	30	G 1 1/4	42.0	55	315	315	200	315	315
GAI38SR	38	G 1 1/2	43.5	60	250	250	160	250	250

For EO-2 part number, insert "Z" between size and pressure series.
Example: GAI06ZLRCF

Dimensions and pressures for reference only, subject to change.

Parker Hannifin Corporation
Tube Fittings Division
Columbus, Ohio
http://www.parker.com/tfd

HPC

Hex Pipe Cap
NPTF

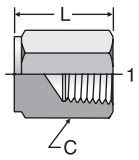

TUBE FITTING PART #	END SIZE 1 NPTF	C HEX (in.)	L (in.)	Dynamic Pressure (x 1,000 PSI) -S	-SS	-B
1/8 HPC	1/8 - 27	9/16	.75	6.0	6.0	3.3
1/4 HPC	1/4 - 18	3/4	.91	6.0	6.0	3.3
3/8 HPC	3/8 - 18	7/8	1.03	6.0	6.0	3.3
1/2 HPC	1/2 - 14	1 1/16	1.34	6.0	6.0	3.3
3/4 HPC	3/4 - 14	1 1/4	1.44	4.8	4.8	3.1
1 HPC	1 - 11 1/2	1 5/8	1.68	3.6	3.6	2.3
1 1/2 HPC	1 1/2 - 1 1/2	2 3/8	1.92	2.4	2.4	1.5

P87OMN

ISO 6149 Hex Head Plug
ISO 6149
(for ISO 6149-1 Port)

SAE J2244-4* 62M0109A

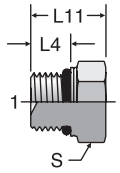

TUBE FITTING PART #	END SIZE 1 THREAD	L4 (mm)	L11 (mm)	S HEX (mm)	Dynamic Pressure (x 1,000 PSI) S	SS	B
M8P87OMN	M8X1	8.5	16.2	12	9.0	9.0	3.3
M10P87OMN	M10X1	8.5	16.2	14	8.0	8.0	3.3
M12P87OMN	M12X1.5	11.0	18.5	17	9.0	9.0	3.3
M14P87OMN	M14X1.5	11.0	19.5	19	9.0	9.0	3.3
M16P87OMN	M16X1.5	11.5	21.5	22	9.0	9.0	3.3
M18P87OMN	M18X1.5	12.5	23.5	24	9.0	9.0	3.3
M20P87OMN	M20X1.5	12.5	24.0	27	6.0	6.0	3.3
M22P87OMN	M22X1.5	13.0	25.5	27	6.0	6.0	3.3
M27P87OMN	M27X2	16.0	32.0	32	6.0	6.0	3.3
M30P87OMN	M30X2	16.0	32.0	36	6.0	6.0	3.3
M33P87OMN	M33X2	16.0	32.0	41	6.0	6.0	3.3
M42P87OMN	M42X2	16.0	34.0	50	4.0	4.0	2.6
M48P87OMN	M48X2	17.5	35.5	55	2.0	2.0	1.3
M60P87OMN	M60X2	17.5	33.0	65	1.0	1.0	0.6

* SAE J2244-4 and ISO 6149-4 are draft standards.

VSTI M-OR

ISO 6149 Hollow Hex Plug
ISO 6149
(for ISO 6149-1 Port)

SAE J2244-4* 62M0109B

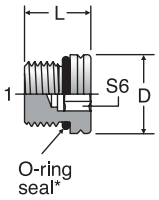

TUBE FITTING PART #	END SIZE 1 METRIC	D (mm)	L (mm)	S6 (mm)	Dynamic Pressure (x 1,000 PSI) CF	71	MS
VSTI10X1ORCF	M10 x 1	13	13.5	5	9.1	9.1	3.3
VSTI12X1.5ORCF	M12 x 1.5	17	15.1	6	9.1	9.1	3.3
VSTI14X1.5ORCF	M14 x 1.5	19	16.0	6	9.1	9.1	3.3
VSTI16X1.5ORCF	M16 x 1.5	21	17.5	8	9.1	9.1	3.3
VSTI18X1.5ORCF	M18 x 1.5	23	19.0	8	9.1	9.1	3.3
VSTI22X1.5ORCF	M22 x 1.5	27	20.0	10	9.1	9.1	3.3
VSTI27X2ORCF	M27 x 2	32	23.5	12	5.8	5.8	3.3
VSTI33X2ORCF	M33 x 2	38	25.0	14	5.8	5.8	3.3
VSTI42X2ORCF	M42 x 2	48	25.5	22	5.8	5.8	3.3

* SAE J2244-4 is a draft standard

VSTI M-ED

Metric Hollow Hex Plug
Metric-ED
(for ISO 9974-1 / DIN 3852-1 Port)

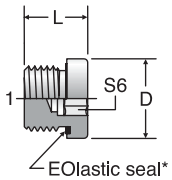

TUBE FITTING PART #	END SIZE 1 THREAD	D (mm)	L (mm)	S6 (mm)	Dynamic Pressure (x 1,000 PSI) CF	71	MS
VSTI10X1ED	M10 x 1	14	12.0	5	5.8	5.8	3.3
VSTI12X1.5ED	M12 x 1.5	17	17.0	6	5.8	5.8	3.3
VSTI14X1.5ED	M14 x 1.5	19	17.0	6	5.8	5.8	3.3
VSTI16X1.5ED	M16 x 1.5	22	17.0	8	5.8	5.8	3.3
VSTI18X1.5ED	M18 x 1.5	24	17.0	8	5.8	5.8	3.3
VSTI20X1.5ED	M20 x 1.5	26	19.0	10	5.8	5.8	3.3
VSTI22X1.5ED	M22 x 1.5	27	19.0	10	5.8	5.8	3.3
VSTI26X1.5ED	M26 x 1.5	32	21.0	12	5.8	5.8	3.3
VSTI27X2ED	M27 x 2	32	21	12	5.8	5.8	3.3
VSTI33X2ED	M33 x 2	40	22.5	17	5.8	5.8	3.3
VSTI42X2ED	M42 x 2	50	22.5	22	4.5	4.5	2.9
VSTI48X2ED	M48 x 2	55	22.5	24	4.5	4.5	2.9

Dimensions and pressures for reference only, subject to change.

Parker Hannifin Corporation
Tube Fittings Division
Columbus, Ohio
http://www.parker.com/tfd